

Opposing Roles for Protein Tyrosine Phosphatases SHP2 and PTPN12 in Breast Cancer

Inauguraldissertation

zur

Erlangung der Würde eines Doktors der Philosophie

vorgelegt der

Philosophisch-Naturwissenschaftlichen Fakultät

Der Universität Basel

von

Nicola Aceto

aus Italien

Basel, 2011

Genehmigt von der Philosophisch-Naturwissenschaftlichen Fakultät
auf Antrag von

Dr. Mohamed Bentires-Alj

Prof. Dr. Nancy E. Hynes

Prof. Dr. Gerhard Christofori

Basel, den 26. April 2011

Prof. Dr. Martin Spiess

Dekan

1. TABLE OF CONTENTS

1. TABLE OF CONTENTS.....	I
2. SUMMARY	i
3. INTRODUCTION	1
3.1 Breast cancer	2
3.2 Luminal A and luminal B breast cancer.....	3
3.3 HER2-enriched breast cancer.....	4
3.4 Triple-negative breast cancer	5
3.5 Breast cancer stem cells	6
3.6 The family of classical PTPs.....	9
3.7 Regulation of classical PTPs.....	12
3.8 Function and regulation of the oncogenic tyrosine phosphatase SHP2	14
3.9 Other oncogenic PTPs in breast cancer.....	17
3.10 Function and regulation of the tumor suppressor phosphatase PTPN12	20
3.11 Other tumor suppressor PTPs in breast cancer.....	21
4. RATIONALE OF THE WORK.....	25
5. RESULTS	28
5.1 Research article submitted to Nature Medicine	28
5.2 Research article published in Cell.....	92

6. DISCUSSION AND OUTLOOK	118
6.1 The role of SHP2 in CSCs	118
6.2 SHP2 as a molecular hub linking stemness and EMT	119
6.3 Mechanism of action of SHP2 in CSCs	119
6.4 The “SHP2 signature” in human breast cancer	120
6.5 SHP2 as a targets in breast cancer and in other malignancies	121
6.6 The role of PTPN12 in TNBCs	121
6.7 Concluding remarks and future directions	122
7. REFERENCES	125
8. ABBREVIATIONS	137
9. ACKNOWLEDGEMENTS	138
10. CURRICULUM VITAE	139

2. SUMMARY

Breast cancer is the most common malignancy among women. It is a very heterogeneous disease that progresses to metastasis, a usually fatal event. The cellular and biochemical mechanisms orchestrating this progression remain largely elusive. The characterization of the cellular heterogeneity of the tumor is crucial for the identification of the source of metastases, and elucidation of the oncogenic and tumor-suppressive networks of cancer cells is fundamental to the development of targeted therapies for this presently incurable disease.

Tumors, like normal organs, appear hierarchically organized at the cellular level. The concept of cancer stem cells (CSCs, a.k.a. tumor-initiating cells) has recently received experimental support in several human malignancies. CSCs are defined as a subpopulation of cells within the tumor capable of self-renewing, differentiating and recapitulating the heterogeneity of the original cancer, and seeding new tumors when transplanted in recipient animals. CSCs are thought to play important roles in the metastatic progression of breast cancers and to resist to classical chemo- and radiation therapies. For these reasons, the identification of the key signaling networks controlling CSCs is of a paramount importance for the development of CSC-targeted therapies.

We demonstrate a fundamental role for protein-tyrosine phosphatase SHP2 in these processes in HER2-positive and triple-negative breast cancers (TNBCs), two subtypes associated with a poor prognosis. Knockdown of SHP2 eradicated breast CSCs *in vitro* and in xenografts, prevented invasion in 3D cultures and progression from *in situ* to invasive breast cancer *in vivo*, and blocked the growth of established tumors and reduced metastases. Mechanistically, SHP2 activated stemness-associated transcription factors including c-Myc and ZEB1, which resulted in the repression of let-7 miRNA and the expression of a set of

“SHP2 signature” genes found co-activated in a large subset of human primary breast tumors. Taken together, our data show that activation of SHP2 and its downstream effectors is required for self-renewal of breast CSCs and for tumor maintenance and progression, thus providing new insights into signaling cascades that regulate CSCs and a rationale for targeting this oncogenic PTP in breast cancer.

Unlike the oncogenic role of SHP2 in breast cancer, we found that another member of the protein-tyrosine phosphatases family, PTPN12, is lost in a subset of TNBCs. Loss of PTPN12 activity by different means, including loss of gene expression induced by upregulation of miRNA-124 or inactivating mutations, promoted cellular transformation *via* activation of oncogenic receptor tyrosine kinases (RTKs) including EGFR, HER2 and PDGFR β . These findings identify PTPN12 as a commonly inactivated tumor suppressor, and provide a rationale for combinatorially targeting proto-oncogenic tyrosine kinases in TNBC and other cancers based on their profile of tyrosine-phosphatase activity.

In summary, our results identify new important targets for the treatment of aggressive subtypes of breast cancer. While targeting SHP2 should result in the depletion of CSCs and tumor regression, combined inhibition of the RTK constrained by PTPN12 in TNBCs should lead to major therapeutic advances for the treatment of this currently incurable disease.

3. INTRODUCTION

Reversible tyrosine phosphorylation is an essential eukaryotic regulatory mechanism for numerous important aspects of cell physiology (Hunter 1987; Alonso, Sasin et al. 2004; Tonks 2006). This enzymatic reaction is governed by the combined action of protein-tyrosine kinases (PTKs) and protein-tyrosine phosphatases (PTPs) (Figure 3-1), and regulates important signaling cascades involved in most of cellular processes (Tonks 2006).

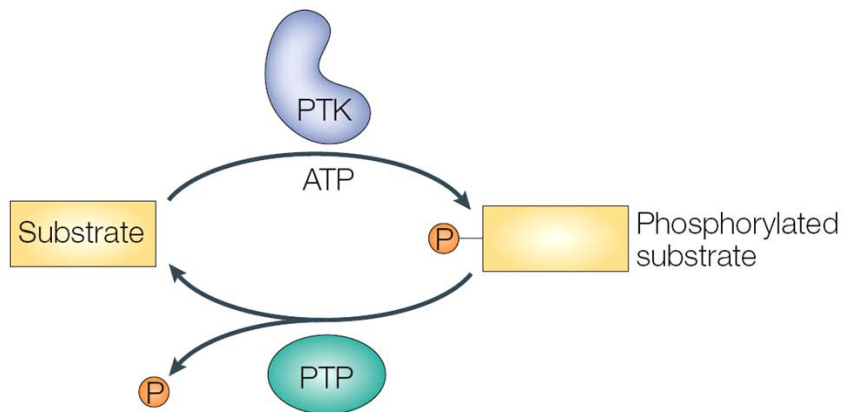


Figure 3-1. Combined action of PTKs and PTPs governs tyrosine phosphorylation. Tyrosine phosphorylation is a key regulatory mechanism in eukaryotes. Proteins are phosphorylated on tyrosine residues by PTK and dephosphorylated by PTPs (Mustelin, Vang et al. 2005).

Deregulation of the balance between PTKs and PTPs activity may result in malignant transformation and cancer, (Hunter 2009), and this work aimed at defining the role of two classical PTPs, SHP2 and PTPN12, in breast cancer.

3.1 Breast cancer

Breast cancer is the most frequently diagnosed cancer in women (Ferlay, Autier et al. 2007; Jemal, Siegel et al. 2010). It is a heterogeneous disease, characterized by different molecular alterations driving its growth, survival and metastatic properties. Breast cancer arises from the epithelial cells of the mammary gland, and progresses into hyperplasia, atypical-hyperplasia, ductal carcinoma *in situ* (DCIS) and invasive ductal carcinoma (IDC). The last and usually fatal step of breast cancer progression is metastasis, particularly frequent in organs like lung, bone, liver and brain (Figure 3-2) (Nguyen, Bos et al. 2009). Notably, this linear progression model has been challenged by several studies showing a “parallel progression” of breast cancer, where the metastatic cells quit the primary tumor site as early as DCIS (Klein 2009).

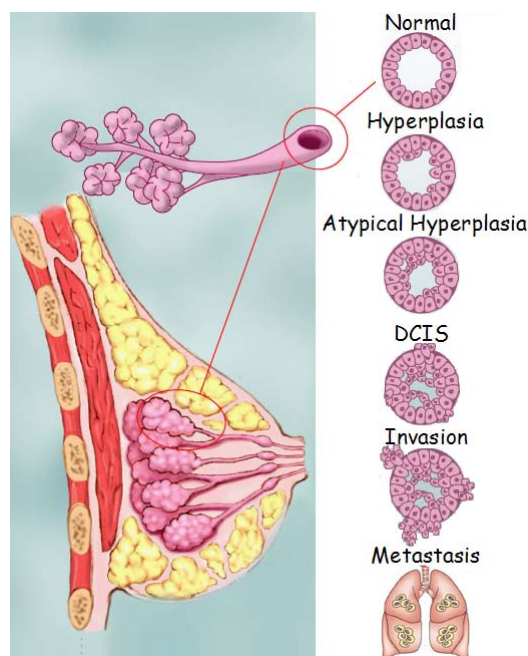


Figure 3-2. Breast cancer linear progression model. Schematic of breast cancer progression steps starting from hyperplasia and progressing into atypical hyperplasia, DCIS, Invasive carcinoma and metastasis (adapted from www.breastcancer.org).

Currently, classification of breast cancers depends on clinical parameters (e.g., age, node status, tumor size, histological grade) and detection of pathological markers like the hormone receptors (HR) estrogen receptor (ER) and progesterone receptor (PR), and the tyrosine kinase receptor c-erbB2/HER2 (Perou, Sorlie et al. 2000; Di Cosimo and Baselga 2010). However, the complexity of breast cancer is not sufficiently recapitulated by these markers. Genome-wide gene-expression profiles identified six breast cancer subgroups: luminal A, luminal B, normal-like, HER2-enriched, basal-like and claudin-low (Perou, Sorlie et al. 2000; Sorlie, Perou et al. 2001; Carey, Perou et al. 2006; Prat, Parker et al. 2010). Each of these subtypes is associated with a different prognosis, mainly influenced by intrinsic aggressiveness of the tumor and current therapeutic options. Basal-like, claudin-low and HER2-enriched breast tumors correlate with the worst prognosis (Perou, Sorlie et al. 2000; Sorlie, Perou et al. 2001; Carey, Perou et al. 2006; Prat, Parker et al. 2010).

3.2 Luminal A and luminal B breast cancer

Luminal tumors are characterized by the expression of ER, with or without co-expression of PR (Sims, Howell et al. 2007) and account for ~60 % of all breast cancers. In particular, luminal A tumors generally express both ER and PR, while the expression of these HRs is more variable in tumors of the luminal B subtype (Sims, Howell et al. 2007). For this reason, patients bearing luminal A tumors are more responsive to hormonal therapy and survive

longer than patients with luminal B tumors (Vargo-Gogola and Rosen 2007). In addition to ER and PR, luminal tumors are characterized by overexpression of other luminal markers like GATA3, X-box binding protein 1 and LIV-1 (Perou, Sorlie et al. 2000; Sorlie, Perou et al. 2001).

The gold standard for treatment of HR-positive breast cancer has been, for over three decades, the ER antagonist tamoxifen. More recently, aromatase inhibitors (AIs), preventing the synthesis of estrogens in the peripheral tissues including breast, have been shown to be more effective compared to tamoxifen in post-menopausal women with early-stage and advanced breast cancer (Thurlimann, Keshaviah et al. 2005; Mauri, Pavlidis et al. 2006; Forbes, Cuzick et al. 2008). Despite these advances in the therapy of HR-positive breast tumors, primary and acquired resistance to endocrine therapy remain a challenge. Resistance mechanisms can occur as a result of the cross-talk between ERs and RTKs or with signaling pathways that function downstream of these receptors, such as the phosphatidylinositol 3-kinase (PI3K)/Akt/mTOR pathway (Prat and Baselga 2008; Creighton, Fu et al. 2010; Meyer and Bentires-Alj 2010; Miller, Hennessy et al. 2010).

3.3 HER2-enriched breast cancer

Another molecular subtype of breast cancer is the HER2-enriched subtype. It accounts for ~20% of patients and it is associated with aggressive disease and decreased survival (Slamon, Clark et al. 1987). In addition to HER2 activation, this subtype is characterized by overexpression of GRB7, TGF β 1-induced anti-apoptotic factor 1 and TNF receptor-associated factor 4. Notably, nearly two-thirds of the HER2-enriched breast tumors bear a gene amplification and overexpression of *HER2*, while one-third of these tumors express

HER2 at a normal level, indicating that mechanisms other than *HER2* amplification drive this subtype; these mechanisms may include HER2 hyperphosphorylation.

Trastuzumab, a humanized monoclonal antibody targeting the extracellular domain of HER2, improves the survival of patients with HER2-positive advanced and early-stage breast cancer (Lewis Phillips, Li et al. 2008). Notably, other therapeutic agents have shown encouraging anti-tumor activity *in vivo* and in early clinical studies, these include lapatinib (a dual HER1 and HER2 tyrosine kinase inhibitor), the humanized monoclonal antibody pertuzumab (which prevents HER2 dimerization by sterically preventing its pairing with other members of the HER receptor family), the trastuzumab-DM1 complex (consisting of trastuzumab conjugated to the anti-microtubule agent DM1) and inhibitors of heat shock protein 90 (a.k.a. HSP90, a molecular chaperone required to maintain HER2 integrity and function) (Agus, Akita et al. 2002; Mendoza, Phillips et al. 2002; Modi, Stopeck et al. 2007; Lewis Phillips, Li et al. 2008; Portera, Walshe et al. 2008; Baselga and Swain 2009; von Minckwitz, du Bois et al. 2009; Baselga, Gelmon et al. 2010). Despite the clinical efficacy of HER2-targeting agents, one third of HER2-positive tumors do not respond to therapy. In addition, nearly half of the patients who initially respond to HER2-targeted agents will relapse within a year (Nagata, Lan et al. 2004).

3.4 Triple-negative breast cancer

Triple-negative breast cancer (TNBC), which accounts for ~20% of cases, is characterized by the lack of expression of ER, PR and lack of *HER2* amplification. TNBCs are divided into basal-like and claudin-low subtypes, which share some common features like low expression of luminal gene clusters and luminal cytokeratins (CKs) 8 and 18. In addition, the basal-like

tumors are further characterized by high expression of the basal CKs 5, 14 and 17, while the claudin-low tumors are more enriched in epithelial-to-mesenchymal transition (EMT) features including loss of E-cadherin, Claudin3, 4 and 7, immune system responses and stem cell-associated biological processes (Sims, Howell et al. 2007; Prat, Parker et al. 2010).

After an initial “dark-phase”, characterized by lack of specific targets, increasing knowledge of the biology of TNBC biology has led to clinical trials using new promising therapies such as EGFR targeted agents, anti-angiogenic factors and poly (ADP-ribose) polymerase (PARP) inhibitors (Anders and Carey 2008; Di Cosimo and Baselga 2010), some of which are currently in clinical trials. Given that the claudin-low subtype shows important features of breast cancers stem cells (Creighton, Li et al. 2009; Hennessy, Gonzalez-Angulo et al. 2009), agents tailored towards depletion of CSCs should be particularly effective in this subtype.

3.5 Breast cancer stem cells

The concept of cancer stem cells (CSCs, a.k.a. tumor-initiating cells), proposed by Pierce and colleagues in 1988 (Pierce and Speers 1988), has recently received experimental support in several human cancers including acute myeloid leukemia, cancers of breast, brain, pancreas, colon, liver and melanoma (Bonnet and Dick 1997; Al-Hajj, Wicha et al. 2003; Singh, Hawkins et al. 2004; Li, Heidt et al. 2007; O'Brien, Pollett et al. 2007; Ricci-Vitiani, Lombardi et al. 2007; Schatton, Murphy et al. 2008; Yang, Ho et al. 2008). CSCs are cells within a tumor which can self-renew, differentiate, and give rise to a tumor when transplanted into recipient mice. Unfortunately, most current cancer therapies are not tailored towards depleting CSCs. Indeed, most current cancer chemotherapeutic agents have been developed

based on their ability to decrease primary tumor size rather than specifically eliminating CSCs. This may explain why, in many solid malignancies including breast cancer, tumor regression does not necessarily translate into increased patient survival. Possible reasons for the failure of current therapeutic agents in the treatment of breast cancer include the suggested inherent drug resistance of CSCs and their propensity to reach distant organs and seed metastases (Dean, Fojo et al. 2005; Li, Tiede et al. 2007; Li, Lewis et al. 2008; Diehn, Cho et al. 2009). The concept of CSCs is developing rapidly, and it yet has not been unanimously accepted by the scientific community. Indeed, an attitude of healthy caution seems to be developing in the maturing CSC community (Clevers 2011). Unfortunately, stem cells and the cellular hierarchy are poorly characterized in most tissues that develop solid cancers. As a consequence, few if any definitive stem cell markers are available for isolating CSC from solid tumors. Markers for identifying CSCs are different across different tumor types and even among different subtypes of the same tumor. Current CSC markers are primarily chosen as robust, heterogeneously expressed FACS markers that allow the sorting of marker-positive and marker-negative populations (e.g. CD133^{high} population in melanoma or CD44^{high}/CD24^{low} population in breast cancer). However, they are not selected on the basis of a deep understanding of the underlying stem cell biology of the pertinent tissue from which the cancer originates (Clevers 2011). In addition, the stability of the CSC phenotype has not yet been experimentally probed. In their study on melanoma, Morrison and colleagues (Quintana, Shackleton et al. 2008; Shackleton, Quintana et al. 2009) showed that tumors arising both from CD133⁻ cells and from CD133⁺ cells sorted from an original melanoma re-establish the original ratios of CD133⁻ and CD133⁺ cells. This experiment indicated that individual cancer cells can recapitulate the marker heterogeneity of the tumors from which they derive. Similarly, Vonderhaar and colleagues showed that the breast CSC markers CD44^{high}/CD24^{low} are under dynamic regulation *in vitro* and *in vivo*; particularly,

they demonstrated that non-invasive, epithelial-like $CD44^{high}/CD24^{high}$ cells gave rise to invasive, mesenchymal $CD44^{high}/CD24^{low}$ progeny (Meyer, Fleming et al. 2009). Plasticity of the CSC state should then be given serious consideration. Therefore, agents targeting both CSCs and the bulk of the tumor will most likely be needed for curing breast cancer.

Potential approaches are to directly kill CSCs or to induce their differentiation by inhibiting their survival mechanisms or blocking their self-renewal (Zhou, Zhang et al. 2009). Alternatively, it is conceivable that interfering with the stem cell niche would also lead to differentiation or death of CSCs (Figure 3-3). Therefore, the identification of the signaling networks that control CSCs is very important for the development of novel therapeutic strategies.

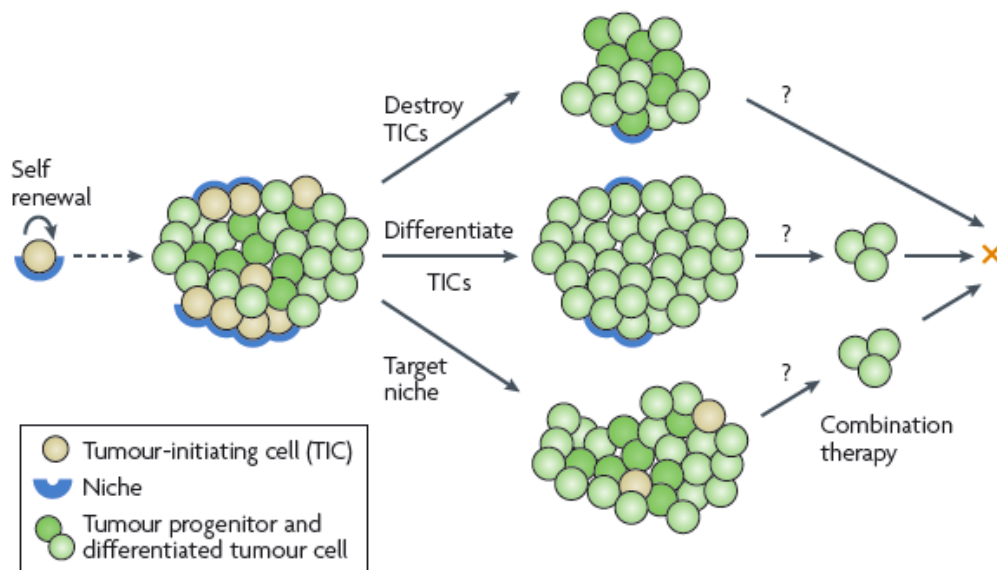


Figure 3-3. Therapeutic strategies to target CSCs. Shown are possible strategies to eradicate CSCs (Zhou, Zhang et al. 2009).

3.6 The family of classical PTPs

Tyrosine phosphorylation plays a pivotal role in virtually all signaling pathways and biological processes mentioned above. Although PTPs were initially thought to act exclusively as tumor suppressors, it is now clear that they can have either inhibitory or stimulatory effects on cancer-associated signaling processes. A better understanding of the mechanisms regulating and regulated by PTPs can lead to the development of new pharmacological targets for breast cancer.

The human genome encodes ~90 PTKs and ~107 PTPs (Robinson, Wu et al. 2000; Alonso, Sasin et al. 2004; Julien, Dube et al. 2011), suggesting similar levels of substrate specificity between these two families of enzymes. PTPs are defined by the catalytic-site motif HC(X)₅R, in which the cysteine residue functions as a nucleophile and is essential for catalysis. This cysteine forms the base of the active-site cleft and recognizes the phosphate of the target substrate. Catalysis proceeds through a two-step mechanism that involves the production of a cysteinyl-phosphate intermediate. In the first step, there is nucleophilic attack on the phosphate by the sulfur atom of the thiolate ion of the essential cysteine residue. This is coupled with protonation of the tyrosyl leaving group of the substrate by the conserved aspartic acid residue. The second step involves the hydrolysis of the phosphoenzyme intermediate, mediated by a glutamine residue, which coordinates a water molecule, and aspartic acid, which now functions as a general base, culminating in the release of phosphate (Figure 3-4).

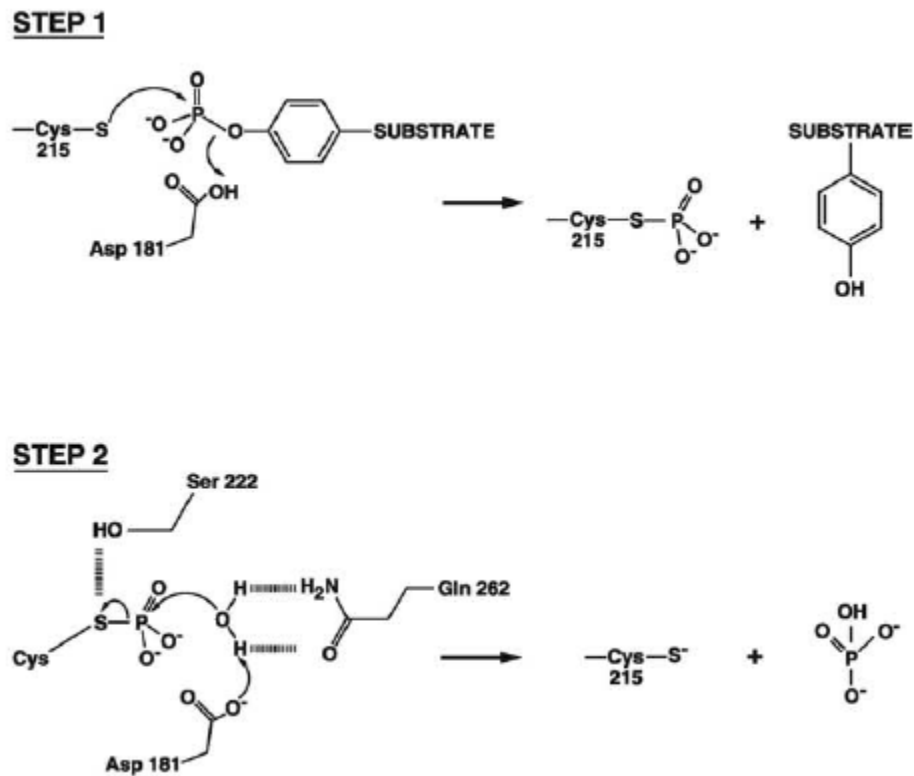


Figure 3-4. Mechanism of action of PTPs. Shown is a schematic representation of the two-step mechanism of action of PTPs (Tonks 2003).

In humans, the ~107 PTPs are divided in 2 groups, classical and dual specificity PTPs. The sub-group of “*classical PTPs*” comprises 37 PTP members, characterized by specificity for phosphotyrosine residues. Classical PTPs are subdivided into two groups, “*transmembrane*” and “*non-transmembrane*” PTPs (Figure 3-5) (Andersen, Mortensen et al. 2001).

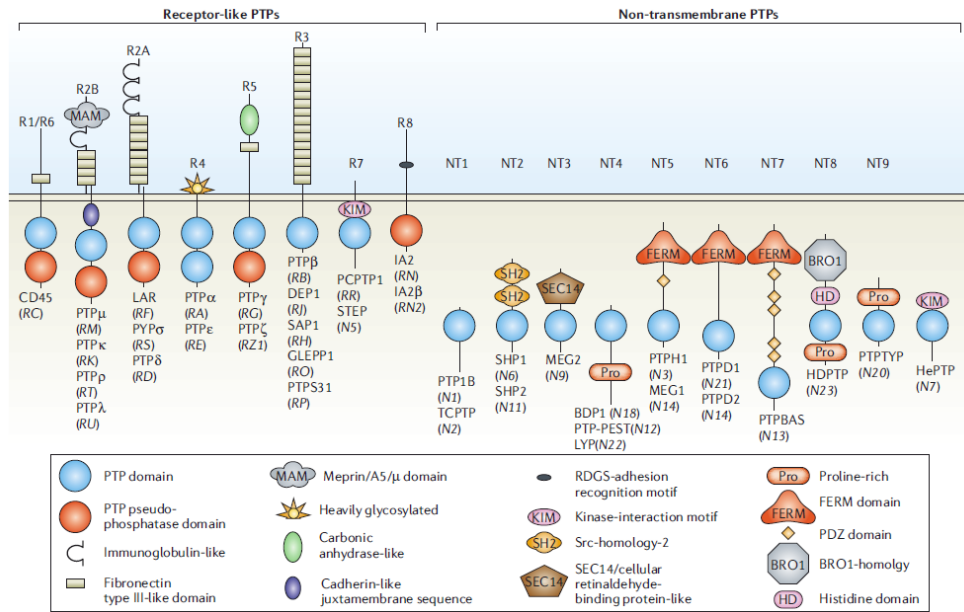


Figure 3-5. The family of classical PTPs. Classical PTPs can be categorized as transmembrane or non-transmembrane proteins (Tonks 2006).

The transmembrane PTPs contain a single-pass transmembrane domain, a variable extracellular domain responsible for cell-to-cell, cell-to-matrix or cell-to-ligand interactions, and an intracellular portion usually containing two tandem catalytically-active domains (with most of the catalytic activity residing in the membrane-proximal domain and with the membrane-distal domain also involved in protein-protein interaction and PTP dimerization) (Streuli, Krueger et al. 1990; Felberg and Johnson 1998). The non-transmembrane PTPs have remarkable structural diversity among each other and contain regulatory sequences that target them to specific subcellular locations or enable their binding to specific proteins (Figure 3-5) (Mauro and Dixon 1994). These regulatory sequences control the activity of the enzyme either directly by interaction with the active site or by controlling substrate specificity (Garton, Burnham et al. 1997; Pulido, Zuniga et al. 1998; Ostman, Hellberg et al. 2006).

3.7 Regulation of classical PTPs

The activity of PTPs is tightly regulated *in vivo* to maintain physiological tyrosine phosphorylation levels. PTPs function can be regulated by different means including the control of gene expression, protein localization and by the post-transcriptional modifications listed below.

First, PTPs can be regulated by reversible oxidation (Meng, Fukada et al. 2002; Meng, Buckley et al. 2004; Persson, Sjoblom et al. 2004; Kamata, Honda et al. 2005). The catalytic-site motif of PTPs contains an invariant cysteine residue which is characterized by an extremely low pK_a (den Hertog, Groen et al. 2005; Salmeen and Barford 2005; Tonks 2005). At neutral pH this cysteine residue is present as a thiolate ion, which promotes its function as a nucleophile in catalysis but also renders it highly susceptible to oxidation, resulting in abrogation of nucleophilic function and inhibition of PTP activity. Therefore, the production of reactive oxygen species (ROS) can be a potent and specific mechanism of regulation of PTPs activity (Finkel 2003; Tonks 2005). Importantly, the oxidation of the catalytic cysteine is reversible, making this modification a dynamic mode of PTP regulation (see Figure 3-4) (Salmeen, Andersen et al. 2003).

Second, PTPs can be regulated through phosphorylation, nitrosylation and/or sumoylation. For example, tyrosine-phosphorylation of PTP1B, SHP1, SHP2 and PTP α or serine-phosphorylation of PTPN12 affects their phosphatase activity as well as their affinity to substrates and interacting partners (Bennett, Tang et al. 1994; den Hertog, Tracy et al. 1994; Garton and Tonks 1994; Dadke, Kusari et al. 2001). In addition, PTP1B was found to be sumoylated in response to insulin leading to a decrease in its catalytic activity (Dadke, Cotteret et al. 2007).

Third, PTPs can be regulated by proteolytic cleavage. Calcium is a critical initiator of protease activity and the calcium-activated protease calpain has been shown to cleave regulatory domains of several PTPs. For example, the non-transmembrane PTP1B, PTP-MEG1 and SHP1 are activated upon calpain-induced cleavage (Frangioni, Oda et al. 1993; Gu and Majerus 1996; Falet, Pain et al. 1998). Transmembrane PTPs like LAR, PTP κ and PTP μ are also subject to proteolysis as a mechanism of regulation of their catalytic activity (Streuli, Krueger et al. 1992; Anders, Mertins et al. 2006; Ruhe, Streit et al. 2006).

Fourth, transmembrane PTPs can be regulated via dimerization and/or binding to ligands. Using PTP α as a model, it was proposed that homodimerization reduced its catalytic activity by reciprocal occlusion of the active sites (Bilwes, den Hertog et al. 1996), although this regulatory mechanism does not seem to be a common feature of all transmembrane PTPs (Nam, Poy et al. 1999; Nam, Poy et al. 2005). In addition, extracellular ligand binding is also a regulatory mechanism for PTPs. For example, while PTP ζ activity is reduced upon binding to its ligand pleiotrophin (Meng, Rodriguez-Pena et al. 2000), LAR activity appears to be regulated by binding to different heparan sulphate proteoglycans at synapses (Fox and Zinn 2005; Johnson, Tenney et al. 2006) (Figure 3-6).

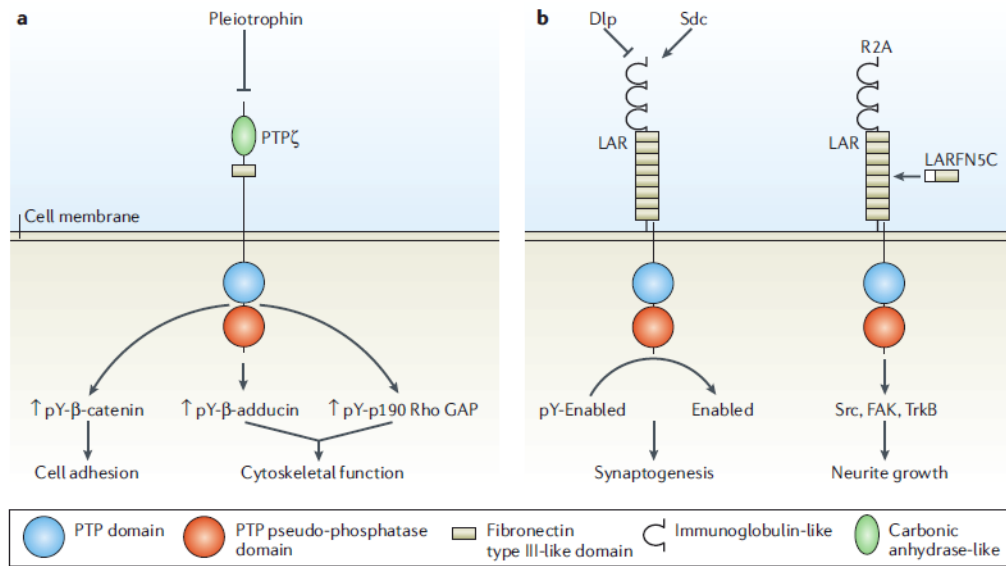


Figure 3-6. Regulation of the function of transmembrane PTPs by ligands. Shown are examples of PTPs regulation mechanisms *via* interaction with extracellular ligands. **a)** The binding of Pleiotrophin to the transmembrane PTP ζ reduces its activity. **b)** The activity of LAR is regulated by binding to different heparan sulphate proteoglycans (Tonks 2006).

3.8 Function and regulation of the oncogenic tyrosine phosphatase SHP2

The Src homology-2 domain-containing phosphatase SHP2 (encoded by *PTPN11*), a ubiquitously expressed PTP, transduces mitogenic, pro-survival, pro-migratory signals from almost all growth factor-, cytokine- and extracellular matrix receptors. SHP2 null-embryos die peri-implantation and fail to yield trophoblast stem cell lines (Yang, Klamann et al. 2006). While SHP2 deficiency increases self-renewal of murine and human embryonic stem cells (Burdon, Stracey et al. 1999; Wu, Pang et al. 2009), it decreases self-renewal in neural stem/progenitor cells and hematopoietic stem cells (HSC), suggesting a cell-type specific role

of SHP2 in regulating cell fate (Chan, Li et al. 2006; Ke, Zhang et al. 2007; Zhu, Ji et al. 2011).

SHP2 contains two SRC homology 2 (SH2) domains (N-SH2 and C-SH2), a PTP domain and a C-terminal tail with a proline-rich motif and two tyrosyl phosphorylation sites (Y542 and Y580). In the absence of upstream stimulation, SHP2 is kept in an inactive state by interaction of the N-terminal SH2 domain with the PTP domain. Upon activation of RTKs, binding and phosphorylation of scaffolding adaptors, SHP2 binds tyrosine phosphorylated residues *via* its SH2 domains. SHP2 can also bind directly to phosphorylated tyrosine residues on RTKs. Binding causes a conformational change in SHP2, resulting in SHP2 activation and dephosphorylation of its substrates. (Figure 3-7) (Chan, Kalaitzidis et al. 2008).

Gain-of-function (GOF) germline *PTPN11* mutations were found in about half of patients with Noonan syndrome (NS), a common autosomal dominant developmental disorder (Tartaglia, Mehler et al. 2001). Moreover, GOF somatic mutations were identified in ~34% of patients with juvenile myelomonocytic leukemia (JMML), ~6% of patients with acute myeloid leukemia (AML), more rarely in solid tumors but not in breast cancer (Tartaglia, Niemeyer et al. 2003; Bentires-Alj, Paez et al. 2004; Loh, Vattikuti et al. 2004). Interestingly, these GOF mutations lead to the activation of key oncogenic signaling cascades including ERK and AKT pathways (Wang, Yu et al. 2009). In addition to GOF mutations, SHP2 can be activated by different means, for example by binding to scaffolding adaptor like GAB2, downstream of constitutive active forms of EGFR and fibroblast growth factor receptor 3 (FGFR3), upon BCR-ABL activation, and downstream of active RTKs RET and HER2 (Sattler, Mohi et al. 2002; Agazie, Movilla et al. 2003; D'Alessio, Califano et al. 2003; Zhan and O'Rourke 2004; Bentires-Alj, Gil et al. 2006). SHP2 has also been found to be a

mediator of *Helicobacter pylori*-induced transformation of gastric epithelial cells via interaction with the CagA protein, a virulence factor secreted by *H. pylori* (Hatakeyama 2004).

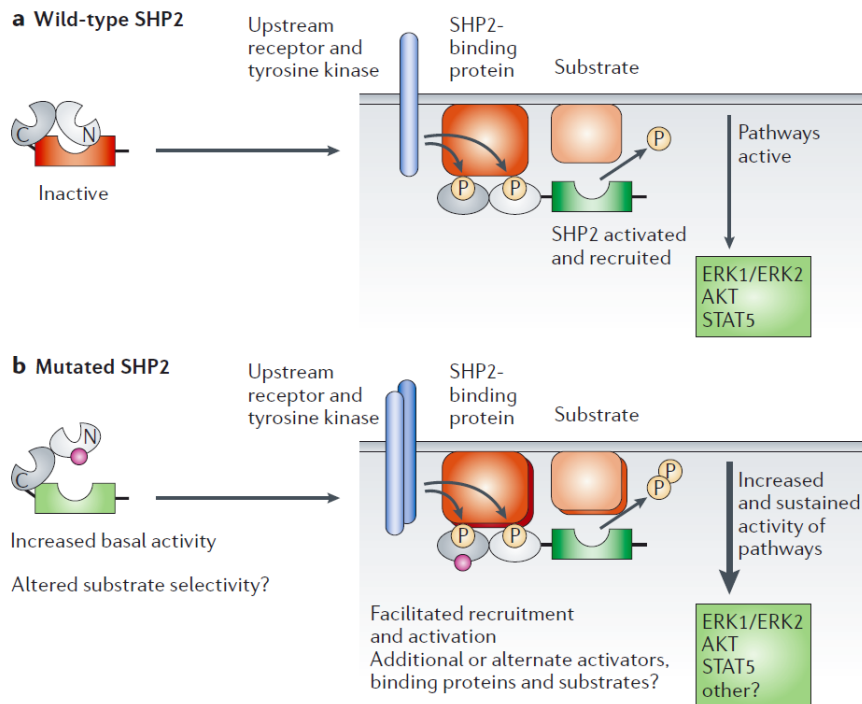


Figure 3-7. Mechanisms of SHP2 activation. Schematic of the mechanism of activation of wild-type and mutated SHP2. **a)** In absence of upstream stimulation, SHP2 is kept in an inactive state by the interaction of the N-terminal SH2 domain with the catalytic PTP domain. Upon activation of surface receptors, SHP2 binds phospho-tyrosine sites via its SH2 domains. This causes a conformational change which leads to an increase of the enzymatic activity of SHP2 and activation of the downstream signaling. **b)** In Leukemia, mutations of SHP2 lead to permanent changes in its structure and activation of the PTP domain, causing an increased and sustained activation of downstream pathways (Ostman, Hellberg et al. 2006).

3.9 Other oncogenic PTPs in breast cancer

Other PTPs have been associated with a potential oncogenic role in breast cancer, like PTP1B (Wiener, Kerns et al. 1994; Bjorge, Pang et al. 2000; Bentires-Alj and Neel 2007; Julien, Dube et al. 2007; Cortesio, Chan et al. 2008; Arias-Romero, Saha et al. 2009; Blanquart, Karouri et al. 2009; Johnson, Peck et al. 2010), PTP α (Ardini, Agresti et al. 2000; Zheng, Resnick et al. 2008), PTP ϵ (Elson 1999; Gil-Henn and Elson 2003), LAR (Yang, Zhang et al. 1999; Levea, McGary et al. 2000) and PTPH1 (Zhi, Hou et al. 2010). However, definitive evidence for their relevance for human breast cancer is still missing. Clearly, additional validation is required before establishing any of these PTPs as drug targets.

The non-transmembrane PTP1B (encoded by *PTPNI*), an important regulator of mammalian metabolism (Elchebly, Payette et al. 1999), has been linked to breast cancer. Mice lacking PTP1B in all tissues are hypersensitive to insulin, lean, and resistant to high fat diet-induced obesity (Elchebly, Payette et al. 1999; Klaman, Boss et al. 2000). Overexpression of PTP1B was observed in human breast tumors, with a strong association with HER2-positive tumors (Wiener, Kerns et al. 1994). In line with this finding, PTP1B was later found to be required for HER2/Neu-evoked mammary tumorigenesis (Bentires-Alj and Neel 2007; Julien, Dube et al. 2007). In contrast, PTP1B deficiency had no effect on polyoma middle T mediated tumorigenesis (Bentires-Alj and Neel 2007). Subsequently, PTP1B has also been associated with breast cancer cell transformation, proliferation, invadopodia dynamics, invasion and resistance to 4-OH tamoxifen treatment (Cortesio, Chan et al. 2008; Arias-Romero, Saha et al. 2009; Blanquart, Karouri et al. 2009). Mechanistically, PTP1B was shown to dephosphorylate and activate c-Src in human breast cancer cell lines *in vitro* (Bjorge, Pang et al. 2000; Cortesio, Chan et al. 2008; Arias-Romero, Saha et al. 2009) and to

suppress prolactin-mediated activation of STAT5 in breast cancer cells through inhibitory dephosphorylation of the STAT5 tyrosine kinase JAK2 (Johnson, Peck et al. 2010). Recent data from our lab show that PTP1B deletion in the mammary epithelium delays MMTV-HER2/NeuNT-induced breast cancer (Balavenkatraman et al., submitted). In contrast, depletion of PTP1B after breast tumor development did not block tumor progression (Balavenkatraman et al., submitted). These data raise the possibility that PTP1B inhibitors could be used for preventing breast cancer, but not for the treatment of advanced stages of this disease.

The transmembrane PTP α is a widely expressed enzyme enriched in brain tissues (Skelton, Ponniah et al. 2003). Full-body PTP α knockout mice show deficits in learning, locomotor activity and anxiety (Skelton, Ponniah et al. 2003). Protein levels of PTP α (encoded by *PTPRA*) were found to vary widely among breast tumors, with ~30% of cases manifesting significant overexpression. High PTP α levels correlated significantly with low tumor grade and positive estrogen receptor status (Ardini, Agresti et al. 2000). In another study, suppression of PTP α in breast cancer cell lines resulted in reduction of Src activity (Zheng, Resnick et al. 2008). Consistently, Src and PTP α depletion induced apoptosis in ER-negative breast cancer cells (Zheng, Resnick et al. 2008), suggesting that this PTP contributes to the activation of oncogenic pathways.

The transmembrane PTP ϵ (encoded by *PTPRE*) has been found upregulated in MMTV-RAS and MMTV-Neu tumors, suggesting that this phosphatase may play a role in transformation by these two oncogenes (Elson and Leder 1995). Multiparous MMTV-PTP ϵ female mice, uniformly developed mammary hyperplasia accompanied by residual milk production and formation of sporadic tumors. The sporadic nature of these tumors, the long latency period and low levels of transgene expression indicated that PTP ϵ provided a

necessary, but insufficient, signal for oncogenesis (Elson 1999). In addition, PTP ϵ was shown to activate Src and support the transformed phenotype of Neu-induced mammary tumors (Gil-Henn and Elson 2003).

The leukocyte common antigen-related (LAR) PTP (encoded by *PTPRF*) is a prototype member of the class of transmembrane PTPs containing cell adhesion domains. Transgenic mice deficient in LAR exhibit defects in glucose homeostasis (Ren, Li et al. 1998). LAR mRNA and protein levels have been found increased in breast cancer tissues (Yang, Zhang et al. 1999). Moreover, LAR expression in human breast cancer specimens has been associated with metastatic potential and ER expression (Levea, McGary et al. 2000), but additional studies are required to understand the importance of this phosphatase in breast cancer.

The non-transmembrane PTPH1 (encoded by *PTPN3*) was shown to be overexpressed in some metastatic human primary breast tumor (Zhi, Hou et al. 2010). Mechanistically, PTPH1 promotes breast cancer growth via its effect on the expression of nuclear vitamin D receptor (VDR) protein. Notably, this effect is independent of its phosphatase activity, but dependent on its ability to increase cytoplasmic translocation of VDR, leading to the mutual stabilization of VDR and PTPH1 (Zhi, Hou et al. 2010).

In summary, *in vitro* and in some cases *in vivo* data suggest an oncogenic role for PTP1B, PTP α , PTP ϵ , LAR and PTPH1 in breast cancer. These observations warrant future experiments to demonstrate the value of each of these phosphatases as therapeutic targets in breast cancer.

3.10 Function and regulation of the tumor suppressor phosphatase PTPN12

Since their discovery, PTPs have been considered potential tumor suppressor because of their antagonistic effects on oncogenic PTK signaling (Hunter 2009).

PTPN12 (a.k.a. PTP-PEST) is a ubiquitously expressed PTP that plays a role in cell motility, cytokinesis, and apoptosis (Angers-Loustau, Cote et al. 1999; Garton and Tonks 1999; Cousin and Alfandari 2004; Playford, Lyons et al. 2006; Sastry, Rajfur et al. 2006; Halle, Liu et al. 2007). In fibroblasts, PTPN12 acts downstream of integrins and receptor tyrosine kinases (Charest, Wagner et al. 1997; Cong, Spencer et al. 2000; Lyons, Dunty et al. 2001) to regulate motility through its action on Rho GTPases (Sahai and Marshall 2002; Sastry, Lyons et al. 2002). Excess levels of PTPN12 suppress Rac1 activity while decreased PTPN12 levels elevate Rac1 and block RhoA activation (Sahai and Marshall 2002; Sastry, Lyons et al. 2002). Importantly, PTPN12 acts, either directly or indirectly, on several tyrosine kinases including c-SRC, c-ABL, and FAK, whose activities contribute to regulation of cell-cell junctions and Rho GTPases (Playford, Vadali et al. 2008; Chellaiah and Schaller 2009; Zheng, Xia et al. 2009). Although the precise function of PTPN12 in epithelial cells has not been determined, few studies implicate this phosphatase in the control of intestinal (Takekawa, Itoh et al. 1994) and pancreatic cancer cell motility (Sirois, Cote et al. 2006) through c-SRC or c-ABL-dependent pathways, respectively. In mammary epithelial cells, PTPN12 was shown to downregulate prolactin signaling in response to EGF (Horsch, Schaller et al. 2001).

3.11 Other tumor suppressor PTPs in breast cancer

Other PTPs have been suggested as tumor suppressor in breast cancer, like PTP γ (Panagopoulos, Pandis et al. 1996; Zheng, Kulp et al. 2000; Liu, Sugimoto et al. 2002; Liu, Sugimoto et al. 2004; Wang, Huang et al. 2006; Shu, Sugimoto et al. 2010), PTP-BAS (Bompard, Puech et al. 2002; Freiss, Bompard et al. 2004; Dromard, Bompard et al. 2007; Revillion, Puech et al. 2009; Glondu-Lassis, Dromard et al. 2010), MEG2 (Yuan, Wang et al.), GLEPP1 (Ramaswamy, Majumder et al. 2009) and PTP ζ (Perez-Pinera, Garcia-Suarez et al. 2007).

The expression of the transmembrane PTP γ (encoded by *PTPRG*) is reduced in breast cancer compared to normal breast (Panagopoulos, Pandis et al. 1996; Zheng, Kulp et al. 2000). Interestingly, the expression of this phosphatase appears to be regulated by estrogen or by conjugated linoleic acid (Zheng, Kulp et al. 2000; Liu, Sugimoto et al. 2002; Wang, Huang et al. 2006). Moreover, PTP γ overexpression was shown to inhibit growth in monolayer cultures, anchorage-independent growth, and tumorigenicity of MCF7 breast cancer cells (Liu, Sugimoto et al. 2004; Shu, Sugimoto et al. 2010). Mechanistically, overexpression of PTP γ in MCF7 cells reduces ERK1/2 phosphorylation and increases the expression of p21(cip) and p27(kip) (Shu, Sugimoto et al. 2010). These data suggest that PTP γ is a potential tumor suppressor, however this possibility needs to be tested in additional breast cancer models.

The non-transmembrane PTP-BAS (encoded by *PTPN13*) was initially found to promote apoptosis following tamoxifen treatment in MCF7 breast cancer cells via direct dephosphorylation of insulin receptor substrate-1 (IRS-1) and consequent inhibition of the PI3K/AKT pathway (Bompard, Puech et al. 2002; Dromard, Bompard et al. 2007). Moreover, PTP-BAS expression is a prognostic indicator of favorable outcome for patients with breast

cancer (Revillion, Puech et al. 2009). Notably, PTP-BAS expression was found decreased in breast cancer and metastasis specimens when compared with nonmalignant tissue (Glondu-Lassis, Dromard et al. 2010). Depletion of PTP-BAS in MCF7 cells drastically increased tumor growth and invasion (Glondu-Lassis, Dromard et al. 2010). Substrate-trapping experiments revealed that PTP-BAS directly dephosphorylated Src on tyrosine 419, leading to the inactivation of the Src downstream substrates FAK and p130cas (Glondu-Lassis, Dromard et al. 2010), and identifying a new mechanisms by which this phosphatase inhibits breast tumor aggressiveness.

The non-transmembrane tyrosine phosphatase MEG2 (encoded by *PTPN9*) was recently shown to directly dephosphorylate and inactivate both EGFR and HER2, and subsequently to impair EGF-induced STAT3 and STAT5 activation, resulting in an inhibition of cell growth in soft agar (Yuan, Wang et al. 2010). MEG2 overexpression also reduced invasion and MMP2 expression in MDA-MB-231 breast cancer cells (Yuan, Wang et al. 2010), suggesting that MEG2 plays a signal-attenuating role in breast cancer.

The transmembrane PTP GLEPP1 (encoded by *PTPRO*) is particularly expressed on the apical cell surface of the glomerular podocyte, and was shown to regulate the glomerular pressure/filtration rate relationship through an effect on podocyte structure and function (Wharram, Goyal et al. 2000). Expression of GLEPP1 was found to be reduced in breast cancer cell lines due to promoter methylation compared to normal mammary epithelial cells (Ramaswamy, Majumder et al. 2009). In line with this observation, treatment with 5-azacytidine restored expression of GLEPP1. Moreover, *PTPRO* promoter region harbors estrogen-responsive elements and treatment with estrogen reduces its expression, while treatment with tamoxifen increases it (Ramaswamy, Majumder et al. 2009). Accordingly, ectopic expression of GLEPP1 sensitized cells to the growth-suppressive effects of

tamoxifen, indicating that this PTP might act as a tumor-suppressor (Ramaswamy, Majumder et al. 2009).

The transmembrane PTP ζ (encoded by *PTPRZ1*) functions as a receptor for the cytokine pleiotrophin (PTN). PTN binding inactivates PTP ζ , leading to increased tyrosine phosphorylation of different proteins including beta-catenin, Fyn, P190RhoGAP and ALK (Perez-Pinera, Garcia-Suarez et al. 2007). PTP ζ was found expressed in different breast cancer subtypes and it correlated with ALK expression (Perez-Pinera, Garcia-Suarez et al. 2007), a RTK with oncogenic activity (Pulford, Morris et al. 2004; Perez-Pinera, Chang et al. 2007). This suggests that inactivation of PTP ζ could activate ALK in breast cancer, and that suppression of this PTP may favor breast tumor growth.

4. RATIONALE OF THE WORK

Targeted therapies for breast cancer are currently available and generally consist of endocrine treatment for ER-positive luminal tumors, and trastuzumab in combination with chemotherapy for HER2-overexpressing tumors. However, despite an initial benefit due to the treatment, patients frequently develop resistance and relapse. Thus, new anticancer agents targeting key signaling nodes are urgently required to improve the survival of breast cancer patients.

We focused on the most aggressive breast cancer subtypes, TNBCs and HER2-positive tumors. This work aims at understanding the role of two PTPs, SHP2 and PTPN12, in these subtypes of breast cancers.

Previous studies suggested that SHP2 might play a positive role in cancer. For example, GOF somatic mutations are found in ~35% of juvenile myelomonocytic leukemias and at various incidences in other myeloid malignancies, but rarely in solid cancers. SHP2 is also activated downstream of oncogenes in gastric carcinoma, anaplastic large cell lymphoma and glioblastoma. Although SHP2 mutations in breast cancer were not found, it was shown that the gene encoding the SHP2-activating protein GAB2 is amplified and overexpressed in 10-15% of human breast tumors. In addition, it has been proposed that SHP2 is overexpressed both in breast cancer cell lines and infiltrating ductal carcinoma of the breast, and that this phosphatase promotes epithelial to mesenchymal transition in breast cancer cells. However, none of these studies have addressed the *in vivo* role of SHP2 in CSCs or in tumor maintenance and progression, and the signaling cascades and transcriptional factors acting downstream of SHP2 remained ill-defined. We therefore used conditional reverse

genetics, 3D cultures and *in vivo* models complemented by bioinformatic analysis to address these important questions.

PTPN12 has been previously shown to inhibit cell motility, cytokinesis, and apoptosis in several cellular systems. Our collaborators T. Westbrook from The Baylor College of Medicine and S. Elledge from Harvard Medical School identified PTPN12 in a screen for tumor suppressor genes in human mammary epithelial cells. We tested the effects of PTPN12 knockdown and/or overexpression of WT and loss of function mutants in the mammary epithelial cell line MCF10A grown in 3D cultures, and investigated the role of PTPN12 as a tumor suppressor in breast cancer.

5. RESULTS

5.1 Research article submitted to Nature Medicine

The Tyrosine Phosphatase SHP2 Promotes Breast Cancer Progression and Maintains the Cancer Stem Cell Population via Activation of Key Transcription Factors and Repression of the let-7 miRNA

Nicola Aceto¹, Nina Sausgruber¹, Heike Brinkhaus¹, Dimos Gaidatzis¹, Georg Martiny-Baron², Giovanni Mazzarol³, Stefano Confalonieri³, Guang Hu^{4,5}, Piotr Balwierz⁶, Mikhail Pachkov⁶, Stephen J. Elledge⁴, Erik van Nimwegen⁶, Michael B. Stadler¹, and Mohamed Bentires-Alj^{1*}

¹ Friedrich Miescher Institute for Biomedical Research (FMI), Basel, Switzerland

² Novartis Institutes for Biomedical Research, Basel, Switzerland

³ IFOM, Fondazione Istituto FIRC di Oncologia Molecolare and IEO, Istituto Europeo di Oncologia, Milan, Italy

⁴ Howard Hughes Medical Institute and Department of Genetics, Harvard Medical School, Division of Genetics, Brigham and Women's Hospital, Boston, USA

⁵ Current address: Laboratory of Molecular Carcinogenesis, National Institute of Environmental Health and Sciences, Research Triangle Park, USA

⁶ Biozentrum, University of Basel and Swiss Institute of Bioinformatics, Basel, Switzerland

Running title: SHP2 is required for breast tumor progression

Keywords: PTPN11, SHP2, tyrosine phosphatases, breast cancer, tumor-initiating cells

Abbreviations: PTP: protein-tyrosine phosphatase. RTK: receptor tyrosine kinase. CSCs: cancer stem cells. SHP2: Src-homology 2 domain-containing phosphatase

*Contact:

Mohamed Bentires-Alj
Friedrich Miescher Institute for Biomedical Research
Maulbeerstr. 66
4058 Basel, Switzerland
E-mail: bentires@fmi.ch

SUMMARY

Cancer stem cells (CSCs) influence tumor maintenance, progression and relapse in many cancers but the signaling networks controlling these cells remain unknown. We demonstrate a fundamental role for protein-tyrosine phosphatase SHP2 in these processes in HER2-positive and triple-negative breast cancers, two subtypes associated with a poor prognosis. Knockdown of SHP2 eradicated breast CSCs *in vitro* and in xenografts. SHP2 depletion prevented invasion in 3D cultures and progression from *in situ* to invasive breast cancer *in vivo*. Importantly, SHP2 knockdown in established breast tumors blocked growth and reduced metastases. Mechanistically, SHP2 activated stemness-associated transcription factors including c-Myc and ZEB1, which resulted in the repression of let-7 microRNA and the expression of a set of “SHP2 signature” genes found co-activated in a large subset of human primary breast tumors. Taken together, these data show that activation of SHP2 and its downstream effectors is required for self-renewal of breast CSCs and for tumor maintenance and progression, thus providing new insights into signaling cascades that regulate CSCs and a rationale for targeting SHP2 in breast cancer.

INTRODUCTION

Breast cancer is a heterogeneous disease that progresses to metastasis, a fatal hallmark of cancer (Nguyen, Bos et al. 2009); and the cellular and biochemical mechanisms orchestrating breast tumor maintenance and progression remain largely elusive. The characterization of the cellular heterogeneity of the tumor is crucial for the identification of the source of metastases, and elucidation of the oncogenic networks of cancer cells is fundamental to the development of targeted therapies for this presently incurable disease.

Tumors, like normal organs, appear hierarchically organized at the cellular level. Indeed, normal human and mouse mammary glands contain cells in a dynamic state of stemness that are long-lived and self-renewing and that differentiate to all breast cell lineages to form a functional gland (Pece, Tosoni et al. ; Kordon and Smith 1998; Shackleton, Vaillant et al. 2006; Stingl, Eirew et al. 2006; Sleeman, Kendrick et al. 2007; Raouf, Zhao et al. 2008; Visvader 2009; Pece, Tosoni et al. 2010). In the neoplastic breast, recent studies have identified subpopulations of cancer cells in a stem-like state that seed and sustain a tumor, recapitulating the heterogeneity of the original cancer. This subpopulation of “cancer stem cells (CSCs)” or “tumor-initiating cells” (Al-Hajj, Wicha et al. 2003; Dontu, Al-Hajj et al. 2003; Stingl and Caldas 2007; Polyak and Weinberg 2009; Rosen and Jordan 2009; Visvader 2009) also plays an important role in metastasis and in resistance to chemo- and radiation therapies (Dontu, Al-Hajj et al. 2003; Dean, Fojo et al. 2005; Li, Tiede et al. 2007; Li, Lewis et al. 2008; Diehn, Cho et al. 2009). Whilst identification of the Achilles heel of CSCs is of paramount clinical importance in the search for therapeutic targets, signaling networks controlling CSCs stemness remain ill-defined.

In cancer, many signaling networks are subverted at the biochemical level (Vogelstein and Kinzler 2004; Pawson and Kofler 2009). Most signaling pathways are modulated by

reversible protein-tyrosine phosphorylation, which is regulated by protein-tyrosine kinases (PTKs) and protein-tyrosine phosphatases (PTPs) (Hunter 2009). Abnormal tyrosine phosphorylation underlies various diseases of deregulated growth and differentiation, including cancer, and although the roles of several PTKs in breast carcinogenesis have been studied extensively (e.g., ErbB2/HER2), elucidation of the roles of specific PTPs in this disease has only started recently (Hynes and Lane 2005; Ostman, Hellberg et al. 2006; Tonks 2006). The first *bona fide* PTP proto-oncogene was the Src-homology 2 domain-containing phosphatase SHP2 (encoded by *PTPN11*), an ubiquitously expressed PTP that transduces mitogenic, pro-survival, cell fate and/or pro-migratory signals from numerous growth factor-, cytokine- and extracellular matrix receptors. SHP2 is required for full activation of the ERK/MAPK pathway downstream of most receptors; however, its regulation of other pathways (e.g., Jak/STAT and PI3K) is cell- and/or receptor-specific (Shi, Yu et al. 2000; Chan, Kalaitzidis et al. 2008). Interestingly, gain-of-function (GOF) germline mutations of SHP2 cause ~50% of cases of the developmental disorder Noonan syndrome (Tartaglia, Mehler et al. 2001). Moreover, mouse genetics, gene silencing and sequencing studies have demonstrated a broad role for SHP2 in development, cell fate and tumorigenesis (Grossmann, Rosario et al. ; Tartaglia, Mehler et al. 2001; Feng 2007; Chan, Kalaitzidis et al. 2008; Grossmann, Rosario et al. 2010). SHP2 null-embryos die peri-implantation and fail to yield trophoblast stem cell lines (Yang, Klaman et al. 2006). While SHP2 deficiency increases self-renewal of murine and human embryonic stem cells (Burdon, Stracey et al. 1999; Wu, Pang et al. 2009), it decreases self-renewal in neural stem/progenitor cells and hematopoietic stem cells (HSC), suggesting a cell-type specific role of SHP2 in regulating cell fate (Chan, Li et al. 2006; Ke, Zhang et al. 2007). Systemic comparative transcriptomics and gene network analysis have shown that SHP2 acts as a hub maintaining the stability and connectivity of the HSC genetic network (Huang, Hsieh et al. 2008).

In malignancies, SHP2 is hyperactivated either by mutations or downstream of oncoproteins. GOF somatic mutations are found in ~35% of juvenile myelomonocytic leukemias and at various incidences in other myeloid malignancies, but rarely in solid cancers (Tartaglia, Niemeyer et al. 2003; Bentires-Alj, Paez et al. 2004; Chan, Kalaitzidis et al. 2008). SHP2 is also activated downstream of oncogenes in gastric carcinoma, anaplastic large cell lymphoma and glioblastoma (Chan, Kalaitzidis et al. 2008; Zhan, Counelis et al. 2009). Although our previous studies have not found SHP2 mutations in breast cancer, we and others have found that the gene encoding the SHP2-activating protein GAB2 is amplified and overexpressed in 10-15% of human breast tumors (Bocanegra, Bergamaschi et al. ; Bentires-Alj, Paez et al. 2004; Bentires-Alj, Gil et al. 2006; Bocanegra, Bergamaschi et al. 2010). It has been proposed that SHP2 is overexpressed both in breast cancer cell lines and infiltrating ductal carcinoma of the breast, and that this phosphatase promotes epithelial to mesenchymal transition in breast cancer cells (Zhou, Coad et al. 2008; Zhou and Agazie 2008). However, none of these studies have addressed the *in vivo* role of SHP2 in CSCs or in tumor maintenance and progression, and the signaling cascades and transcriptional factors acting downstream of SHP2 remain ill-defined.

In this present study, using conditional reverse genetics, 3D cultures and *in vivo* models complemented by bioinformatics analysis, we have not only uncovered an SHP2-dependent positive feedback signaling loop but have also shown that SHP2 regulates breast CSCs and is required for breast tumor maintenance and progression. This demonstrates that SHP2 is an important target in breast cancer.

RESULTS

SHP2 is necessary for invasion, proliferation and loss of polarity in a 3D culture model of invasive breast cancer

To assess the roles of SHP2 in breast cancer progression, we developed a 3D culture model of invasive breast cancer and used inducible small hairpin RNA^{miRs} (miRs) to deplete SHP2. We established that overexpression of HER2 and HER3 caused immortalized but non-transformed human breast epithelial cells MCF10A to form invasive, unpolarized and hyperproliferative 3D structures with a filled lumen (**Supplementary Fig. 1a,b**). These hallmarks are key events in breast cancer initiation and progression (Bissell, Radisky et al. 2002). Next, we constructed doxycycline (dox)-inducible lentiviral vectors expressing two independent SHP2 miRs (SHP2 miR1/2) (**Fig. 1a** and **Supplementary Fig. 2a**), generated pools of MCF10A-HER2/3 cells expressing the SHP2 miRs and grew them in 3D cultures. SHP2 knockdown blocked HER2/3-evoked invasion by 85% (**Fig. 1b**). To exclude off-target effects, we rescued MCF10A-HER2/3 cell-invasiveness by expressing a non-targetable SHP2 cDNA (Rescue) in cells expressing SHP2 miR2 (**Fig. 1a, b** and **Supplementary Fig. 2a**), thereby confirming that SHP2 depletion blocks invasiveness in MCF10A-HER2/3 cells.

To examine other markers in SHP2-depleted MCF10A-HER2/3 cells, we stained for the proliferation marker Ki67, the apical Golgi marker GM130 and the basal marker laminin-5 (Debnath, Mills et al. 2002) in MCF10A-HER2/3 cells expressing CTRL or SHP2 miRs. SHP2 inhibition prevented the hyperproliferative, unpolarized and filled-lumen phenotypes of MCF10A-HER2/3 in 3D cultures (**Supplementary Fig. 2b**). Thus, SHP2 is required not only for invasiveness but also for hyperproliferation, luminal filling and loss of cell polarity.

SHP2 promotes the transition from *in situ* to invasive carcinoma *in vivo*

Ductal carcinoma *in situ* (DCIS), in which cancer cells remain within the milk duct, is believed to be the precursor of invasive ductal carcinoma (IDC), the most common type of breast cancer (Allred, Wu et al. 2008), yet the signaling networks underlying this transition remain ill-defined. To determine the effect of SHP2 knockdown on the transition from DCIS to IDC, we used the human-in-mouse intraductal transplantation model (Behbod, Kittrell et al. 2009). The onset of DCIS was detected 10 days after intraductal injection of pools of the human breast cancer cell line BT474 expressing GFP and CTRL or SHP2 miR1 (**Fig. 1c,d** and **Supplementary Fig. 2c**), at which point we treated mice with dox for 54 days. Whereas CTRL cells invaded the surrounding stroma, indicating progression from DCIS to IDC (**Fig. 1d-f**), SHP2 miR1 cells did not progress to invasive carcinoma (**Fig. 1d-f**). These results show that SHP2 is fundamental for breast cancer progression from DCIS to IDC and suggest that targeting SHP2 could be useful for blocking breast tumor progression.

SHP2 is essential for tumor maintenance

The roles of SHP2 in breast tumor growth and progression *in vivo* are unknown. To test whether SHP2 is required for tumor maintenance, we used dox-inducible miRs to deplete SHP2 after overt tumor development (**Fig. 2a**). Pools of three HER2-positive (BT474, SKBR3 and MCF10A-NeuNT) and two triple-negative (SUM159 and SUM1315) breast cancer cell lines expressing either CTRL or SHP2 miRs were injected orthotopically into mammary fat pads of immunodeficient mice. In the absence of dox, tumor growth was not affected in SHP2 miR tumors (**Supplementary Fig. 3a**). Dox treatment dramatically blocked the growth of xenografts expressing SHP2 miRs. In contrast, dox administered when tumors

from CTRL or SHP2 miRs cells were palpable did not affect the growth of tumors expressing CTRL miR or SHP2 miR2 rescued with exogenous SHP2 (**Fig. 2b,c**). We quantified this effect in terms of tumor volume, area and weight (**Fig. 2b,c** and **Supplementary Fig. 3b,c**). These results show that SHP2 expression is absolutely required for the growth and maintenance of established HER2-positive and triple-negative tumors, two breast cancer subtypes associated with a poor prognosis.

At the end of the above experiment, we confirmed that SHP2 expression levels remained lower in xenografts of cells expressing SHP2 miRs than in CTRL miR (**Supplementary Fig. 3d**). Immunohistochemical analysis of Ki67 revealed a decrease in proliferation in tumors lacking SHP2 (**Fig. 2d**), while staining for CD31 showed no differences in microvessel density. Thus, in addition to its role in promoting proliferation *ex vivo* (**Supplementary Fig. 2b**), SHP2 also increased proliferation *in vivo*. Altogether, our results show that SHP2 increases cell proliferation and is required for the growth and maintenance of two aggressive breast tumor subtypes.

SHP2 promotes metastases

Given our observations that SHP2 increases invasion *ex vivo* and *in vivo* and that this phosphatase is required for tumor maintenance *in vivo*, we asked whether SHP2 knockdown in breast tumors also reduces their metastatic capacity. To mimic the neoadjuvant setting when patients are treated prior to tumor removal, mice bearing BT474 CTRL or SHP2 miR1 xenografts were dox-treated for 30 days, tumors were removed and the mice were monitored for a further 16 weeks without dox before lung metastases were quantified (**Fig. 2e**). H&E and HER2 staining of the lungs showed that SHP2 knockdown reduced the metastatic

capacity of BT474 tumors. Remarkably, the mean number of metastases per mouse was ~4 times less in the absence of SHP2 than in CTRL (**Fig. 2f**). These observations demonstrate that knockdown of SHP2 in the primary tumor decreased lung metastases.

SHP2 is required for the maintenance and tumor-seeding ability of CSCs

The role of SHP2 in the maintenance of breast CSCs is unknown. We addressed this question using different assays, initially with the tumorsphere-formation assay in which CSCs form floating spherical colonies when grown in non-adherent conditions (Dontu, Abdallah et al. 2003; Ponti, Costa et al. 2005). We measured the tumorsphere-formation efficiency of HER2-positive and triple-negative breast cancer cell lines in the presence or absence of SHP2 (**Fig. 3a top panels**). To assess whether SHP2 controls self-renewal of CSCs, the primary tumorspheres were dissociated into single cells and reseeded. Interestingly, the ratio of the number of secondary and primary tumorspheres was lower upon SHP2 knockdown than in the control, showing that SHP2 depletion decreases self-renewal capacity of CSCs in the tested models (**Fig. 3a bottom panels**). This suggests that SHP2 knockdown reduces self-renewal of breast CSCs of both HER2-positive and triple-negative tumors.

Second, we examined CSCs distribution in the presence or absence of SHP2 by analyzing the expression of the cell-surface markers CD44 and CD24, as the CD44^{high}/CD24^{low} cell population has been shown to be enriched in breast CSCs (Al-Hajj, Wicha et al. 2003). HER2/HER3 co-overexpression in MCF10A cells increased the number of CD44^{high}/CD24^{low} cells *in vitro*. Interestingly, knockdown of SHP2 depleted the population of CSCs in MCF10A-HER2/3 cells (**Fig. 2b,c** and **Supplementary Fig. 4a,b**). We also

observed a decrease in the number of CD44^{high}/CD24^{low} cells when we depleted SHP2 in the triple-negative breast cancer cells SUM159 (**Supplementary Fig. 4c,d**).

Third, to assess directly the effects of SHP2 on the tumor-seeding capacity of breast CSCs *in vivo*, we assayed the ability of human cancer cells to seed tumors or to grow as tumorspheres following SHP2 knockdown in xenografts. We isolated single cells from tumors with or without SHP2 and either transplanted them in mice at serial dilutions or grew them as tumorspheres in the absence of dox (**Fig. 3d**). Notably, we found that whereas CTRL cells efficiently seeded new tumors, deletion of SHP2 *in vivo* strongly impaired both tumorsphere formation and tumor seeding capacity (**Fig. 3e,f** and **Supplementary Fig. 4e**). The fact that neither mice transplanted with cells, nor the cells grown as tumorspheres were treated with dox, indicated that depletion of CSCs upon knockdown of SHP2 happened *in vivo* during dox treatment of the primary tumors. These data indicate a strong requirement for SHP2 in the maintenance of breast CSCs *in vitro* and *in vivo*.

SHP2 effects on stemness and tumor progression are dependent on activation of the ERK pathway

We next sought to define the biochemical pathways whose activity in breast cancer *in vivo* requires SHP2. Screening for changes in phosphorylation upon SHP2 knockdown in tumors using a reverse-phase protein array (RPA) revealed a decrease in phosphorylation of several signaling molecules (**Fig. 4a** and **Supplementary Fig. 5a**). Immunoblotting of tumor lysates confirmed the decrease in phosphorylation of ERK5, ERK1/2, AKT, PLC γ , EGFR and HER2 (**Supplementary Fig. 5b**). To distinguish tumor-specific changes in phospho-proteins from changes in the mouse stroma, we also analyzed protein phosphorylation in lysates from

BT474 tumorspheres. SHP2 deletion dramatically reduced the phosphorylation of ERK5 and to a lesser extent of ERK1/2, PLC γ , AKT, EGFR and HER2 (**Fig. 4b**). Consistently, we also observed reduced phosphorylation of ERK5 and ERK1/2 in MCF10A-HER2/3 tumorspheres upon knockdown of SHP2 (**Supplementary Fig. 5c**).

We then used two independent shRNAs to knockdown ERK5 (ERK5 sh1 and sh2) and measured the tumorsphere-formation efficiency of BT474 and MCF10A-HER2/3 cells in the presence (CTRL vector) or absence of ERK5. Knockdown of ERK5 reduced tumorsphere formation (~30% fewer primary and secondary tumorspheres in ERK5 shRNA cells than in CTRL cells) but did not affect self-renewal (**Fig. 4c** and **Supplementary Fig. 5d**). These results show that ERK5 depletion is not sufficient to phenocopy the effect of SHP2 loss on CSCs. Interestingly, upon ERK5 knockdown, BT474 and MCF10A-HER2/3 tumorspheres expressed higher levels of active ERK1/2, suggesting that phosphorylation of ERK1/2 may compensate for ERK5 loss (**Fig. 4d** and **Supplementary Fig. 5d**). We next combined ERK5 depletion with pharmacological inhibition of ERK1/2 using PD184352. Consistent with previous observations (Mody, Leitch et al. 2001), we found that PD184352 specifically inhibited ERK1/2 activation at 1 μ M and both ERK1/2 and ERK5 activation at 10 μ M (**Supplementary Fig. 5e**). Knockdown of ERK5 and treatment of BT474 and MCF10A-HER2/3 tumorspheres with PD184352 at 1 μ M, or treatment with 10 μ M PD184352 that abrogates activation of both ERK5 and ERK1/2, reduced tumorsphere-formation efficiency and self-renewal similar to SHP2 knockdown (**Fig. 4e** and **Supplementary Fig. 5e,f**). To assess whether inhibition of both ERK1/2 and ERK5 is required for mimicking the effect of SHP2 knockdown on CSCs, we treated BT474 and MCF10A-HER2/3 tumorspheres with PD184352 at 1 μ M, which inhibits ERK1/2 but not ERK5, and found this to dramatically reduce tumorsphere formation and self-renewal, recapitulating the effect of SHP2 knockdown

(**Fig. 4e** and **Supplementary Fig. 5e,f**). These results suggest that SHP2 action on CSCs is predominantly dependent on ERK1/2 activation.

To further investigate the effects of SHP2-evoked activation of ERK5 and ERK1/2 on the number of CSC, we examined CSC distribution in MCF10A-HER2/3 cells lacking ERK5 and/or treated with PD184352 by measuring the proportion of CD44^{high}/CD24^{low} cells. ERK5 depletion decreased the CD44^{high}/CD24^{low} cell population by ~35%. Similar to the results of the tumorsphere assay, simultaneous inhibition of ERK5 and ERK1/2, or ERK1/2 inhibition alone, led to complete depletion of the CD44^{high}/CD24^{low} population (**Fig. 4f** and **Supplementary Fig. 5g**), exactly as we observed upon SHP2 knockdown (**Fig. 3b,c**). These results show that although ERK5 is hyperactivated in the presence of SHP2, it contributes only partially to the role of SHP2 in CSCs, and that SHP2 increases CSCs self-renewal predominantly by activating ERK1/2.

We then investigated whether inactivation of ERK1/2 and/or ERK5 affects the invasiveness of MCF10A-HER2/3 cells grown in 3D cultures. ERK5 knockdown in MCF10A-HER2/3 cells decreased invasion by ~20%. Notably, the inhibition of ERK1/2 alone or in combination with ERK5 inactivation completely blocked HER2/3-evoked invasion (**Fig. 4g**).

Altogether, our data show that the requirement for SHP2 in self-renewal of breast CSCs and tumor progression is predominantly due to SHP2-evoked activation of ERK1/2.

SHP2 increases the activity of stemness-associated transcription factors that repress let-7 miRNA and increase stemness and invasion of breast tumors

The effect of SHP2 on gene expression in cancer has not been examined. To address this, we analyzed the gene expression profiles of BT474 CTRL and SHP2 miRs tumors after 30 days of dox and identified 180 downregulated genes, referred to as the “SHP2 signature” (**Fig. 5a** and **Supplementary Table 1**). Gene ontology analysis of the signature revealed enrichment in development-associated genes, mainly of the HOX family (**Supplementary Fig. 6a,b**). To identify the transcription factors whose activity is responsible for the observed changes, we used a computational method (Suzuki, Forrest et al. 2009) to model global gene expression patterns in terms of genome-wide predictions of transcription factor binding sites. This analysis identified 10 transcription regulators that are inferred to cause significant downregulation of their targets upon SHP2 inactivation (**Fig. 5b**). Among these transcription factors is ZEB1, a zinc finger E-box-binding homeobox 1 that was shown to induce EMT (Wellner, Schubert et al. 2009). Consistently, ZEB1 was downregulated in microarrays of BT474 tumors lacking SHP2 (**Supplementary Table 1**). Analysis of RNA from BT474 and SUM159 tumors by real-time PCR confirmed that ZEB1 expression was repressed upon SHP2 knockdown (**Fig. 5c**). The repression of ZEB1 was accompanied by downregulation of the EMT markers Fibronectin1, Vimentin and N-cadherin (**Supplementary Fig. 7**), indicating a role for SHP2 in EMT *in vivo*. To assess the functional role of ZEB1 downstream of SHP2, we generated pools of MCF10A-HER2/3 cells expressing inducible ZEB1 miR (**Supplementary Fig. 8a**). Knockdown of ZEB1 dramatically reduced invasion in MCF10A-HER2/3 cells grown in 3D cultures (**Fig. 5d**). Moreover, ZEB1 depletion reduced the self-renewal of MCF10A-HER2/3 cells (**Fig. 5e**), although not to the same extent as depletion of SHP2 (**Fig. 3a**). These data indicate that ZEB1 acts downstream of SHP2 in promoting invasion and stemness and suggest that additional mediators are required for the effect of SHP2 on self-renewal capacity of CSCs.

To address this question, we analyzed transcriptome changes upon SHP2 knockdown *in vivo* with the Ingenuity resource. This analysis revealed that SHP2 knockdown strongly affected genes belonging to the c-Myc network (**Supplementary Fig. 8b**), confirming that c-Myc transcriptional activity is reduced upon SHP2 knockdown *in vivo* (**Fig. 5b**). Moreover, the expression of the known c-Myc target LIN28B (Chang, Zeitels et al. 2009), a suppressor of miRNA biogenesis, was decreased in microarrays from tumors lacking SHP2 (**Supplementary Table 1**). These observations prompted us to dissect the role of c-Myc and LIN28B downstream of SHP2 in CSCs. First, we quantified the expression of LIN28B by real-time PCR in BT474 and SUM159 tumors, and confirmed that it was transcriptionally repressed upon SHP2 knockdown in both models (**Fig. 5f**). LIN28B has been shown previously to suppress the biogenesis of the let-7 miRNA (Viswanathan, Daley et al. 2008; Chang, Zeitels et al. 2009; Iliopoulos, Hirsch et al. 2009). Consistently, we observed that 20 genes among the “SHP2 signature” genes were predicted let-7 targets (**Supplementary Table 2**), the majority of which are tightly associated with the c-Myc pathway (**Supplementary Fig. 8c**). To avoid cross-detection of stromal mouse let-7 miRNA present in the tumors, we analyzed its expression in MCF10A-HER2/3 cells grown in 3D cultures in the presence or absence of SHP2. Remarkably, we found increased biogenesis of mature let-7a and let-7b in the absence of SHP2 in these cells (**Fig. 5g**). Consistently, whole gene expression analysis of MCF10A-HER2/3 cells grown in 3D cultures or xenografts of BT474 cells showed a stronger decrease in the expression of RNAs encoding predicted let-7 target genes than other genes in the absence of SHP2 (**Fig. 5h**). We further confirmed the downregulation, at the protein level, of the let-7 targets RAS and c-Myc in tumors lacking SHP2 (**Fig. 5i**).

Next, we assessed whether the expression levels of ZEB1 and LIN28B are dependent on activation of ERK1/2. Treatment with PD184352 showed that ERK1/2 inhibition reduced

the expression of ZEB1 and LIN28B in both SUM159 and MCF10A-HER2/3 cells (**Fig. 5j** and **Supplementary Fig. 8d**). These data suggest that the effects of SHP2 on ZEB1 and LIN28B expression are mediated by ERK1/2.

Our findings suggest that SHP2 activation of ERK1/2 increases the expression of c-Myc and LIN28B in breast cancer. To test this model directly, we asked whether restoring the expression of c-Myc or LIN28B rescues the effects of SHP2 knockdown. Notably, expression of c-Myc restored expression of LIN28B in MCF10A-HER2/3 cells lacking SHP2 (**Supplementary Fig. 8e**). Consistently, expression of either c-Myc or LIN28B restored invasion and self-renewal of CSCs in MCF10A-HER2/3 cells lacking SHP2 (**Fig. 5k,l**).

In summary, we show that SHP2 is required for stemness and invasion of breast tumors. Our data demonstrate that SHP2 promotes ERKs activation, causing upregulation of ZEB1 and c-Myc-dependent expression of LIN28B, which leads to repression of let-7 miRNA and overexpression of let-7 target genes including RAS (**Fig. 5m**). These data identify a key feed forward signaling loop required for the maintenance of breast CSCs and invasiveness of breast tumors.

SHP2 is expressed and active in a large subset of primary breast tumors

SHP2 has been previously found expressed in a large number of breast tumors (Zhou, Coad et al. 2008), although its expression in normal tissue and its activity in breast cancer patients are still unclear. We first examined the expression of SHP2 in normal breast, primary tumors and in breast cancer cell lines. We found high levels of SHP2 expression in ~88% of breast tumors, but no consistent changes in SHP2 expression between normal and neoplastic tissue (**Fig. 6a,b** and **Supplementary Fig. 9a,b**). Moreover, SHP2 expression levels did not

significantly correlate with any tumor histotype or clinicopathological parameter (**Supplementary Table 3**). These results suggest that SHP2 activation by oncogenes rather than SHP2 overexpression determines its roles in breast tumorigenesis.

We then used the “SHP2 signature” genes as a readout for SHP2 activation. To assess whether expression of the “SHP2 signature” could be used to stratify patients with breast cancer, we asked whether the genes from this signature are co-overexpressed in human breast tumors. In four independent publicly available datasets, we found that the “SHP2 signature” genes are co-regulated and cluster the patients into two groups: one with downregulation (group 1) and the other with overexpression (group 2) of the “SHP2 signature” genes. Notably, the clear split into “SHP2 signature” low- and high-expression groups was hardly ever observed in 10,000 randomly-selected gene groups of the same size (**Fig. 6c** and **Supplementary Fig 10**).

We next grouped the data from the four datasets and found that ~55% of all primary breast cancers overexpress the “SHP2 signature” genes (**Fig. 6d**). Strikingly, analysis of two of these datasets for which the molecular subtypes were reported showed that the “SHP2 signature” was high more frequently in triple-negative breast cancers (**Fig. 6e**), a subtype characterized by poor outcome and lack of efficient therapy and thought to be enriched in CSCs (Stingl and Caldas 2007; Nakshatri, Srour et al. 2009).

Taken together, our findings indicate that the “SHP2 signature” genes are overexpressed in ~55% of human primary breast tumors, particularly those of the triple-negative subtype. Importantly, these data suggest that, of all breast cancer subtypes, SHP2 inhibition might be very effective in patients bearing tumors with high “SHP2 signature” genes and might prove particularly effective in triple-negative breast cancer, a currently incurable disease.

DISCUSSION

Recent studies have demonstrated the importance of CSCs in breast cancer (Al-Hajj, Wicha et al. 2003; Dontu, Al-Hajj et al. 2003; Li, Tiede et al. 2007; Stingl and Caldas 2007; Li, Lewis et al. 2008). The signaling networks that govern CSCs remain ill-defined, however, and their delineation should pave the way for development of targeted, potentially curative cancer therapies. In this study, we provide new insights into the multiple roles of SHP2 in cancer. We found that SHP2 increases self-renewal of breast CSCs and is required for breast tumor maintenance and progression, demonstrating that SHP2 is a high quality target in human breast cancer.

Evidence that SHP2 increases self-renewal of breast CSCs is shown by several *in vitro* and *in vivo* models. Knockdown of SHP2 *in vitro* reduced the proportion of the CD44^{high}/CD24^{low} population and decreased tumorsphere-forming efficiency. In several different *in vivo* models, SHP2 knockdown inhibited tumor growth, reduced tumorsphere-forming efficiency of the cancer cells and dramatically decreased their capacity to seed new tumors when transplanted back at limiting dilutions in mice. Evidence for SHP2 requirement for breast tumor maintenance and progression comes from our *in vivo* and 3D culture experiments. First, SHP2 knockdown blocked the growth of established breast tumors and decreased the number of lung metastases. SHP2 depletion in invasive 3D cultures also reduced proliferation and prevented loss of polarity, two critical steps in the oncogenic process (Bissell, Radisky et al. 2002; Zhan, Rosenberg et al. 2008), further supporting a role for SHP2 in tumor maintenance and progression. Third, knockdown of SHP2 prevented invasion in 3D cultures and blocked the transition from DCIS to IDC in a human-in-mouse intraductal transplantation model, supporting a role of SHP2 in tumor progression.

It was reported recently that induction of an invasive phenotype in normal or neoplastic mammary epithelial cell populations increases the number of cells with CSC-like properties, suggesting a functional overlap between the invasion phenotype and the state of stemness (Mani, Guo et al. 2008). In line with this concept, CSCs are thought to be responsible for metastases (Li, Tiede et al. 2007). Our observations that SHP2 regulates CSCs and EMT, mediates the progression from DCIS to IDC and promotes metastatic spread suggest that SHP2 acts as a molecular hub for these fundamental phenomena.

Mechanistically, we found that the effects of SHP2 on self-renewal of CSC and invasion of breast cancer cells require ERK pathway activation. Further, we show that SHP2 activation of ERK1/2 induces expression of the transcription factors ZEB1 and c-Myc, the latter mediating increase in LIN28B expression. Notably, the EMT-activator ZEB1 has been previously suggested to increase stemness in pancreatic and colorectal cancers (Wellner, Schubert et al. 2009). Moreover, LIN28B, an RNA-binding protein and a marker of undifferentiated human embryonic stem cells (Richards, Tan et al. 2004), promoted c-Myc-mediated proliferation and invasion in several cancer models (Chang, Zeitels et al. 2009; Wang, Chen et al. 2011). In our studies, c-Myc-induced LIN28B expression repressed let-7 miRNA leading to overexpression of let-7 targets, including RAS and other regulators of stemness (Johnson, Grosshans et al. 2005; Iliopoulos, Hirsch et al. 2009). These findings uncover a novel mechanism of ERK regulation by SHP2 and identify an SHP2-dependent positive feedback loop required for the maintenance of CSC and for the invasiveness of breast cancer cells.

Importantly, our work has led to the discovery of an “SHP2 signature”, a set of genes that we found to be co-overexpressed in ~55% of human primary breast tumors. This signature reflects the existence of an SHP2-driven gene network, mainly controlled by c-Myc

and ZEB1 activity, and capable of maintaining stemness and invasiveness of breast tumors. Notably, the SHP2 signature genes are co-overexpressed in ~55% of all breast tumors and more frequently in triple-negative breast cancers, an aggressive subtype that lacks efficient therapies and is thought to be enriched in CSCs (Stingl and Caldas 2007; Nakshatri, Srour et al. 2009). These results suggest that inhibiting SHP2 might be particularly effective in human triple-negative breast cancer, specially the ones recently found to be dependent on active RTKs (Sun, Aceto et al. 2011), that require SHP2 for full activation of ERK (Chan, Kalaitzidis et al. 2008).

As SHP2 has been shown to act downstream of most growth factor and cytokine receptors, targeting SHP2 might be therapeutic in other cancers in which SHP2 is hyperactivated, e.g., downstream of the cytotoxin-associated antigen A (CagA) encoded by virulent *H. pylori* strains in gastric carcinoma, of the fusion protein NPM-ALK in anaplastic large cell lymphoma, and of EGFRvIII in glioma (Chan, Kalaitzidis et al. 2008). Our findings warrant experiments to address whether SHP2 also regulates CSCs, tumor maintenance and progression in these malignancies.

In summary, we have shown that knockdown of SHP2 depletes the breast CSC-population and inhibits breast cancer maintenance and progression. These findings reveal a fundamental SHP2-dependent positive feedback loop regulating CSCs and reinforce the need for developing selective inhibitors of SHP2 for treating aggressive malignancies.

ACKNOWLEDGEMENTS

We thank N. Hynes (FMI) and G. Christofori (University of Basel) for helpful comments on the manuscript, W. Filipowicz, J. Krol and H. Grosshans (FMI) for helpful discussions, W. Xian (in the lab of J. Brugge, Harvard Medical School), D. Medina (Baylor College of Medicine) for help with the intraductal protocol, T. Westbrook (Baylor College of Medicine) for providing the dox-inducible lentiviral vector, and Alice Terrier (Novartis Institutes for Biomedical Research) and Micaela Quarto (IFOM, Fondazione Istituto FIRC di Oncologia Molecolare) for excellent technical assistance, further members of the Bentires-Alj lab for advice and discussions and various colleagues for reagents. We also thank IGC and expO (<https://expo.intgen.org/geo/home.do>) for offering free access to clinically annotated tumor data. Research in the lab of M.B-A. is supported by the Novartis Research Foundation, the European Research Council (ERC starting grant 243211-PTPsBDC), the Swiss Cancer League and the Krebsliga Beider Basel.

AUTHOR CONTRIBUTIONS

N.A. and M.B-A. designed and performed most experiments and composed the main body of the manuscript. N.S. and H.B. performed real-time PCR and lung metastases experiments. D.G. and M.B.S. performed bioinformatic analyses. G.M-B. performed the RPA. G.M. and S.C. performed the TMA analysis and examined histological sections from xenografts. P.B., M.P. and E.v.N. performed the MARA analysis. G.U. and S.J.E. generated the dox-inducible lentiviral vector. All the authors participated in the preparation of the manuscript.

FIGURE LEGENDS

Fig. 1. SHP2 promotes invasion, proliferation and loss of polarity in 3D cultures and *in vivo*. (a) Dox treatment of MCF10A-HER2/3 cells deleted SHP2 in cells expressing SHP2 miR1 and 2 (90.5% and 91.1%, respectively), but not in cells expressing firefly (CTRL) miR or in cells expressing SHP2 cDNA (Rescue) or SHP2 miR2, which targets the 3' UTR. Immunoblot showing expression of SHP2, HER2, HER3 and ERK2 (loading control) in the presence (+) or absence (-) of dox. (b) SHP2 knockdown decreased the percentage of HER2/3-evoked invasive structures (9% versus 94% in CTRL). Representative phase contrast images of MCF10A-HER2/3 cells grown in 3D culture for 20 days and expressing the indicated miRs. The bar graph shows the percentage of invasive structures. Results represent means \pm SEM from five independent experiments; $**P < 0.0001$. (c) Schematic of DCIS onset following injection of cells into the primary mouse mammary duct of immunodeficient mice. BT474-GFP cells formed DCIS-like lesions 10 days (DCIS Onset) after intraductal injection. The miR was activated by treating the mice with dox at the onset of DCIS. (d,e) Representative images of whole-mount (d), H&E-stained, GFP-stained and Keratin18-stained (e) mammary glands at DCIS onset (*top*) and after 54 days of treatment with dox (*bottom*) ($n=6$). DAPI (*blue*) stained the nuclei. IDC is seen in the presence (*bottom left*) but not in the absence of SHP2 (*bottom right*). (f) Bar graph showing the mean percentage of mammary glands with IDC \pm SEM ($n=6$, $*P < 0.05$).

Fig. 2. SHP2 is required for tumor maintenance, growth and progression to lung metastases. (a) Schematic of the experiment. Cells were injected orthotopically and the mice after tumors became palpable were treated continuously with dox to express the miRs. (b, c) Tumor growth curves of HER2-positive (b) and triple-negative (c) breast cancer cell lines in the presence or absence of SHP2 showing the mean tumor volume (mm^3) \pm SEM (BT474

$n=15$, SKBR3 $n=10$, MCF10A-NeuNT $n=8$, SUM159 $n=10$, SUM1315 $n=9$; $*P<0.0005$, $**P<0.0001$). (d) SHP2 knockdown reduced proliferation. Representative images of H&E-, Ki67- and CD31-stained sections of BT474 tumors expressing CTRL or SHP2 miR1 dissected after 30 days of treatment with dox. Note the decrease in number of mitoses (from $21/\text{mm}^2$ to $12/\text{mm}^2$) without any sign of necrosis and the increased presence of mature collagen (*arrows*) upon knockdown of SHP2. Immunostaining for Ki67 showed a twofold decrease in proliferation in the absence of SHP2. Immunostaining for CD31 revealed no differences in microvessel density in the presence or absence of SHP2. The bar graphs show the percentage of Ki67- or CD31-positive cells \pm SEM ($n=8$, $**P<0.00002$) (*right*). (e) Schematic of the lung metastases study. Mice were injected with 10^6 BT474 cells expressing CTRL or SHP2 miR1 and treated with dox for 30 days after the tumors became palpable. The primary tumors were then dissected and the mice kept alive without dox for a further 16 weeks, after which the lungs were analyzed for the presence of metastases. (f) SHP2 knockdown after overt tumor development reduced the metastatic capacity of BT474 tumors. Representative H&E- and HER2-stained histological sections of lungs from mice bearing BT474-CTRL or BT474-SHP2 miR1 tumors as indicated. HER2 staining identifies BT474 foci specifically. Metastases were found in 3 out of 4 animals in the control group and in 4 out of 8 animals bearing tumors lacking SHP2. The bar graph shows the mean number of metastases per animal \pm SEM ($n=3$ in the CTRL group and $n=4$ in the SHP2 miR1 group; $*P<0.04$).

Fig. 3. SHP2 maintains the cancer stem cell population *in vitro* and *in vivo*. (a) Self-renewal was reduced in the absence of SHP2. Mean tumorsphere formation and self-renewal capacities. Results represent means \pm SEM from four independent experiments; $*P<0.003$, $**P<0.0008$. (b) Representative flow cytometry dot plots showing that HER2/HER3 increased the CD44^{high}/CD24^{low} subpopulation (*green rectangle*) in MCF10A cells (*left*

panels). Knockdown of SHP2 decreased the CD44^{high}/CD24^{low} subpopulation. Dot plots of CD44/CD24 expression in MCF10A-HER2/3 cells expressing CTRL or SHP2 miR and treated with dox for 7 days (*right panels*). Only RFP^{high} cells corresponding to high miR expression were counted (Supplementary Fig. 4a). (c) Mean percentage of CD44^{high}/CD24^{low} cells in MCF10A cells. Results represent means \pm SEM from four independent experiments; ** $P=0.0001$. (d) Schematic of the approach used to assess the requirement for SHP2 of CSCs *in vivo*. Mice bearing tumors expressing CTRL or SHP2 miR were treated with dox *in vivo*. Single cells were then generated from the tumors and were either transplanted as serial dilutions or seeded for the tumorspheres assay without dox. (e) SHP2 knockdown in xenografts reduced the tumorsphere-forming capacity of BT474 cells. Representative images of tumorspheres are shown. The bar graph shows the mean number of tumorspheres/ 10^4 cells \pm SEM from four independent experiments; ** $P<0.00001$. (f) Limiting dilution transplantations show that SHP2 knockdown in xenografts reduced the tumor-formation ability of BT474, SUM159 and SUM1315 cells. The transplanted mice were kept without dox for 8 weeks, after which the number of mice with tumors was counted; $P=2.1\times 10^{-9}$ for BT474, $P=3.3\times 10^{-6}$ for SUM159 and $P=0.0015$ for SUM1315 calculated by Poisson test.

Fig. 4. SHP2 promotion of breast CSCs self-renewal and tumor progression is dependent on the ERK pathway. (a) RPA analysis of BT474 tumors treated with dox for 30 days. Array spot images of three dilutions of lysates from tumors. (b) Immunoblot of lysates from BT474 primary tumorspheres in the presence or absence of SHP2. The bar graph shows the percentage of normalized protein \pm SEM ($n=3$). (c) ERK5 knockdown partially reduces the tumorsphere-forming capacity but does not affect self-renewal of BT474 cells. Bar graphs showing self-renewal capacities and the mean number of BT474 tumorspheres/ 10^4 cells \pm SEM ($n=3$); ** $P<0.004$. (d) Immunoblot of lysates from BT474 primary tumorspheres in the presence or absence of ERK5 ($n=3$). (e) Inhibition of ERK1/2 activity alone ($1\ \mu\text{M}$

PD184352) or in combination with ERK5 inactivation (1 μ M PD184352 and ERK5 shRNA, or 10 μ M PD184352 alone) decreases BT474 tumorsphere-formation efficiency and self-renewal. The bar graph shows self-renewal capacities and the mean number of BT474 tumorspheres/ 10^4 cells \pm SEM ($n=3$); $*P<0.001$, $**P<0.0008$. (f) Mean percentage of the CD44^{high}/CD24^{low} population in MCF10A-HER2/3 cells in the presence or absence of ERK5 and/or treated with PD184352 for 7 days. Results represent means \pm SEM ($n=3$); $*P<0.005$, $**P<5\times 10^{-7}$. (g) The bar graph shows the percentage of invasive structures of MCF10A-HER2/3 cells grown in 3D culture for 15 days in the presence or absence of ERK5 and/or treated with PD184352. Results represent means \pm SEM ($n=4$); $*P<0.05$, $**P<0.003$.

Fig. 5. SHP2 increases the activity of key transcription factors and represses let-7 microRNA, enhancing invasion and self-renewal of CSCs. (a) Plot of the gene expression contrast in BT474 SHP2 miR1-CTRL miR tumors versus SHP2 miR2-CTRL miR tumors. The green line circles genes of the SHP2 signature. (b) Table showing the MARA mean activity scores (\pm SD) of 10 transcription factors whose activity was reduced upon SHP2 knockdown. “ P down” values show for each factor the probability of a decreased activity in SHP2 miRs compared with CTRL miR samples. (c) Quantitative Real-Time PCR of ZEB1. Bar graph showing the percentage of ZEB1 expression in BT474 and SUM159 tumors in the presence or absence of SHP2. Results represent means \pm SEM ($n=3$); $*P<0.029$, $**P<0.018$. (d) Bar graph showing the mean percentage of invasive structures of MCF10A-HER2/3 grown in 3D cultures for 15 days in the presence or absence of ZEB1 \pm SEM ($n=3$); $**P<0.01$. (e) Bar graphs showing the self-renewal capacities and the mean number of MCF10A-HER2/3 tumorspheres/ 10^4 cells in the presence or absence of ZEB1 \pm SEM ($n=3$); $*P<0.05$. (f) Quantitative Real-Time PCR of LIN28B. Bar graph showing the percentage of LIN28B expression in BT474 and SUM159 tumors in the presence or absence of SHP2. Results represent means \pm SEM ($n=3$); $*P<0.03$, $**P<0.02$. (g) Quantitative Real-Time PCR

on mature let-7a and let-7b miRNAs. The bar graph shows the mean percentage of let-7a and let-7b expression in MCF10A-HER2/3 cells grown in 3D cultures for 15 days in the presence or absence of SHP2 \pm SEM ($n=3$); $*P<0.04$. **(h)** Downregulation of let-7 target genes in the absence of SHP2. Curves showing the relative frequency (density) of genes that are not targeted by let-7 (non-target), genes that are predicted let-7 targets (let-7 targets), and genes that are the 100 most likely let-7 targets (top 100 let-7 targets) according to TargetScan 5.1 resource (www.targetscan.org) upon SHP2 knockdown in MCF10A-HER2/3 cells grown in 3D cultures (3D cultures) or in BT474 tumors (*in vivo*). P values are shown in the plot area. **(i)** Immunoblot showing the expression of SHP2, P-ERK, ERK and the let-7 targets c-Myc and RAS in lysates from BT474 tumors treated with dox for 30 days. **(j)** Quantitative Real-Time PCR of ZEB1 and LIN28B. Bar graph showing the mean percentage of ZEB1 and LIN28B expression in SUM159 cells upon treatment with 1 μ M PD184352 for 7 days \pm SEM ($n=3$); $*P<0.016$. **(k)** Bar graph showing the percentage of invasive structures of MCF10A-HER2/3 cells grown in 3D cultures for 15 days in the presence or absence of SHP2 and expressing a c-Myc or LIN28B rescue. Results represent means \pm SEM ($n=3$); $**P<2.9\times 10^{-5}$. **(l)** Bar graph showing the self-renewal capacities of MCF10A-HER2/3 cells in the presence or absence of SHP2 and expressing a c-Myc or LIN28B rescue. Results represent means \pm SEM ($n=3$); $**P<0.0015$. **(m)** Model of the mechanism of action of SHP2 in CSCs: SHP2 activates the ERK pathway, which in turn promotes ZEB1 transcription and c-Myc-dependent LIN28B expression. The expression of LIN28B blocks the processing of let-7, maintaining high levels of let-7 target genes including RAS and c-Myc.

Fig. 6. SHP2 is expressed and active in a large subset of breast cancer patients. **(a)** Representative images of human primary normal breast and breast tumors scoring from 0 to 3 depending on the abundance of SHP2 expression. **(b)** Quantification of SHP2 expression in human normal and neoplastic breast. **(c)** Expression heatmap for SHP2 signature genes in

human primary breast tumors. Mean expression of each gene is indicated in gray, and expression level Z-scores are mapped to colors from red ($z=-5.0$, below mean) to blue ($z=5.0$, above mean). Genes (rows) and patients (columns) are clustered by expression (see Methods), resulting in the patient groups 1 and 2. Expression polarization between the groups of patients is shown as a red line for the SHP2 signature against 10,000 randomly-selected gene signatures of the same size (*bottom*); $P=0.0001$ for the Bos, Wang and Bittner datasets, $P=0.0002$ for the Stockholm dataset. **(d)** Bar graph showing the percentage of all patients (including the Bos, Wang, Bittner and Stockholm datasets) belonging to group 1 (low SHP2 signature genes, i.e. inactive SHP2) or group 2 (high SHP2 signature genes, i.e. active SHP2). **(e)** Bar graph showing the percentage of group 1 and group 2 patients in each breast cancer molecular subtype. Genes of the SHP2 signature are upregulated in all the molecular subtypes, but more frequently in the triple-negative tumors; $P=6.24 \times 10^{-7}$ for the Bittner and $P=2.02 \times 10^{-12}$ for the Stockholm dataset.

METHODS

3D cultures. MCF10A cells were grown and stained as previously described (Bentires-Alj, Gil et al. 2006). For experiments with inducible miRs, 500 ng/ml of dox and 10 ng/ml of heregulin (Sigma) were added to the medium 2 days after seeding the cells and refreshed every 2 days.

Chemicals and vectors. For the inducible RNAi studies, 97-mer shRNAmiR (miR) were obtained from Sigma, PCR-amplified, sequence-confirmed and cloned into the dox-inducible lentiviral vector pINDUCER (Meerbrey, Hu et al. 2011). We used 2 miRs targeting SHP2,

SHP2 miR1 (5'-TGCTGTTGACAGTGAGCGCGGGCACGAATATACAAATATTTAGTGAAGCCACAGATGTAAATATTTGTATATTCGTGCCCTGCCTACTGCCTCGGA-3')

and SHP2 miR2 (5'-TGCTGTTGACAGTGAGCGACCACGTATATTATGTAGTCTATAGTGAAGCCACAGATGTATAGACTACATAATATACGTGGGTGCCTACTGCCTCGGA-3')

and miR targeting ZEB1 (5'TGCTGTTGACAGTGAGCGAGCGCAATAACGTTACAAATTATAGTGAAGCCACAGATGTATAATTTGTAACGTTATTGCGCCTGCCTACTGCCTCGGA-3').

As a control, we used an miR targeting firefly luciferase (CTRL miR). Constitutive ERK5 shRNAs were obtained from Sigma. Rescue experiments were performed with pMSCV-neo-SHP2-WT, pBabe-puro-LIN28B (Addgene) and pSD-94-c-Myc (Duss, Andre et al. 2007). PD184352 (CI-1040) was purchased from Biovision and the cells were treated with fresh inhibitor every 2 days.

Animal experiments. Experiments with SCID-beige mice (Jackson Labs) were carried out according to FMI guidelines. For the intraductal transplantation, 50,000 BT474 cells were

injected as previously described (Behbod, Kittrell et al. 2009). For the other studies, 10^6 BT474, 5×10^6 SKBR3, 10^6 MCF10A-NeuNT, 10^6 SUM159 or 10^6 SUM1315 cells were suspended in a 100- μ l mixture of Basement Membrane Matrix Phenol Red-free (BD Biosciences) and PBS 1:1 and injected orthotopically. For BT474 cells injections, the mice were pre-implanted with a 17-Beta-Estradiol (Sigma) pellet. Expression of miRs was induced by dox in the drinking water (2 g/l of dox in a 5% sucrose solution), which was refreshed every 48 h.

Tumorsphere assay. Single cells were seeded on Ultra Low Attachment Plates (Corning) at a concentration of 100,000/ml. For experiments with inducible miRs, dox was added at the beginning of the tumorsphere assay and refreshed every 2 days. Tumorspheres larger than 50 μ m diameter were counted 7 days after seeding (1^o tumorspheres). The primary spheres were dissociated with HyQTase and 20,000/ml cells seeded in the presence of dox. The number of tumorspheres was counted after 7 days (2^o tumorspheres).

Immunohistochemistry. For TMA studies, paraffin sections from a cohort of 19 normal human breast tissues and 354 human breast tumors were stained with SHP2 (1:200) antibodies (Santa Cruz) as previously described (Zhou, Coad et al. 2008). For the intraductal studies, mouse mammary gland tissue was fixed in MethCarnoy's (60% methanol, 30% chloroform and 10% glacial acetic acid) for 4 h, stained in Carmine-Alum solution, embedded in paraffin and stained with hematoxylin and eosin (H&E), anti-GFP (MBL) or anti-Keratin18 (Fitzgerald) antibodies. For the other xenograft studies, tumors were fixed in Formal Fix solution (Thermo Electro Corporation) for 16 h, embedded in paraffin and stained with H&E, anti-Ki67 (Thermo Scientific) or anti-CD31 (Dianova) antibodies. Mouse lungs were fixed in Bouin's fixative, embedded in paraffin and stained with H&E or anti-HER2 (Dako) antibodies.

FACS analysis. MCF10A or SUM159 cells were dissociated with HyQTase and stained with a 1:5 dilution of Alexa fluor 647 anti-CD24 and a 1:200 dilution of Alexa fluor 488 anti-CD44 antibodies (Biolegend).

Microarray analysis. Total RNA was extracted from tumors with TRIzol reagent (Invitrogen). RNA was processed, hybridized to GeneChip Human Gene 1.0 ST arrays (Affymetrix, Santa Clara, CA) and scanned according to the manufacturer's instructions. All gene arrays were processed in R (www.r-project.org) using bioconductor and the package oligo. Robust multi-array mean (RMA) was performed using the following command:

```
expr <- rma(read.celfiles(filenamees, pkgname="pd.hugene.1.0.st.v1"), target="probeset")
```

. Expressions for transcript clusters were calculated by averaging corresponding probeset values (using array annotation from Affymetrix).

The contrast between SHP2 miR1-CTRL miR and SHP2 miR2-CTRL miR expressing tumors was plotted and 210 Affymetrix IDs were found to be either upregulated or downregulated in both SHP2 miRs-expressing tumors (*black asterisks* in Fig. 5a). Of these 210 IDs, 182 had a human gene annotation. 180 genes were downregulated whereas only two were upregulated in SHP2 miR1/2 tumors (Supplementary Table 1). The 180 downregulated genes were considered to be the "SHP2 signature".

Analysis of let-7 target genes from microarray data. Contrasts between SHP2 miRs samples – CTRL miR were calculated as described above for both MCF10A-HER2/3 cells grown in 3D cultures and BT474 tumors in the presence or absence of SHP2. Using the TargetScan 5.1 resource (www.targetscan.org), we defined three groups of expressed genes (average log₂ expression level greater than 4.0): genes that are not targeted by let-7, genes that are predicted let-7 targets and genes that are the 100 most likely let-7 targets sorted by

TargetScan scores. For each group of genes, we plotted the relative frequency (density) of log₂ fold changes induced by SHP2 knockdown.

Analysis of public microarray data. CEL files were downloaded (<http://www.ncbi.nlm.nih.gov/geo>, accessions: GSE12276 for the Bos dataset (Bos, Zhang et al. 2009), GSE2034 for the Wang dataset (Wang, Klijn et al. 2005), GSE1456 for the Stockholm dataset (Pawitan, Bjohle et al. 2005) and GSE2109 for the Bittner dataset) and normalized using `gcrma` from R/bioconductor. Probesets were linked to genes using Affymetrix annotation and, for genes represented by multiple probesets, those with maximal variance across tumors were selected. Genes not clearly detected (mean log₂ level below 4.0) were removed. For clustering and visualization, Z-scores were calculated from expression levels of each gene by subtracting the mean and dividing by the standard deviation. Patients were split into two groups by k-means clustering and expression polarization was defined as the absolute difference between the mean expression levels over genes and patients in each group.

Motif activity response analysis (MARA). We used MARA (Suzuki, Forrest et al. 2009) to model genome-wide gene expression patterns in terms of computationally predicted transcription factor binding sites. We calculated the means and standard errors of the activities of over 200 human regulatory motifs in the CTRL, SHP2 miR1 and SHP2 miR2 samples, identifying those motifs that were consistently downregulated in both SHP2 miR1 and SHP2 miR2 samples.

Immunoblotting and Reverse-Phase Protein Array (RPA). Total protein lysates for immunoblotting were obtained using L-buffer (2.5% SDS, Tris-HCl 250 mM pH 7.4). RPA was performed as previously described (Voshol, Ehrat et al. 2009). For immunoblotting, we used anti-SHP2, HER3, ERK2, EGFR, PLC γ (Santa Cruz), HER2 (Calbiochem), P-EGFR

(Invitrogen), P-HER2, Ras (Millipore), P-PLC γ (Upstate), c-Myc (Sigma), P-ERK1/2, P-ERK5 and ERK5 (Cell Signaling) antibodies. For RPA, we used anti-SHP2 (Santa Cruz), P-EGFR, P-MEK3/6 (Invitrogen), P-HER2 (Millipore), P-PDGFRbeta, P-ERK5, P-ERK1/2, P-p38, P-JNK, P-AKT, P-GSK3 α/β , P-S6, P-mTOR, P-PLC γ , P-STAT1, P-STAT3, P- β Catenin, P-ACC, P-TUBERIN, and P-PP1a (Cell Signaling) antibodies.

Quantitative Real-Time PCR. Total RNA was extracted with TRIzol reagent (Invitrogen) and used as a template for production of cDNA (Invitrogen). cDNA was used for SYBR-based quantitative real time PCR for quantification of transcript levels of HOXA5 (F: 5'-GCTGCAAAACGGGGGAAATAAAG-3'; R: 5'-TTCCCTCGCAGTTCCATTAGGA-3'), HOXA9 (F: 5'-GAGGGGAGGGGACAGAGAGGTAG-3'; R: 5'-CTCCGCTGCTTTATGTTTCCTGCT-3'), HOXA13 (F: 5'-GGCTCCAAGAAACACCCATTCTG-3'; R: 5'-GCAGTGGGGACAGGTCAGGTAAT-3'), HOXB5 (F: 5'-AAAGCCCAACCCTGCTCTAAAA-3'; R: 5'-AGTCGCCGGGAGAGAAAGAAAC-3'), HOXB6 (F: 5'-CGACTGAGAAAAGGGTTGCTGGT-3'; R: 5'-CAATCGCTGGATTCAACCACTCA-3'), HOXB9 (F: 5'-ACGCTTTATCAGGCAGTCGGAAA-3'; R: 5'-CCTGCTCAACTTCTCAGCCAACA-3'), HOXD10 (F: 5'-TTCCAGTTTAGAGCCTGCCTTGC-3'; R: 5'-GATGATATATGGGCGGGCACAG-3'), HOXD11 (F: 5'-CGGGTGGAAGAGAAATCTGGAAC-3'; R: 5'-GTCTAAGGACAGTGGGGCAGTCG-3'), HOXD13 (F: 5'-TTTATAAACGTCCCGCGATGAGC-3'; R: 5'-TAGCCCTCTCTCCCTCTGTGAGC-3'), ZEB1 (F: 5'-GCACCTGAAGAGGACCAGAG-3'; R: 5'-TGCATCTGGTGTTCATTTT-3'), Fibronectin1 (F: 5'-CAGTGGGAGACCTCGAGAAG-3'; R: 5'-TCCCTCGGAACATCAGAAAC-3'), Vimentin (F: 5'-GAGAACTTTGCCGTTGAAGC-3'; R: 5'-GCTTCCTGTAGGTGGCAATC-3'), N-cadherin (F: 5'-

ACAGTGGCCACCTACAAAGG-3'; R: 5'-CCGAGATGGGGTTGATAATG-3') and LIN28B (F: 5'-CTGTCAGAGCATCATGCACATG-3'; R: 5'-GGGTGGCTGTGCAACATTTT-3'). GAPDH (F: 5'-ACCCAGAAGACTGTGGATGG-3'; R: 5'-TCTAGACGGCAGGTCAGGTC-3') and ACTIN (F: 5'-TTGCCGACAGGATGCAGAA-3'; R: 5'-GCCGATCCACACGGAGTACT-3') were used as loading controls. All the primers were designed to specifically amplify human transcripts.

Statistical analysis. Paired data were evaluated by Student's t-test. The transplantation frequency analysis was performed using R and the "statmod" package as previously described (Shackleton, Vaillant et al. 2006). The single-hit assumption was tested as recommended and was not rejected for any dilution series ($P > 0.05$). P values for let-7 target genes downregulation were calculated with Wilcoxon rank sum test. P values for observed expression polarization were calculated as $P = (b+1)/(R+1)$, where R is the number of randomly selected gene groups of the same size as our signature (10,000), and b is the number of times that a random gene group produced an expression polarization value equal to or greater than the one obtained for our signature. P values for association of patient groups with molecular tumor subtypes were calculated using Fisher's exact test.

FIGURES

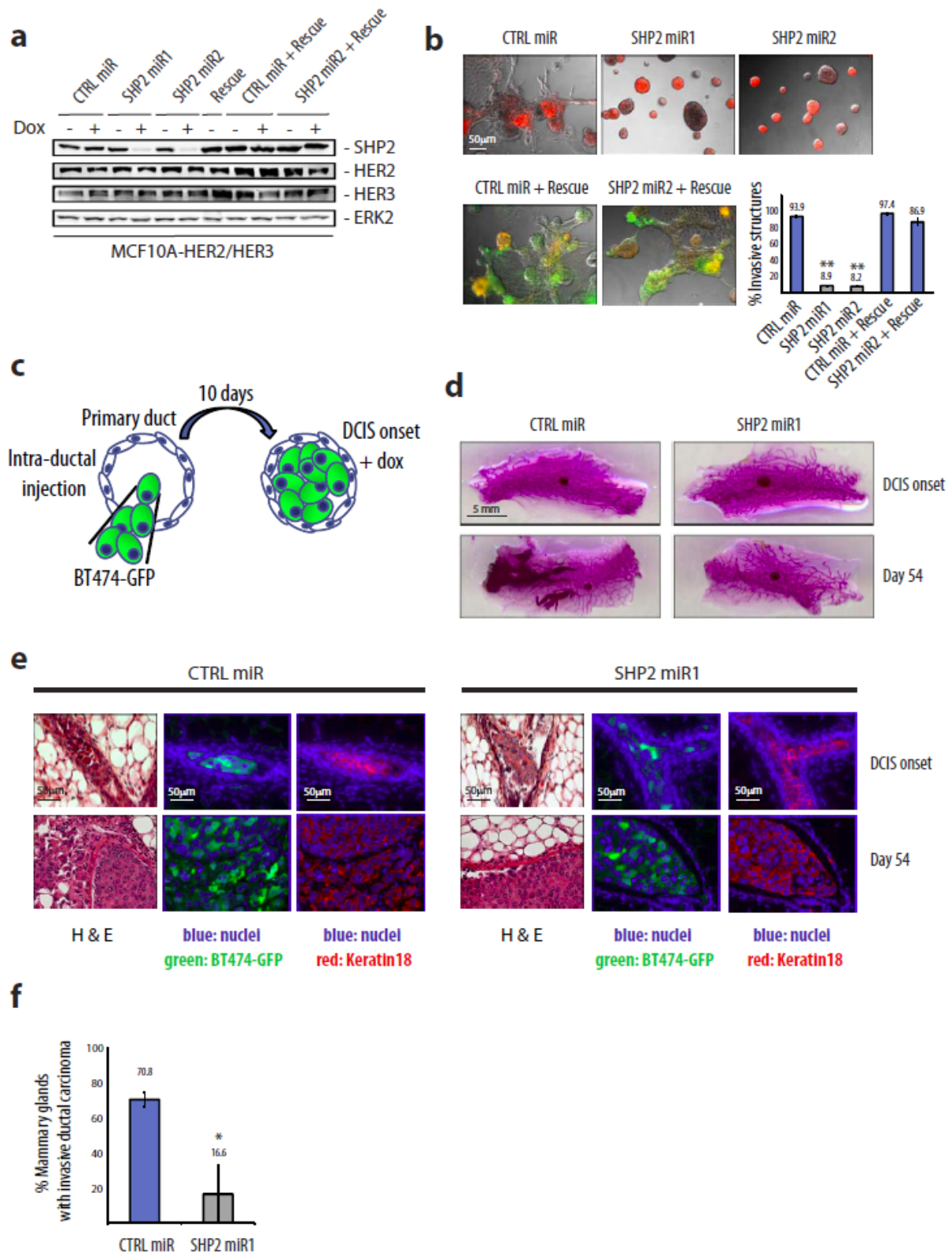


Figure 1 Aceto et al.

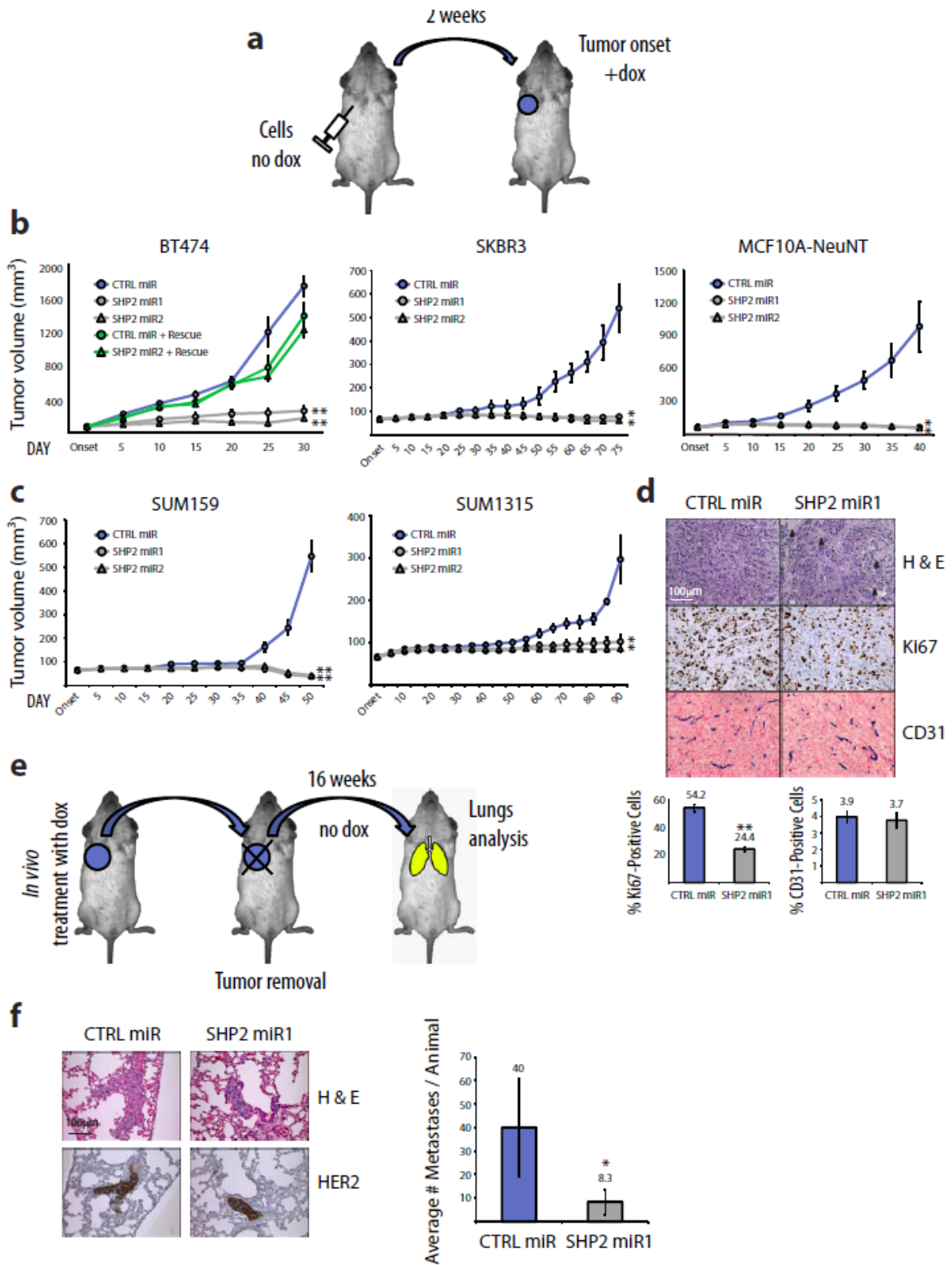


Figure 2 Aceto et al.

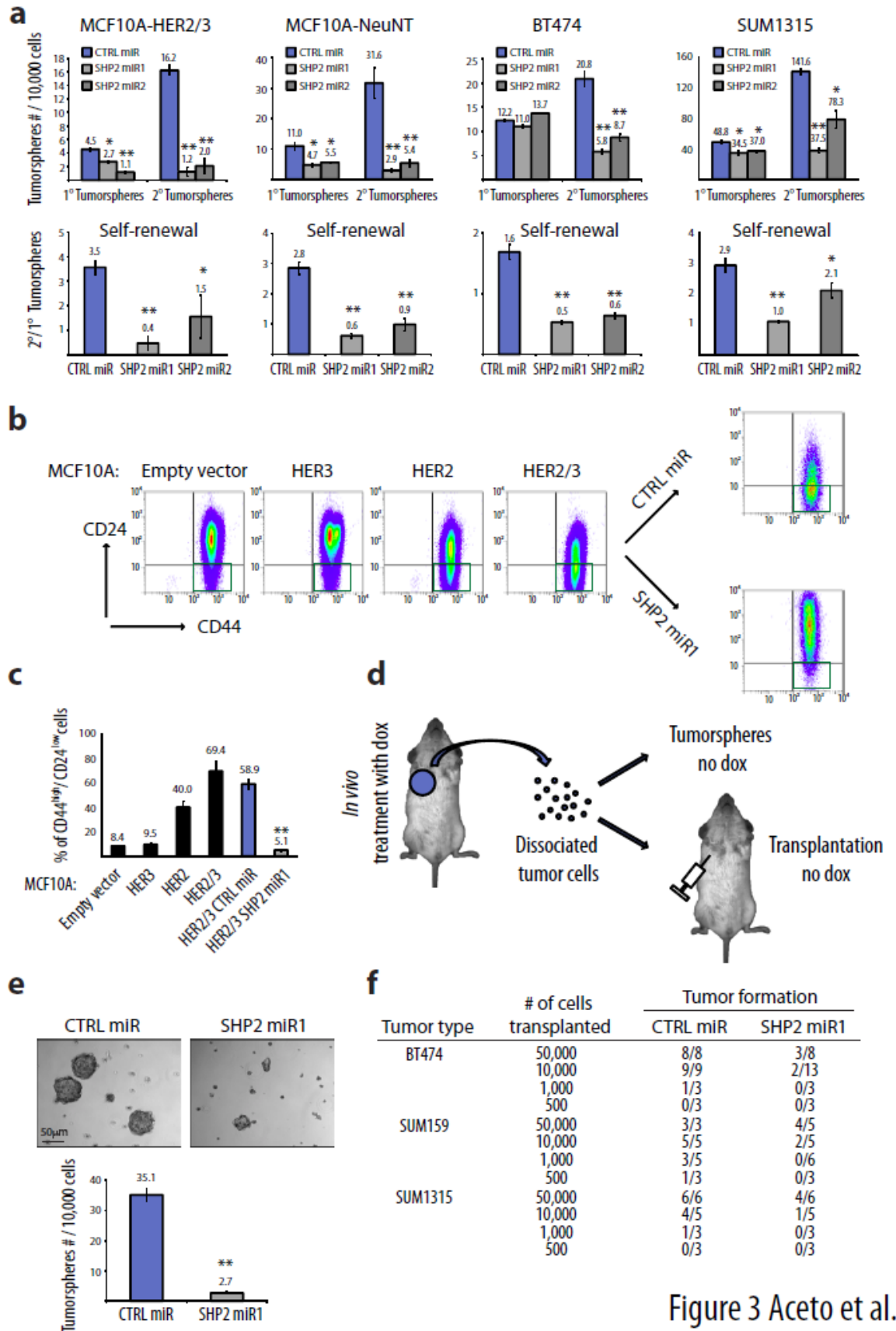


Figure 3 Aceto et al.

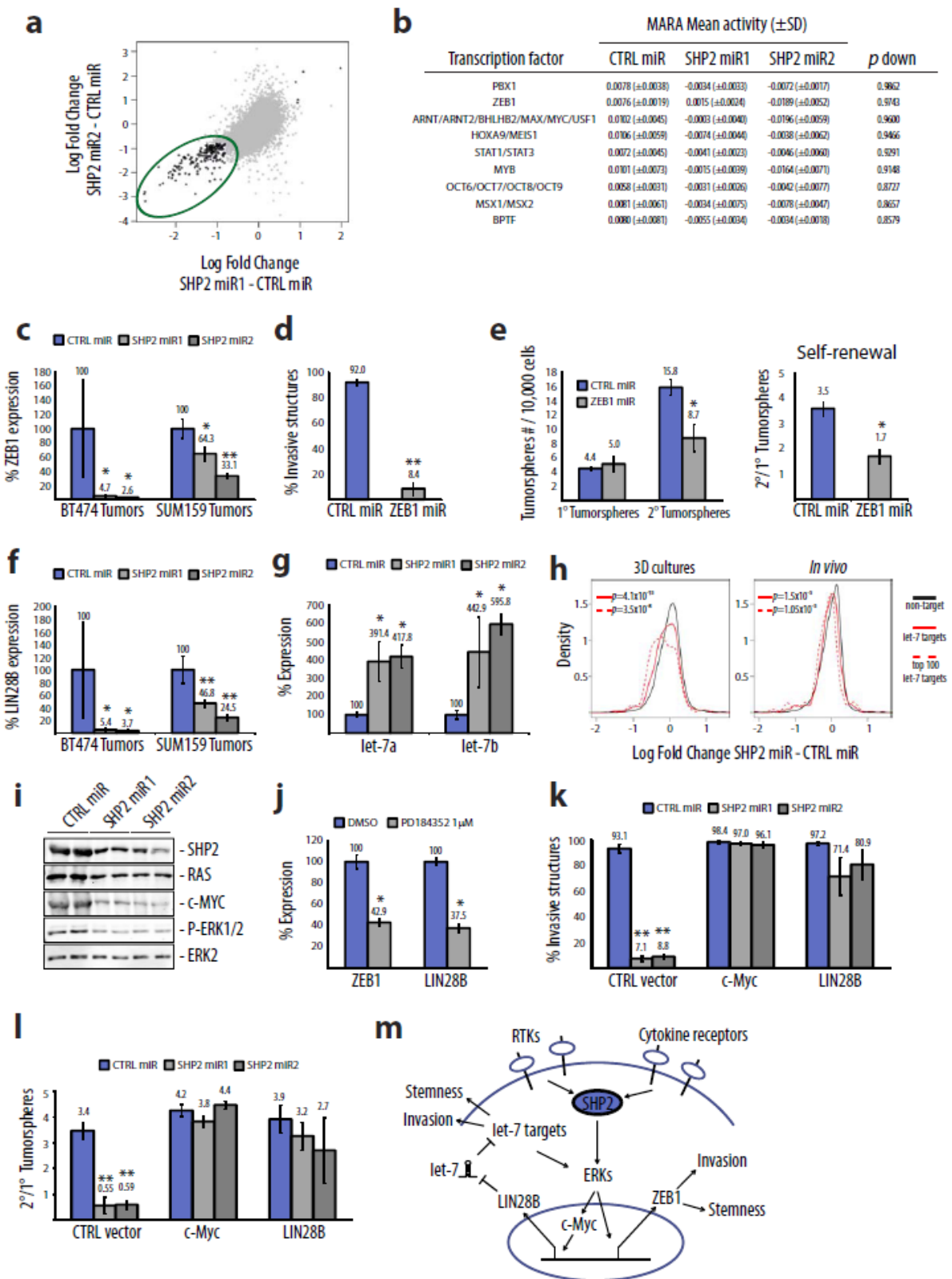


Figure 5 Aceto et al.

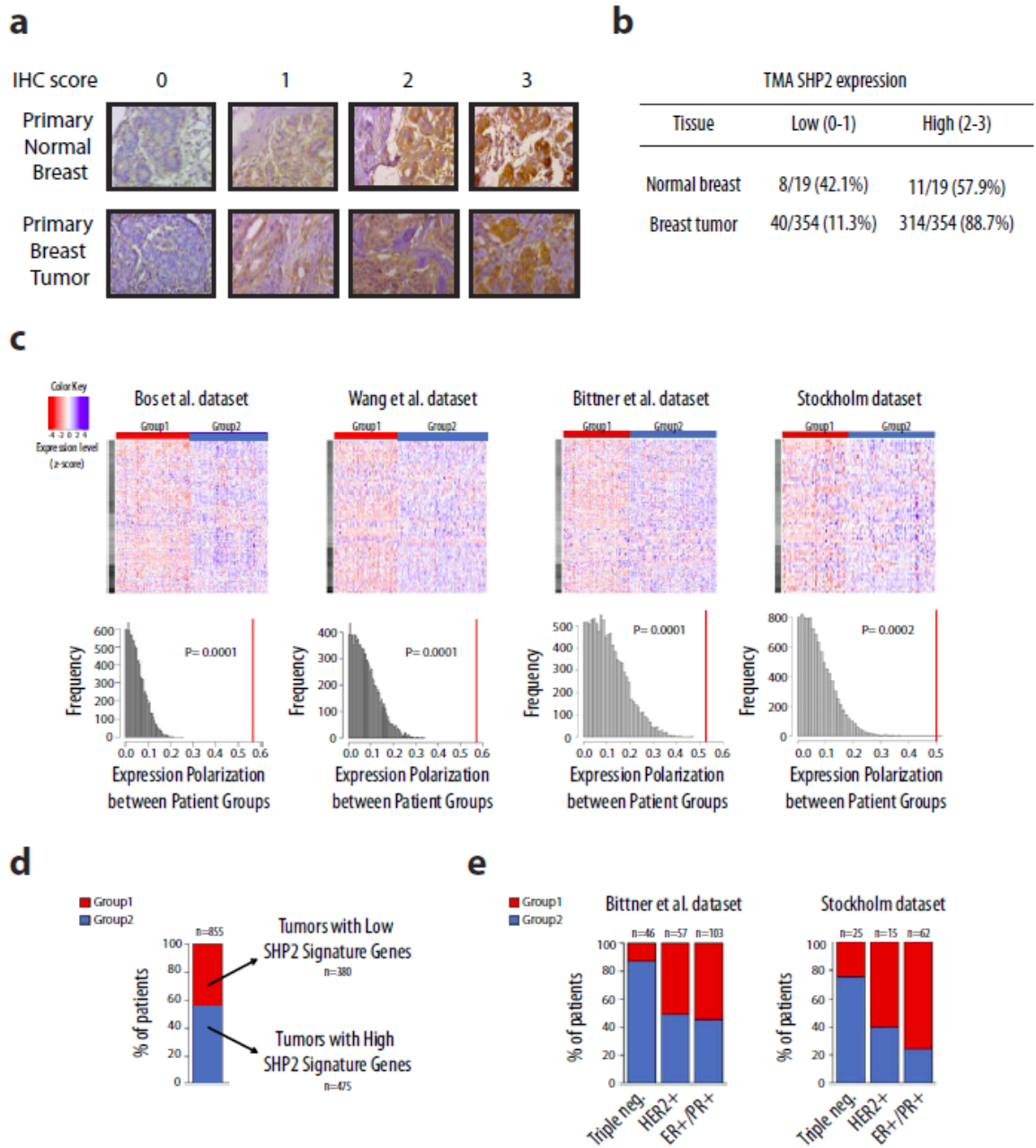
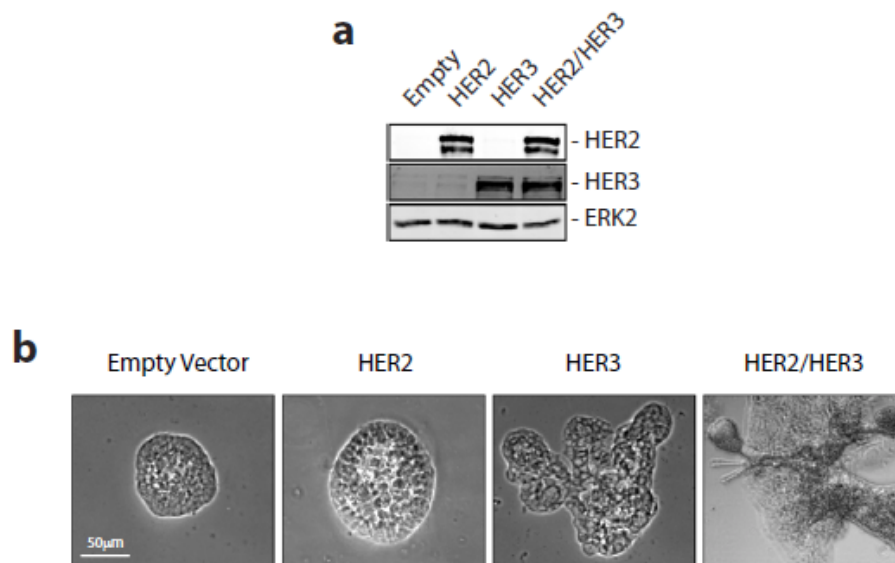


Figure 6 Aceto et al.

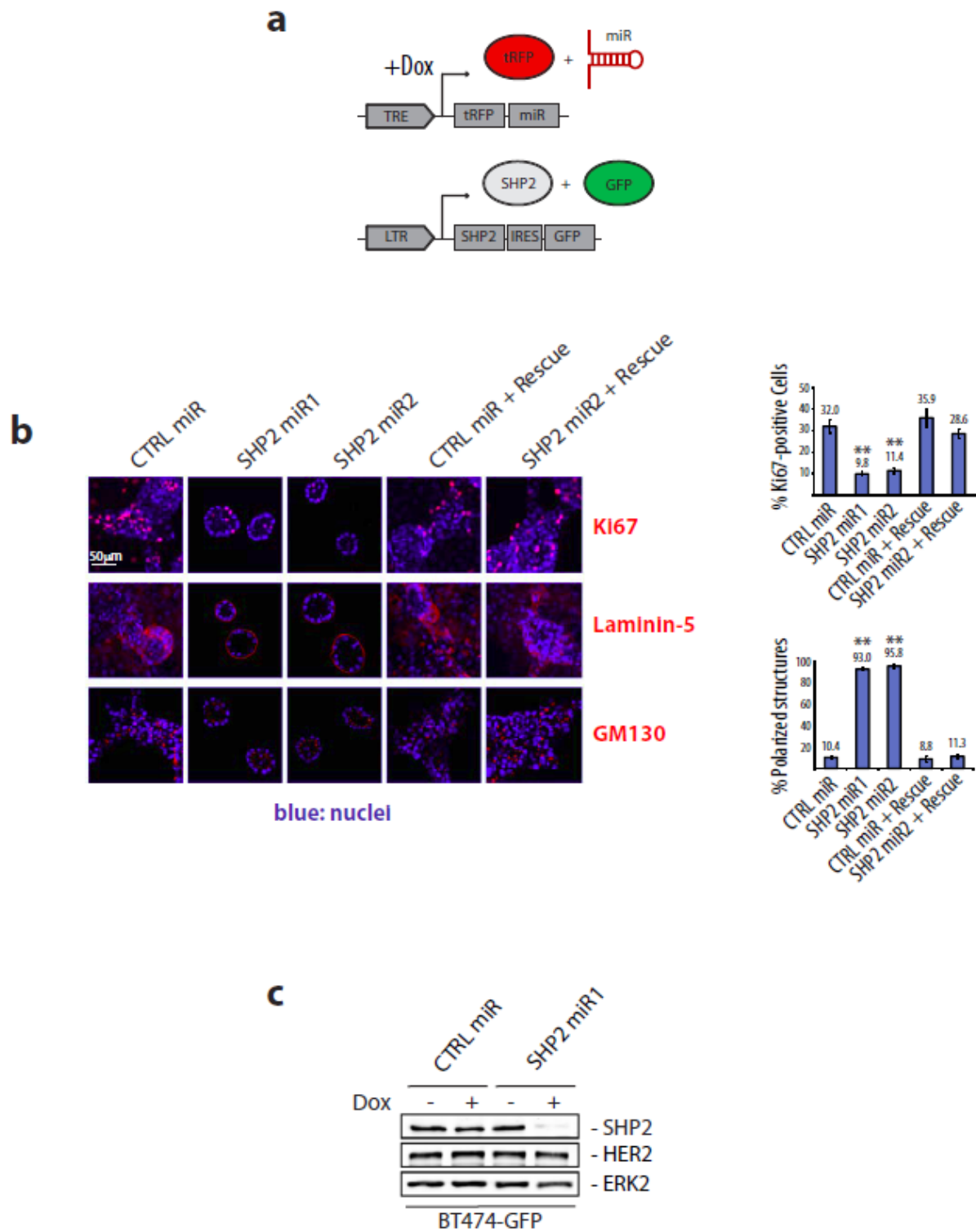
SUPPLEMENTARY INFORMATION

Supplementary Figure 1 Aceto et al.



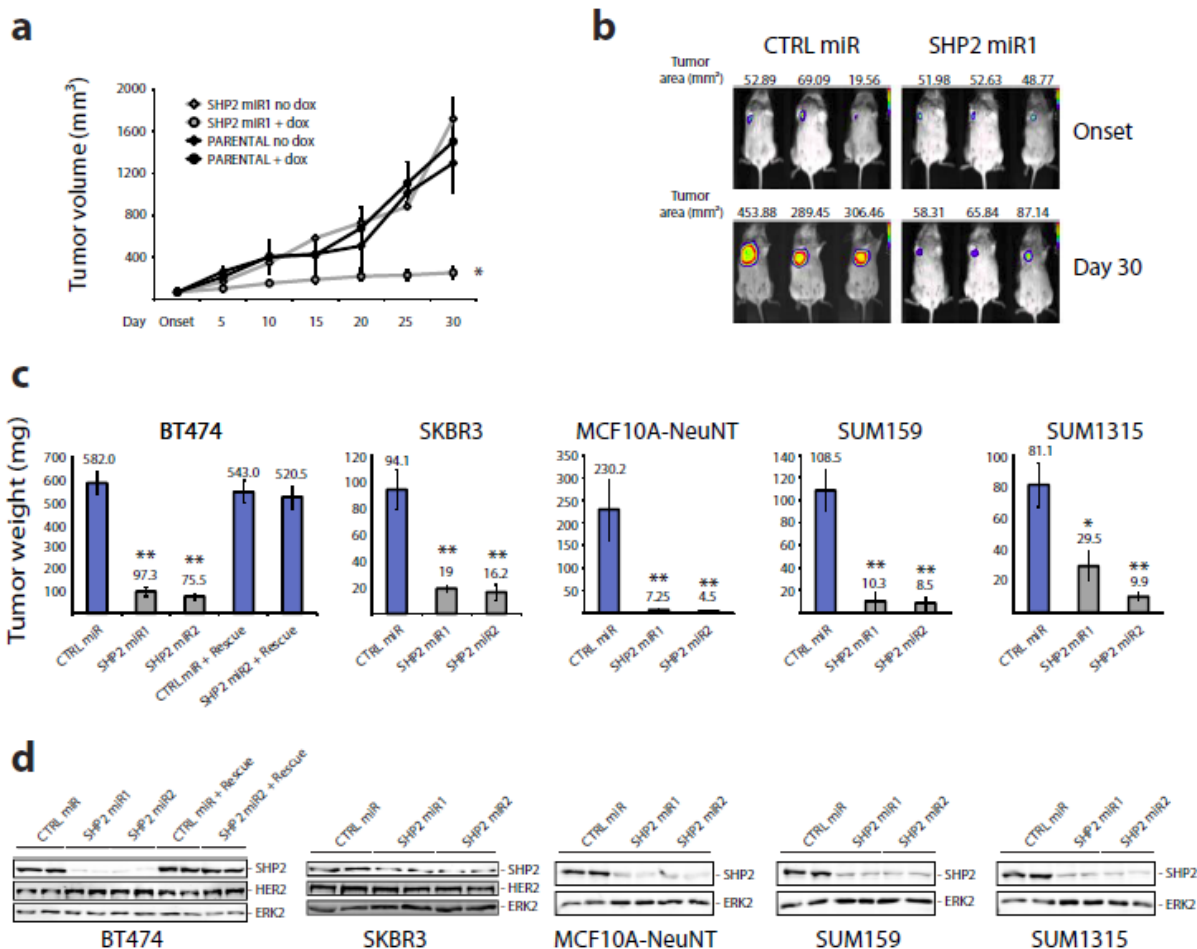
Supplementary Fig. 1. HER2 and HER3 co-overexpression confers an invasive phenotype on MCF10A cells. (a) Immunoblot showing expression levels of HER2, HER3 and ERK2 (loading control) in MCF10A cells. **(b)** Representative phase contrast images of MCF10A cells expressing the empty vector, HER2, HER3 or HER2/HER3 grown in 3D cultures for 20 days.

Supplementary Figure 2 Aceto et al.



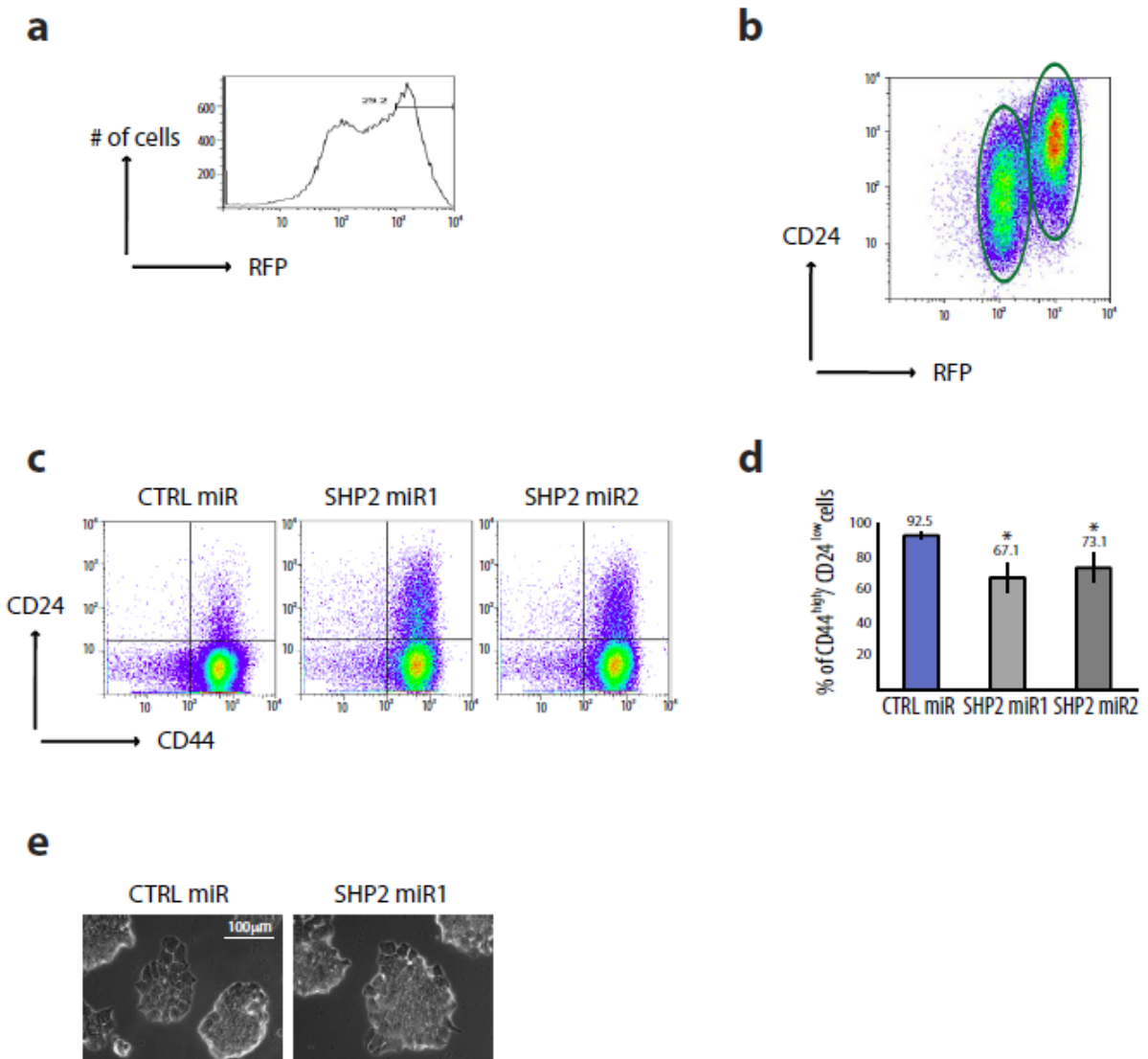
Supplementary Fig. 2. SHP2 promotes invasion, proliferation and loss of polarity in 3D cultures and *in vivo*. (a) *Top*: Schematic of the inducible lentiviral vector that expresses shRNA^{miR} (miR) and turbo red fluorescent protein (tRFP) upon treatment with dox. *Bottom*: Schematic of the pMSCV vector expressing human wild-type SHP2 and GFP cDNAs. (b) SHP2 knockdown reduced proliferation, restored polarity and blocked invasion. Representative confocal images of equatorial cross-sections of MCF10A-HER2/3 structures grown in 3D culture for 20 days in the presence or absence of SHP2 and stained as indicated. The bar graphs show the percentage of Ki67-positive cells and the percentage of polarized structures. Results represent means \pm SEM from four independent experiments; **** $P < 0.001$** . (c) Treatment with dox of BT474 cells expressing GFP (for marking the cells) and an inducible SHP2 miR1, but not cells expressing CTRL miR, resulted in the downregulation of SHP2. Immunoblot shows levels of SHP2, HER2 and ERK2 (loading control) in the presence (+) or absence (-) of dox.

Supplementary Figure 3 Aceto et al.



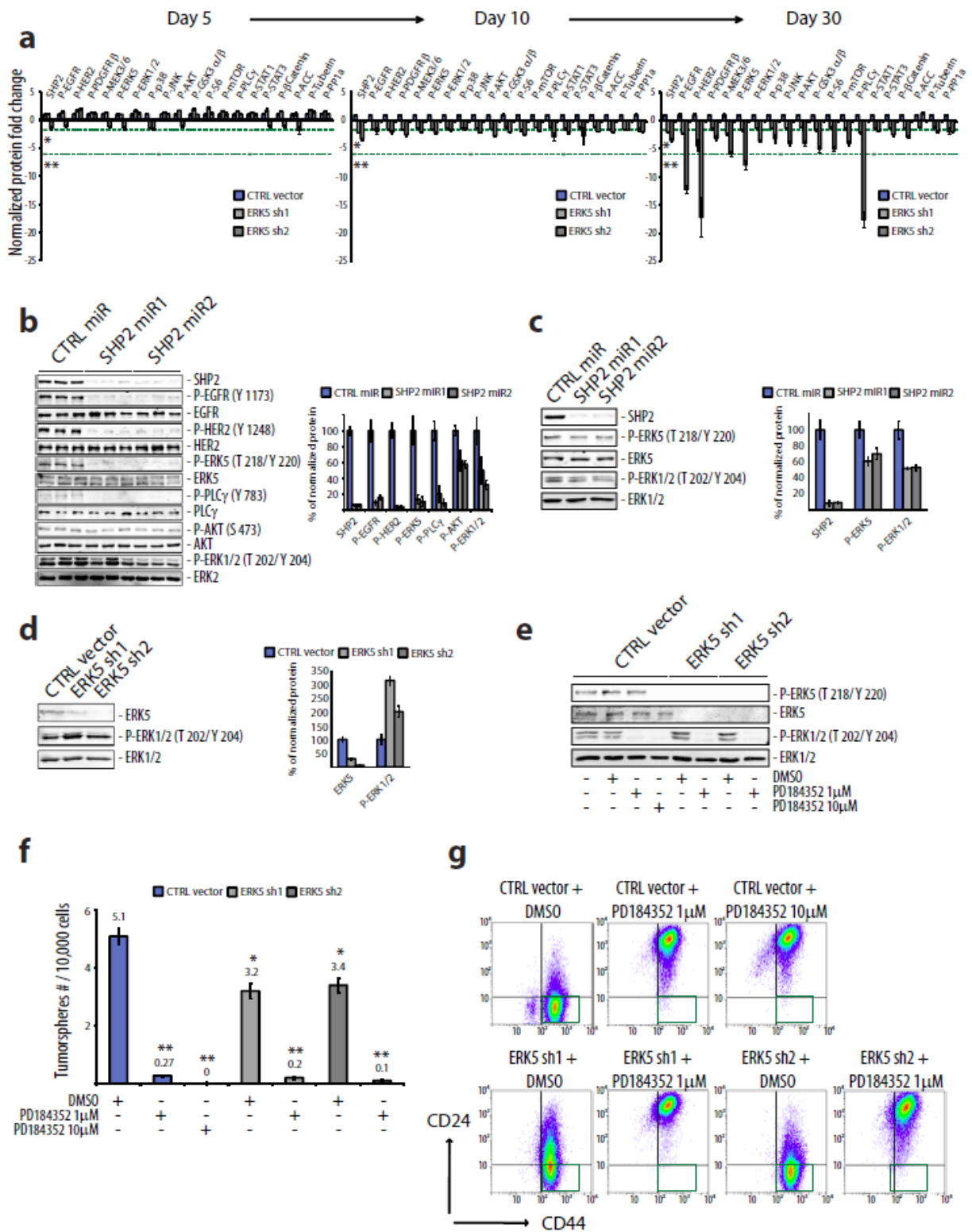
Supplementary Fig. 3. SHP2 is essential for tumor maintenance. (a) Tumor growth curves of BT474 parental cells or those expressing SHP2 miR1 in the presence or absence of dox. Dox was added at the onset of tumors and maintained until the end of the experiment. The curves show the average tumor volume (mm^3) \pm SEM ($n=6$ per group, $*P<0.006$). (b) SHP2 knockdown decreased tumor area ~ 5 times. Representative bioluminescence images of BT474 primary tumors after 30 days of treatment with dox. (c) SHP2 knockdown decreased tumor weight. Bar graph showing mean tumor weight (mg) \pm SEM after treatment with dox (BT474 $n=15$, SKBR3 $n=10$, MCF10A-NeuNT $n=8$, SUM159 $n=10$, SUM1315 $n=9$; $*P<0.04$, $**P<0.00003$). (d) Persistent reduction of SHP2 expression in tumors expressing SHP2 miRs compared with CTRL miR after treatment with dox. Immunoblot showing expression of SHP2, HER2 and ERK2 (loading control) in lysates from the indicated tumors.

Supplementary Figure 4 Aceto et al.



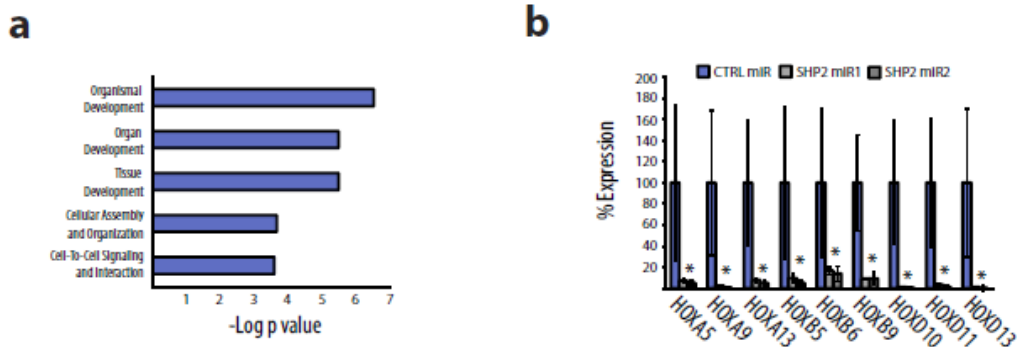
Supplementary Fig. 4. SHP2 knockdown depletes the CSC population. (a) Distribution of RFP-positive cells after dox-mediated activation of CTRL or SHP2 miR1 in MCF10A-HER2/3 cells. Only the RFP^{high} cells (29.2% of the total) were considered for the CD44^{high}/CD24^{low} analysis. (b) As an internal control, we evaluated the distribution of RFP and CD24 expression in MCF10A-HER2/3 cells expressing SHP2 miR1. High RFP expression, which correlates with low SHP2 expression, was associated with an increase in the CD24^{high} population lacking CSCs. Representative flow cytometry dot plot of CD24 and RFP expression in MCF10A-HER2/3 cells expressing SHP2 miR1. (c) Representative flow cytometry dot plots showing CD44/CD24 expression in SUM159 cells expressing CTRL or SHP2 miRs and treated with dox for 7 days. (d) Mean percentage of CD44^{high}/CD24^{low} cells in SUM159 cells. Results represent means \pm SEM from three independent experiments; * $P < 0.05$. (e) To exclude the possibility that BT474 cells lacking SHP2 died before transplantation, we seeded them *in vitro* immediately after single cell isolation and found that they were viable and proliferating when grown as monolayer cultures. Representative phase contrast images of monolayer cultures of cells derived from BT474 tumors expressing CTRL or SHP2 miR treated with dox for 30 days.

Supplementary Figure 5 Aceto et al.



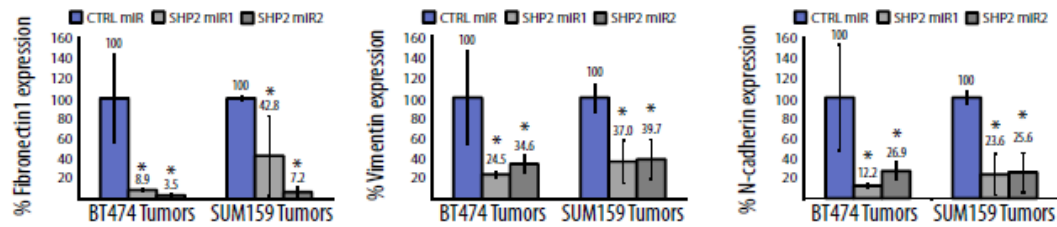
Supplementary Fig. 5. SHP2 promotes maintenance of breast CSCs and tumor progression via activation of the ERK pathway. (a) RPA screening using lysates from BT474 CTRL, miR1 and miR2 tumors after 5, 10 and 30 days of treatment with dox. The bar graph shows the average fold change of the indicated proteins \pm SEM ($n=8$, $*P<0.05$, $**P<0.01$). (b) Immunoblot of lysates from BT474 tumors. The bar graph shows the percentage of normalized protein \pm SEM ($n=3$). (c) Immunoblot of lysates from MCF10A-HER2/3 primary tumorspheres in the presence or absence of SHP2. The bar graph shows the percentage of normalized protein \pm SEM ($n=3$). (d) Immunoblot of lysates from MCF10A-HER2/3 primary tumorspheres in the presence or absence of ERK5. The bar graph shows the percentage of normalized protein \pm SEM ($n=3$). (e) Immunoblot of lysates from BT474 primary tumorspheres expressing ERK5 shRNA alone or in combination with PD184352 treatment. (f) ERK5 knockdown partially reduces the tumorsphere-forming capacity of MCF10A-HER2/3 cells, whereas ERK1/2 inhibition almost completely abolishes it. Bar graph showing the average number of MCF10A-HER2/3 tumorspheres/ 10^4 cells \pm SEM ($n=3$); $*P<0.001$, $**P<5.5\times 10^{-5}$. (g) Representative flow cytometry dot plots showing that ERK1/2 and ERK5 inhibition decreased the CD44^{high}/CD24^{low} subpopulation (*green rectangle*) in MCF10A-HER2/3 cells.

Supplementary Figure 6 Aceto et al.



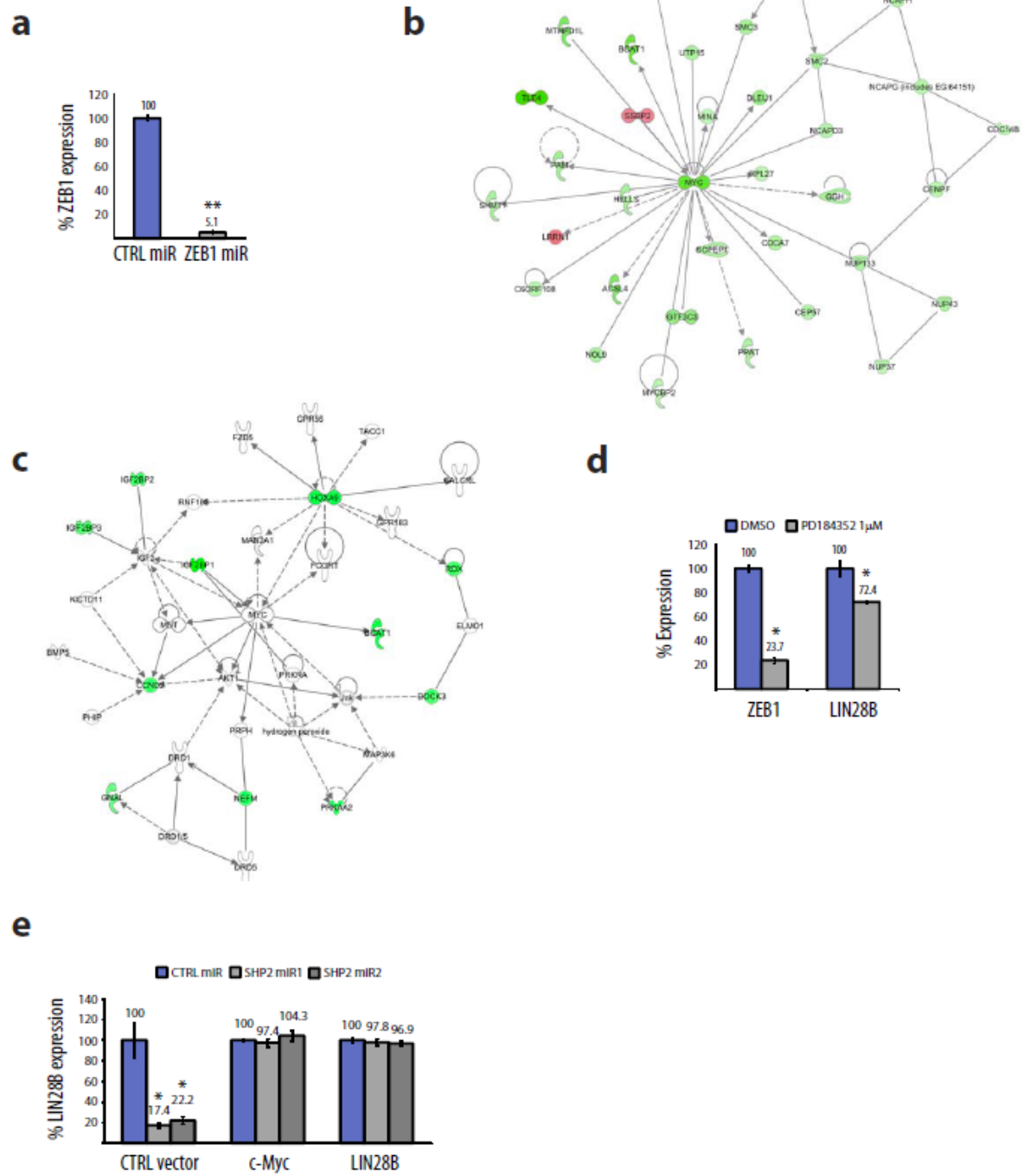
Supplementary Fig. 6. SHP2 induces the expression of a set of development-associated genes. (a) Gene ontology analysis (Ingenuity) of the “SHP2 signature” described in Figure 5a revealed a remarkable enrichment in development-associated genes. This enrichment was mainly determined by the presence of 9 HOX genes (HOXA5, HOXA9, HOXA13, HOXB5, HOXB6, HOXB9, HOXD10, HOXD11 and HOXD13) in the SHP2 signature. (b) Quantitative Real-Time PCR confirmed the decrease in the expression of HOX genes upon depletion of SHP2. RNA was isolated from BT474 tumors expressing CTRL or SHP2 miRs treated for 30 days with dox. Quantitative Real-Time PCR was performed using primers against HOXA5, HOXA9, HOXA13, HOXB5, HOXB6, HOXB9, HOXD10, HOXD11 and HOXD13. Results represent means \pm SEM ($n=3$); $*P<0.05$.

Supplementary Figure 7 Aceto et al.



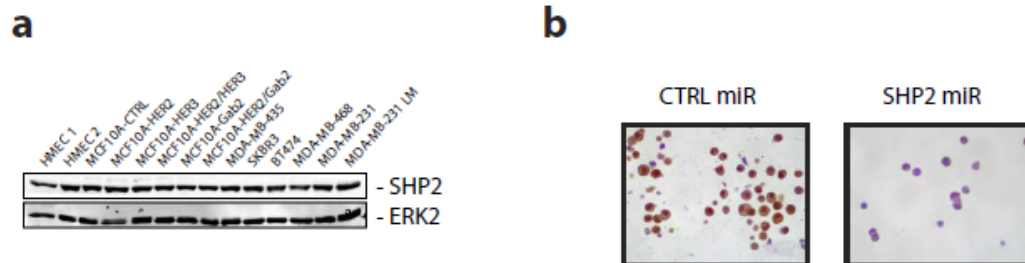
Supplementary Fig. 7. SHP2 induces EMT *in vivo*. Quantitative Real-Time PCR of the EMT markers Fibronectin1, Vimentin and N-cadherin. The bar graphs show the percentage of EMT marker expression in BT474 and SUM159 tumors in the presence or absence of SHP2. Results represent means \pm SEM ($n=3$); * $P<0.05$.

Supplementary Figure 8 Aceto et al.



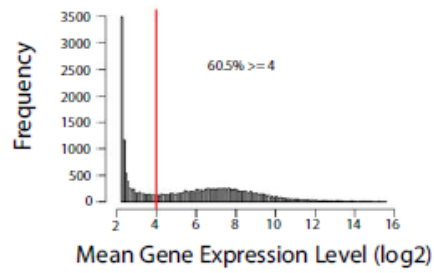
Supplementary Fig. 8. SHP2 maintains CSCs via ERK1/2-mediated activation of ZEB1 and c-Myc transcription factors. (a) Quantitative Real-Time PCR of the transcription factor ZEB1. The bar graph shows the mean percentage of ZEB1 expression in MCF10A-HER2/3 cells expressing an inducible ZEB1 miR \pm SEM ($n=3$); $**P<0.00054$. (b) Network analysis (Ingenuity) of downregulated and upregulated genes (greater than ± 0.5 logarithmic fold change) upon SHP2 knockdown in BT474 tumors. The top-ranked network is shown, displaying c-Myc as a key factor. Downregulated genes are shown in green, upregulated genes in red. *Ingenuity network score=47* (c) Network analysis (Ingenuity) of predicted let-7 targets within the SHP2 signature (listed in Supplementary Table 2). The top ranked network is shown, indicating that let-7 target genes within the SHP2 signature strongly associate with the c-Myc network. *Ingenuity network score=28* (d) Quantitative Real-Time PCR of ZEB1 and LIN28B. The bar graph shows the mean percentage of ZEB1 and LIN28B expression in MCF10A-HER2/3 cells upon treatment with 1 μ M PD184352 for 7 days \pm SEM ($n=3$); $*P<0.5$. (e) Quantitative Real-Time PCR of LIN28B. The bar graph shows the percentage of LIN28B expression in MCF10A-HER2/3 cells in the presence or absence of SHP2 and expressing a c-Myc or LIN28B rescue. Results represent means \pm SEM ($n=3$); $*P<0.048$.

Supplementary Figure 9 Aceto et al.



Supplementary Fig. 9. SHP2 is expressed in normal human breast and primary breast tumors. (a) Immunoblot shows levels of SHP2 and ERK2 (loading control) expression in a panel of normal human mammary epithelial cells (first three lines) and human breast cancer cell lines. **(b)** Validation of the SHP2 antibody for immunohistochemistry. Representative images of sections of BT474 cells expressing a CTRL or SHP2 miR1 stained with anti-SHP2 antibodies.

Supplementary Figure 10 Aceto et al.



Supplementary Fig. 10. SHP2 signature genes are expressed in a large subset of breast cancer patients. Representative mean gene expression levels (log2) of the genes from the “SHP2 signature” from the Bos dataset. In all datasets used, genes above 4 (*threshold, red line*) were considered expressed and used for the polarization analysis.

Supplementary Table 1. Upregulated and downregulated genes in SHP2 miR1 and SHP2 miR2 tumors

UPREGULATED (2 genes)			
Log FC	Entrez gene ID	Gene name	Description
2.146	283463	MUC19	mucin 19, oligomeric
0.977	27328	PCDH11X	protocadherin 11 X-linked
DOWNREGULATED (180 genes, "SHP2 signature")			
Log FC	Entrez gene ID	Gene name	Description
-0.812	6443	SGCB	sarcoglycan, beta (43kDa dystrophin-associated glycoprotein)
-0.822	9753	ZSCAN12	zinc finger and SCAN domain containing 12
-0.843	3400	ID4	inhibitor of DNA binding 4, dominant negative helix-loop-helix protein
-0.854	7547	ZIC3	Zic family member 3 (odd-paired homolog, Drosophila)
-0.861	54504	CPVL	carboxypeptidase, vitellogenic-like
-0.881	3105	HLA-A	major histocompatibility complex, class I, A
-0.893	55283	MCOLN3	mucolipin 3
-0.894	132671	SPATA18	spermatogenesis associated 18 homolog (rat)
-0.897	55076	TMEM45A	transmembrane protein 45A
-0.904	2774	GNAL	guanine nucleotide binding protein (G protein), alpha activating activity polypeptide, olfactory type
-0.911	79901	CYBRD1	cytochrome b reductase 1
-0.917	7102	TSPAN7	tetraspanin 7
-0.917	6935	ZEB1	zinc finger E-box binding homeobox 1

Results

-0.921	54875	CNTLN	centlein, centrosomal protein
-0.921	4747	NEFL	neurofilament, light polypeptide
-0.934	201161	CENPV	centromere protein V
-0.937	84100	ARL6	ADP-ribosylation factor-like 6
-0.940	3251	HPRT1	hypoxanthine phosphoribosyltransferase 1
-0.940	151827	LRRC34	leucine rich repeat containing 34
-0.942	10630	PDPN	podoplanin
-0.944	222389	BEND7	BEN domain containing 7
-0.948	117247	SLC16A10	solute carrier family 16, member 10 (aromatic amino acid transporter)
-0.951	158318	FAM27E1	family with sequence similarity 27, member E1
-0.959	59338	PLEKHA1	pleckstrin homology domain containing, family A (phosphoinositide binding specific) member 1
-0.960	51191	HERC5	hect domain and RLD 5
-0.962	53344	CHIC1	cysteine-rich hydrophobic domain 1
-0.967	84295	PHF6	PHD finger protein 6
-0.968	6785	ELOVL4	elongation of very long chain fatty acids (FEN1/Elo2, SUR4/Elo3, yeast)-like 4
-0.975	84168	ANTXR1	anthrax toxin receptor 1
-0.981	23532	PRAME	preferentially expressed antigen in melanoma
-0.983	6322	SCML1	sex comb on midleg-like 1 (Drosophila)
-0.986	79745	CLIP4	CAP-GLY domain containing linker protein family, member 4
-0.988	27443	CECR2	cat eye syndrome chromosome region, candidate 2
-0.997	25904	CNOT10	CCR4-NOT transcription complex, subunit 10

Results

-1.007	10643	IGF2BP3	insulin-like growth factor 2 mRNA binding protein 3
-1.008	4675	NAP1L3	nucleosome assembly protein 1-like 3
-1.011	2719	GPC3	glypican 3
-1.012	84451	KIAA1804	mixed lineage kinase 4
-1.015	8526	DGKE	diacylglycerol kinase, epsilon 64kDa
-1.015	355	FAS	Fas (TNF receptor superfamily, member 6)
-1.031	285220	EPHA6	EPH receptor A6
-1.031	79070	KDEL1C1	KDEL (Lys-Asp-Glu-Leu) containing 1
-1.038	83690	CRISPLD1	cysteine-rich secretory protein LCCL domain containing 1
-1.040	1795	DOCK3	dedicator of cytokinesis 3
-1.043	2182	ACSL4	acyl-CoA synthetase long-chain family member 4
-1.045	79937	CNTNAP3	contactin associated protein-like 3
-1.046	389072	PLEKHM3	pleckstrin homology domain containing, family M, member 3
-1.047	5962	RDX	radixin
-1.049	9096	TBX18	T-box 18
-1.055	58528	RRAGD	Ras-related GTP binding D
-1.061	3215	HOXB5	homeobox B5
-1.063	6622	SNCA	synuclein, alpha (non A4 component of amyloid precursor)
-1.065	65991	FUNDC2	FUN14 domain containing 2
-1.067	8516	ITGA8	integrin, alpha 8
-1.069	164045	HFM1	HFM1, ATP-dependent DNA helicase homolog (S. cerevisiae)

Results

-1.072	10644	IGF2BP2	insulin-like growth factor 2 mRNA binding protein 2
-1.073	894	CCND2	cyclin D2
-1.079	54557	SGTB	small glutamine-rich tetratricopeptide repeat (TPR)-containing, beta
-1.085	283078	MKX	mohawk homeobox
-1.086	131544	CRYBG3	beta-gamma crystallin domain containing 3
-1.087	51186	WBP5	WW domain binding protein 5
-1.089	23284	LPHN3	latrophilin 3
-1.095	56271	BEX4	brain expressed, X-linked 4
-1.098	144402	CPNE8	copine VIII
-1.104	2731	GLDC	glycine dehydrogenase (decarboxylating)
-1.111	222553	SLC35F1	solute carrier family 35, member F1
-1.114	3209	HOXA13	homeobox A13
-1.114	5176	SERPINF1	serpin peptidase inhibitor, clade F (alpha-2 antiplasmin, pigment epithelium derived factor), member 1
-1.117	4741	NEFM	neurofilament, medium polypeptide
-1.119	221711	SYCP2L	synaptonemal complex protein 2-like
-1.121	2273	FHL1	four and a half LIM domains 1
-1.123	27350	APOBEC3C	apolipoprotein B mRNA editing enzyme, catalytic polypeptide-like 3C
-1.124	800	CALD1	caldesmon 1
-1.130	60681	FKBP10	FK506 binding protein 10, 65 kDa
-1.131	3237	HOXD11	homeobox D11
-1.136	163259	DENND2C	DENN/MADD domain containing 2C
-1.141	54839	LRRC49	leucine rich repeat containing 49

Results

-1.143	91775	FAM55C	family with sequence similarity 55, member C
-1.151	9729	KIAA0408	KIAA0408
-1.154	3219	HOXB9	homeobox B9
-1.160	57020	C16ORF62	chromosome 16 open reading frame 62
-1.166	57001	ACN9	ACN9 homolog (<i>S. cerevisiae</i>)
-1.167	7991	TUSC3	tumor suppressor candidate 3
-1.171	54898	ELOVL2	elongation of very long chain fatty acids (FEN1/Elo2, SUR4/Elo3, yeast)-like 2
-1.173	50859	SPOCK3	sparc/osteonectin, cwcv and kazal-like domains proteoglycan (testican) 3
-1.184	3216	HOXB6	homeobox B6
-1.186	57539	WDR35	WD repeat domain 35
-1.190	4354	MPP1	membrane protein, palmitoylated 1, 55kDa
-1.196	81545	FBXO38	F-box protein 38
-1.200	5563	PRKAA2	protein kinase, AMP-activated, alpha 2 catalytic subunit
-1.201	122060	SLAIN1	SLAIN motif family, member 1
-1.204	27031	NPHP3	nephronophthisis 3 (adolescent)
-1.208	57650	KIAA1524	KIAA1524
-1.211	5631	PRPS1	phosphoribosyl pyrophosphate synthetase 1
-1.213	10052	GJC1	gap junction protein, gamma 1, 45kDa
-1.224	154796	AMOT	angiominin
-1.225	10479	SLC9A6	solute carrier family 9 (sodium/hydrogen exchanger), member 6
-1.233	115207	KCTD12	potassium channel tetramerisation domain containing 12
-1.236	54830	NUP62CL	nucleoporin 62kDa C-terminal like

Results

-1.243	9666	DZIP3	DAZ interacting protein 3, zinc finger
-1.244	83700	JAM3	junctional adhesion molecule 3
-1.245	3205	HOXA9	homeobox A9
-1.257	138649	ANKRD19	ankyrin repeat domain 19
-1.262	1029	CDKN2A	cyclin-dependent kinase inhibitor 2A (melanoma, p16, inhibits CDK4)
-1.266	586	BCAT1	branched chain aminotransferase 1, cytosolic
-1.269	4942	OAT	ornithine aminotransferase (gyrate atrophy)
-1.271	23266	LPHN2	latrophilin 2
-1.274	79780	CCDC82	coiled-coil domain containing 82
-1.306	51170	HSD17B11	hydroxysteroid (17-beta) dehydrogenase 11
-1.306	25939	SAMHD1	SAM domain and HD domain 1
-1.308	116966	WDR17	WD repeat domain 17
-1.316	65975	STK33	serine/threonine kinase 33
-1.321	2950	GSTP1	glutathione S-transferase pi 1
-1.325	7220	TRPC1	transient receptor potential cation channel, subfamily C, member 1
-1.327	1152	CKB	creatine kinase, brain
-1.335	389421	LIN28B	lin-28 homolog B (C. elegans)
-1.339	160428	ALDH1L2	aldehyde dehydrogenase 1 family, member L2
-1.354	26278	SACS	spastic ataxia of Charlevoix-Saguenay (sacsin)
-1.360	1047	CLGN	calmegin
-1.366	53904	MYO3A	myosin IIIA
-1.373	23136	EPB41L3	erythrocyte membrane protein band 4.1-like 3
-1.378	9481	SLC25A27	solute carrier family 25, member 27

Results

-1.406	1462	VCAN	versican
-1.441	493869	GPX8	glutathione peroxidase 8 (putative)
-1.457	114805	GALNT13	UDP-N-acetyl-alpha-D-galactosamine:polypeptide N-acetylgalactosaminyltransferase 13 (GalNAc-T13)
-1.460	25945	PVRL3	poliovirus receptor-related 3
-1.461	26002	MOXD1	monooxygenase, DBH-like 1
-1.498	23462	HEY1	hairy/enhancer-of-split related with YRPW motif 1
-1.506	79649	MAP7D3	MAP7 domain containing 3
-1.527	2098	ESD	esterase D/formylglutathione hydrolase
-1.531	51678	MPP6	membrane protein, palmitoylated 6 (MAGUK p55 subfamily member 6)
-1.535	2070	EYA4	eyes absent homolog 4 (Drosophila)
-1.555	23111	SPG20	spastic paraplegia 20 (Troyer syndrome)
-1.555	57683	ZDBF2	zinc finger, DBF-type containing 2
-1.574	7754	ZNF204	zinc finger protein 204 pseudogene
-1.576	55081	IFT57	intraflagellar transport 57 homolog (Chlamydomonas)
-1.579	231	AKR1B1	aldo-keto reductase family 1, member B1 (aldose reductase)
-1.580	134637	ADAT2	adenosine deaminase, tRNA-specific 2, TAD2 homolog (S. cerevisiae)
-1.580	100131827	ZNF717	zinc finger protein 717
-1.589	55704	CCDC88A	coiled-coil domain containing 88A
-1.596	7762	ZNF215	zinc finger protein 215
-1.601	4281	MID1	midline 1 (Opitz/BBB syndrome)
-1.605	2201	FBN2	fibrillin 2

Results

-1.606	100130876	LOC1001308 76	hypothetical LOC100130876
-1.607	90843	TCEAL8	transcription elongation factor A (SII)-like 8
-1.614	10642	IGF2BP1	insulin-like growth factor 2 mRNA binding protein 1
-1.632	441459	ANKRD18B	ankyrin repeat domain 18B
-1.647	5325	PLAGL1	pleiomorphic adenoma gene-like 1
-1.661	135293	PM20D2	peptidase M20 domain containing 2
-1.673	3945	LDHB	lactate dehydrogenase B
-1.675	196968	C15ORF51	dynamamin 1 pseudogene
-1.704	5781	PTPN11	protein tyrosine phosphatase, non-receptor type 11
-1.730	2037	EPB41L2	erythrocyte membrane protein band 4.1-like 2
-1.753	7091	TLE4	transducin-like enhancer of split 4 (E(sp1) homolog, Drosophila)
-1.764	51280	GOLM1	golgi membrane protein 1
-1.765	116843	C6ORF192	chromosome 6 open reading frame 192
-1.821	3239	HOXD13	homeobox D13
-1.833	9353	SLIT2	slit homolog 2 (Drosophila)
-1.874	7345	UCHL1	ubiquitin carboxyl-terminal esterase L1 (ubiquitin thiolesterase)
-1.875	79659	DYNC2H1	dynein, cytoplasmic 2, heavy chain 1
-1.888	1373	CPS1	carbamoyl-phosphate synthetase 1, mitochondrial
-1.900	160897	GPR180	G protein-coupled receptor 180
-1.962	5836	PYGL	phosphorylase, glycogen, liver
-1.968	51299	NRN1	neuritin 1
-1.975	56952	PRTFDC1	phosphoribosyl transferase domain containing 1

Results

-1.990	6566	SLC16A1	solute carrier family 16, member 1 (monocarboxylic acid transporter 1)
-2.049	1825	DSC3	desmocollin 3
-2.083	54499	TMCO1	transmembrane and coiled-coil domains 1
-2.084	57631	LRCH2	leucine-rich repeats and calponin homology (CH) domain containing 2
-2.088	55117	SLC6A15	solute carrier family 6 (neutral amino acid transporter), member 15
-2.094	22873	DZIP1	DAZ interacting protein 1
-2.156	3202	HOXA5	homeobox A5
-2.163	22824	HSPA4L	heat shock 70kDa protein 4-like
-2.182	1038	CDR1	cerebellar degeneration-related protein 1, 34kDa
-2.203	5358	PLS3	plastin 3 (T isoform)
-2.375	55862	ECHDC1	enoyl Coenzyme A hydratase domain containing 1
-2.444	6594	SMARCA1	SWI/SNF related, matrix associated, actin dependent regulator of chromatin, subfamily a, member 1
-2.767	55086	CXORF57	chromosome X open reading frame 57
-2.818	3236	HOXD10	homeobox D10
-2.953	8471	IRS4	insulin receptor substrate 4

All the genes listed were either upregulated or downregulated in SHP2 miR1/2 BT474 tumors compared with CTRL tumors. The logarithmic fold change (Log FC), the Entrez gene ID, the gene name and description are shown.

Supplementary Table 2. Predicted let-7 targets within the “SHP2 signature” genes

Log FC	Entrez gene ID	Gene name	Description	Conserved sites	Total context score
-1.335	389421	LIN28B	lin-28 homolog B (<i>C. elegans</i>)	4	-1.12
-1.614	10642	IGF2BP1	insulin-like growth factor 2 mRNA binding protein 1	5	-0.82
-1.204	27031	NPHP3	nephronophthisis 3 (adolescent)	1	-0.53
-1.213	10052	GJC1	gap junction protein, gamma 1, 45kDa	1	-0.51
-1.266	586	BCAT1	branched chain aminotransferase 1, cytosolic	1	-0.43
-1.007	10643	IGF2BP3	insulin-like growth factor 2 mRNA binding protein 3	1	-0.38
-1.072	10644	IGF2BP2	insulin-like growth factor 2 mRNA binding protein 2	2	-0.37
-1.015	355	FAS	Fas (TNF receptor superfamily, member 6)	1	-0.35
-1.047	5962	RDX	radixin	1	-0.29
-1.378	9481	SLC25A27	solute carrier family 25, member 27	1	-0.28
-1.2	5563	PRKAA2	protein kinase, AMP-activated, alpha 2 catalytic subunit	1	-0.24
-1.073	894	CCND2	cyclin D2	3	-0.18
-1.245	3205	HOXA9	homeobox A9	1	-0.18
-0.968	6785	ELOVL4	elongation of very long chain fatty acids (FEN1/Elo2, SUR4/Elo3, yeast)-like 4	1	-0.18
-2.094	22873	DZIP1	DAZ interacting protein 1	1	-0.18
-1.117	4741	NEFM	neurofilament, medium polypeptide	1	-0.17
-0.948	117247	SLC16A10	solute carrier family 16, member 10 (aromatic amino acid transporter)	1	-0.15
-0.904	2774	GNAL	guanine nucleotide binding protein (G protein), alpha activating activity polypeptide, olfactory type	1	-0.09
-0.962	53344	CHIC1	cysteine-rich hydrophobic domain 1	1	-0.09
-1.04	1795	DOCK3	dedicator of cytokinesis 3	1	-0.08

All the genes listed are the predicted let-7 targets within the “SHP2 signature” genes according to the TargetScan 5.1 software (www.targetscan.org). The logarithmic fold change (Log FC), the Entrez gene ID, the gene name, the description, the number of conserved let-7 sites and the total context score (representing the sum of 1) site-type contribution, 2) 3' pairing contribution, 3) local AU contribution, and 4) position contribution) are shown.

Supplementary Table 3. Correlation of SHP2 expression and clinicopathological parameters in invasive breast carcinomas

	SHP2 Low	SHP2 High	OR (C.I.)	p value
ALL PATIENTS	40	314 (88.7%)		
AGE				
<50	20	136 (87.2%)	1.301 (0.671 - 2.526)	0.433
>=50	20	177 (89.8%)		
HISTOTYPE				
Ductal	34	263 (88.6%)	0.883 (0.371 - 2.452)	0.793
Lobular	6	41 (87.2%)		
pT				
1	21	179 (89.5%)	0.847 (0.434 - 1.669)	0.627
2-3-4	18	130 (87.8%)		
LN				
Neg.	18	165 (90.2%)	0.734 (0.375 - 1.419)	0.359
Pos.	22	148 (87.1%)		
GRADE				
G1	6	58 (90.6%)	0.814 (0.278 - 2.117)	0.686
G2 vs G1	15	118 (88.7%)		
G3 vs G1	14	100 (87.7%)	0.739 (0.25 - 1.951)	0.557
ER				
<10%	15	90 (85.7%)	1.5 (0.738 - 2.965)	0.25
>=10%	24	216 (90%)		
PR				
<10%	17	126 (88.1%)	1.124 (0.564 - 2.214)	0.735
>=10%	21	175 (89.3%)		
HER2				
Neg.	34	259 (88.4%)	1.838 (0.624 - 7.869)	0.33
Pos.	3	42 (93.3%)		
Ki67				
<16%	14	139 (90.8%)	0.68 (0.331 - 1.349)	0.278
>=16%	24	162 (87.1%)		
NPI				
GPG	10	92 (90.2%)	0.96 (0.388 - 2.327)	0.928
MPG	12	106 (89.8%)		
PPG	12	64 (84.2%)	0.58 (0.231 - 1.423)	0.234

SHP2 expression was measured by immunohistochemistry on tissue microarray (IHC-TMA). Odds ratio (OR) and 95% confidence intervals (CI) were obtained from logistic regression models. SHP2 expression was analyzed for correlation with the following clinicopathological parameters: age, tumor histotype, pathological assessment of the primary tumor (pT), lymph node status (LN), tumor grade, estrogen receptor status (ER), progesteron receptor status (PR), HER2 receptor status (HER2), Ki67 and nottingham prognostic index (NPI), divided into good (GPG), moderate (MPG) and poor (PPG) prognosis groups. The number of scored cases is lower than the total number of cases because: i) in some cases, individual cores detached from the slides during the manipulations; ii) clinical information was not available for all patients.

5.2 Research article published in Cell

Cell

Activation of Multiple Proto-oncogenic Tyrosine Kinases in Breast Cancer via Loss of the PTPN12 Phosphatase

Tingting Sun,¹ Nicola Aceto,^{1,10,14} Kristen L. Meerbrey,^{1,2,14} Jessica D. Kessler,^{1,2} Chunshui Zhou,¹¹ Ilenia Migliaccio,⁶ Don X. Nguyen,¹³ Natalya N. Pavlova,¹¹ María Botero,⁶ Jian Huang,⁶ Ronald J. Bernardi,³ Earlene Schmitt,^{1,2} Guang Hu,¹¹ Mamie Z. Li,¹¹ Noah Dephoure,¹² Steven P. Gygi,¹² Mitchell Rao,² Chad J. Creighton,^{4,5} Susan G. Hilsenbeck,^{4,5} Chad A. Shaw,² Donna Muzny,⁹ Richard A. Gibbs,^{2,5,9} David A. Wheeler,^{5,9} C. Kent Osborne,^{5,6,7,8} Rachel Schiff,^{5,6,7,8} Mohamed Bentires-Aij,^{10,15} Stephen J. Elledge,^{11,15} and Thomas F. Westbrook^{1,2,3,5,4}

¹Verna & Marrs McLean Department of Biochemistry & Molecular Biology

²Department of Molecular & Human Genetics

³Department of Pediatrics

⁴Division of Biostatistics

⁵Dan L. Duncan Cancer Center

⁶The Lester & Sue Smith Breast Center

⁷Department of Medicine

⁸Department of Molecular & Cellular Biology

⁹The Human Genome Sequencing Center

Baylor College of Medicine, One Baylor Plaza, Houston, TX 77030, USA

¹⁰Friedrich Miescher Institute for Biomedical Research, Basel CH-4002, Switzerland

¹¹Howard Hughes Medical Institute, Department of Genetics, Harvard Medical School, Division of Genetics, Brigham & Women's Hospital, Boston, MA 02115, USA

¹²Department of Cell Biology, Harvard Medical School, Boston, MA 02115, USA

¹³Department of Pathology, Yale University School of Medicine, New Haven, CT 06520, USA

¹⁴These authors contributed equally to this work

¹⁵These authors contributed equally to this work

*Correspondence: thomasw@bcm.edu

DOI 10.1016/j.cell.2011.02.003

SUMMARY

Among breast cancers, triple-negative breast cancer (TNBC) is the most poorly understood and is refractory to current targeted therapies. Using a genetic screen, we identify the PTPN12 tyrosine phosphatase as a tumor suppressor in TNBC. PTPN12 potently suppresses mammary epithelial cell proliferation and transformation. PTPN12 is frequently compromised in human TNBCs, and we identify an upstream tumor-suppressor network that posttranscriptionally controls PTPN12. PTPN12 suppresses transformation by interacting with and inhibiting multiple oncogenic tyrosine kinases, including HER2 and EGFR. The tumorigenic and metastatic potential of PTPN12-deficient TNBC cells is severely impaired upon restoration of PTPN12 function or combined inhibition of PTPN12-regulated tyrosine kinases, suggesting that TNBCs are dependent on the proto-oncogenic tyrosine kinases constrained by PTPN12. Collectively, these data identify PTPN12 as a commonly inactivated tumor suppressor and provide a rationale for combinatorial targeting proto-oncogenic tyrosine

kinases in TNBC and other cancers based on their profile of tyrosine-phosphatase activity.

INTRODUCTION

Breast cancer is the most common malignancy among women and is comprised of a heterogeneous group of diseases stratified into three major subtypes (Di Cosimo and Baselga, 2010; Jemal et al., 2008). Two of these are defined by expression of steroid hormone receptors (estrogen receptor [ER] and progesterone receptor [PR]) or amplification/overexpression of the receptor tyrosine kinase (RTK) HER2. Agents targeting these proteins have led to significant increases in patient survival (Osborne, 1998; Slamon et al., 1999). In contrast, the triple-negative breast cancer (TNBC) subtype is defined only by the absence of ER and PR expression or HER2 amplification, underscoring our lack of understanding of key pathways driving TNBC. TNBC comprises approximately 20% of breast cancer, and the prognosis for patients with TNBC is poor because of its propensity for recurrence and metastasis and a lack of effective targeted therapeutics (Hurvitz and Finn, 2009). Consequently, a major challenge remaining in breast cancer treatment is to identify aberrant signaling networks underlying this aggressive subtype of breast cancer.

Cell 144, 703–718, March 4, 2011 ©2011 Elsevier Inc. 703



Protein tyrosine phosphorylation plays a central role in cellular physiology and in cancer (Hunter, 2009). For instance, aberrant activation of the human epidermal growth factor receptor (HER) family of RTKs occurs frequently in many malignancies, including breast, lung, and brain cancer (Yarden and Sliwkowski, 2001). Although HER2 signaling is required for tumor maintenance in HER2-amplified disease (Slamon et al., 1989), the role of HER2 and other HER family tyrosine kinases (TKs) in breast cancer subtypes lacking HER2 amplification is unclear. Notably, in the absence of TK mutational activation or amplification, other pathways that regulate HER2 and other TKs may also be involved in tumorigenesis but remain to be elucidated.

Protein tyrosine phosphatases (PTPs) also regulate the equilibrium of tyrosine phosphorylation and, in principle, can serve as antagonists to TK signaling to play a prominent role in tumor suppression (Tonks, 2006). However, much less is known about the role of PTPs in suppressing tumorigenesis. In this study we have employed an unbiased functional screen for tumor suppressors and identified a role for the tyrosine phosphatase PTPN12 in TNBC. Loss of PTPN12 leads to malignant transformation of human mammary epithelial cells (HMECs) through multi-TK activation. PTPN12 function is frequently compromised in TNBC by deletions, defective sequence variants, or loss of expression, suggesting that HER2/EGFR and other RTK signaling is aberrantly activated in non-HER2-amplified breast cancers. Restoring PTPN12 expression in PTPN12-deficient TNBC cells inhibits their proliferation, tumorigenicity, and metastatic potential *in vivo*. These results identify PTPN12 as a tumor suppressor and suggest that combinatorial TK signaling is a key dependency in TNBC and, therefore, a target for cancer therapies.

RESULTS

PTPN12 Suppresses Transformation of HMECs

Signal transduction networks play key roles in the malignant behavior of cancer cells. To identify new networks that regulate cellular transformation in human breast cancer, we performed a genetic screen for kinases and phosphatases that suppress cellular transformation in genetically engineered HMECs (Figure 1A). HMECs isolated from healthy human breast tissue were transduced with lentiviruses expressing hTERT and SV40-Large T. These cells (herein termed TLM-HMECs) are immortal but do not proliferate in the absence of extracellular matrix (ECM) (Westbrook et al., 2005). For the screen we generated a shRNA library targeting all human kinases and phosphatases (six shRNAs/gene). TLM-HMECs were transduced with the shRNA library and assessed for cellular transformation by culturing in the absence of ECM. We isolated 530 anchorage-independent colonies from two independent screens and identified proviral shRNAs by sequencing. Genes identified in both replicate screens were considered candidate suppressors of transformation. Several genes were targeted by multiple independent shRNAs, including the well-documented tumor suppressors PTEN and LKB1 (Hemminki et al., 1998; Li et al., 1997).

The top-scoring candidate from this genetic screen was the PTP PTPN12 (aka PTP-PEST) (Yang et al., 1993). Many TKs have been shown to be important drivers of human cancer, but PTPs that antagonize proto-oncogenic TKs have not received

equal attention. Notably, PTPN12 has not been previously implicated in tumor suppression. Three independent PTPN12 shRNAs exhibited robust cellular transformation in TLM-HMECs (Figure 1C), and the degree of depletion correlated with the severity of the phenotype (Figures 1B and 1C). In addition, restoring PTPN12 expression with an exogenous PTPN12 cDNA completely suppressed transformation (Figure 1D), ruling out RNAi off-target effects. Collectively, these data indicate that PTPN12 is a potent suppressor of transformation in mammary epithelial cells.

Loss of PTPN12 Disrupts Proper 3D Acinar Formation of Mammary Epithelial Cells

Proper control of cell proliferation, survival, and polarity in the mammary epithelium is critical for normal mammary gland function, and dysregulation of these processes is considered to be a driver in breast cancer initiation and progression (Bissell et al., 2002). To determine whether PTPN12 regulates these processes during acini formation, we tested the effects of PTPN12 loss of function in 3D culture of MCF10A cells, a nontumorigenic mammary epithelial cell line. When cultured in semisolid ECM, these cells form a polarized acinar structure that resembles mammary acini *in vivo* (Petersen et al., 1992). MCF10A cells transduced with control- or PTPN12-shRNAs were analyzed for PTPN12 expression and formation of 3D acini (Figure 1E, and see Figure S1E available online). PTPN12 depletion significantly disrupted normal acini formation, with >85% forming aberrant structures (Figure 1E). Confocal microscopy revealed that PTPN12 loss of function significantly increased ectopic proliferation (Figures S1B and S1C) but did not lead to a compensatory increase in apoptosis (data not shown) like other oncogenic insults (Debnath et al., 2002), consistent with the significantly expanded cellularity and filled lumen in acini upon PTPN12 depletion. These observations suggest that PTPN12 is required to establish proper proliferative arrest during acinar formation.

To determine whether PTPN12 is required to maintain proliferative arrest in preestablished acini, we utilized an inducible shRNA vector that encodes a shRNA and tRFP on the same inducible transcript (Figure S1D, top panel) (Meerbrey et al., 2011). Addition of doxycycline (dox) results in tRFP fluorescence and PTPN12 depletion within 72 hr (Figure S1E). MCF10A cells encoding an inducible control- or PTPN12-shRNA were seeded in 3D culture, and after acini formation (day 9), dox was added to the culture medium, and acini morphology was assessed at day 15. Addition of dox had no effect in cells expressing control shRNA, but cells expressing PTPN12 shRNA exhibited a significant increase in aberrant acini (Figure S1F). Thus, PTPN12 is required to establish and maintain proliferative arrest in mammary epithelial acini.

PTPN12 Phosphatase Activity Is Required to Suppress Cellular Transformation

To determine the role of the PTPN12 phosphatase activity in transformation, we mutated amino acid C231 to S, which is known to ablate phosphatase activity (Garton et al., 1996). A shRNA-resistant PTPN12-C231S cDNA was transduced into TLM-HMECs expressing a PTPN12 shRNA. Unlike wild-type

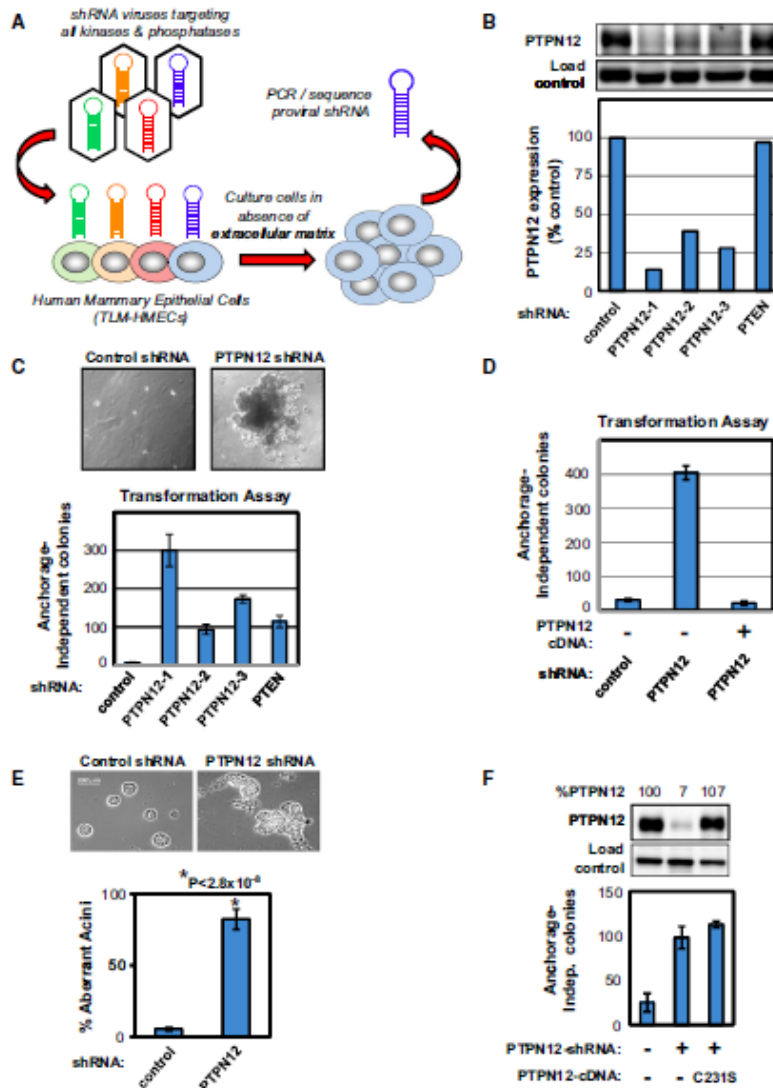


Figure 1. A Genetic Screen for Tumor Suppressors Identifies PTPN12

(A) Schematic of genetic screen for suppressors of HMEC transformation. A pool of retroviral shRNAs was transduced into TLM-HMECs in duplicate, and assessed for anchorage-independent proliferation. shRNAs were PCR amplified and sequenced from macroscopic colonies.

(B) Depletion of PTPN12. PTPN12 protein expression in TLM-HMECs transduced with vectors expressing the indicated shRNAs with quantification below.

(C) PTPN12 loss of function transforms TLM-HMECs. Anchorage-independent proliferation in TLM-HMECs transduced with the indicated shRNAs.

(D) Restoring PTPN12 expression suppresses transformation by PTPN12 shRNA. Anchorage-independent proliferation in TLM-HMECs transduced with control or PTPN12-shRNA in combination with PTPN12 cDNA as indicated.

(E) PTPN12 regulates acinar morphogenesis. MCF10A cells expressing the indicated shRNAs were analyzed for 3D acinar morphogenesis in vitro (day 15 after seeding) and quantified for the number of aberrant mammary acini.

(F) The enzymatic activity of PTPN12 is required for transformation suppression. TLM-HMECs expressing a PTPN12 shRNA were transduced with lentivirus-encoding control or shRNA-resistant PTPN12-C231S mutant cDNA and assessed for PTPN12 expression by western (top) and anchorage-independent proliferation (bottom).

Error bars represent standard error.

PTPN12 (Figure 1D), the C231S mutant had no effect on HMEC transformation (Figure 1F), suggesting that the tyrosine-phosphatase activity of PTPN12 is required for suppressing transformation.

PTPN12 Regulates an EGFR/HER2-Centered RTK Network in HMECs

To elucidate the role of the phosphatase activity of PTPN12 in suppressing transformation, it is critical to identify the phosphorylation events altered in response to PTPN12 loss. Thus, we used a quantitative proteome-wide method that combines anti-phosphotyrosine peptide immunoprecipitation, differential peptide labeling, and LC-MS/MS-based phosphopeptide identification and quantitation (Hsu et al., 2003) to search for phosphotyrosine-peptides whose abundance increases when PTPN12 is depleted. TLM-HMECs engineered with an inducible PTPN12-shRNA were profiled with and without PTPN12 depletion. We identified 99 phosphotyrosine peptides corresponding to 69 proteins whose tyrosine phosphorylation increased by greater than 1.5-fold in the absence of PTPN12 (see Table S1). Many of these proteins have been previously described to interact with PTPN12, including the known substrate p130CAS (or BCAR1). However, whereas p130CAS was highly phosphorylated, depletion experiments indicate it plays only a minor role in cellular transformation due to PTPN12 loss (Figure S2), suggesting that other signaling proteins may play more important roles in the tumor-suppressive function of PTPN12.

Analysis of these PTPN12-regulated proteins using Ingenuity and the Human Protein Reference Database (HPRD) resources revealed two highly connected protein-protein interaction networks. The number of interactions within this PTPN12-regulated network was highly enriched ($p < 0.001$, Monte Carlo procedure), consisting of 46% of all PTPN12-regulated proteins identified (Figures 2A and 2B). The first network consists of proteins and signaling pathways known to govern proliferation and survival in human cancer, with the RTK EGFR being a central component of both the literature-based Ingenuity network and the protein interaction-based HPRD network ($p < 0.001$, Monte Carlo procedure) (Figures 2A and 2B). The second network is comprised of proteins controlling the actin cytoskeleton, consistent with the role of PTPN12 in regulating cell motility and possibly metastasis (Angers-Loustau et al., 1999) (Figures S2A and S2B). Because EGFR and its related receptors play critical roles in breast cancer initiation and progression (Brandt et al., 2000; Muller et al., 1988; Slamon et al., 1989), we focused our

attention on the potential regulatory interaction between PTPN12 and the EGFR family of receptor TKs.

EGFR is one of four RTKs in the HER family, with HER2 playing the most prominent role in human breast cancer. These RTKs are known to promote cell survival and proliferation and signal via autophosphorylation and recruitment of additional substrates through recognition of these autophosphorylation sites (Yarden and Slwkowski, 2001). In principle, tyrosine phosphatases can counter the activity of these RTKs by dephosphorylation of RTK substrates or the RTKs themselves. To determine if PTPN12 interacts with EGFR and other RTKs in HMECs, we employed a bimolecular fluorescence complementation (BiFC) system (Giepmans et al., 2006; Kerppola, 2006). Each of the HER family RTKs (EGFR, HER2, HER3, and HER4) was fused on its C termini with the C-terminal half of YFP. These fusion cDNAs were transduced into TLM-HMECs expressing PTPN12 fused to the N terminus of YFP. If an interaction occurs between PTPN12 and the candidate RTK, this enables folding of the N- and C-terminal fragments of YFP to produce a fluorescent YFP protein (Figure 2C, left panel). EGFR and HER2 exhibited strong interaction with PTPN12, as determined by cellular YFP fluorescence (Figure 2C, right panel). In addition, HER2 interaction was enhanced with the substrate-trapping C231S mutant of PTPN12 (Figure 2D). These data suggest that PTPN12 may directly interact with and inhibit EGFR/HER2 signaling to suppress transformation.

PTPN12 Inhibits an EGFR/HER2-MAPK Signaling Axis to Suppress Cellular Transformation

HER2 and EGFR signal via homo- and heterodimerization and subsequent phosphorylation of their C-terminal tails on sites that serve as hubs for recruitment and activation of signaling complexes (Yarden and Slwkowski, 2001). To determine whether PTPN12 controls EGFR and HER2, we assessed the phosphorylation status of EGFR and HER2 in cells expressing an inducible PTPN12 shRNA. Depletion of PTPN12 led to an increase in HER2 (Y1248) and EGFR (Y1148) phosphorylation. Consistent with our phosphoproteomic data, the Y1148 residue of EGFR showed the strongest differential phosphorylation (>2-fold) in response to PTPN12 depletion (Figure 2E). Reciprocally, inducible expression of a PTPN12 cDNA in TLM-HMECs decreased HER2-pY1248 and EGFR-pY1148, but not other phosphotyrosine residues on EGFR (Figure 2F; data not shown). Thus, PTPN12 selectively regulates phosphorylation of a subset of tyrosine residues on EGFR and HER2.

Figure 2. PTPN12 Interacts with and Inhibits the HER2/EGFR Signaling Axis
(A and B) Tyrosine phosphoproteins regulated by PTPN12. HMECs expressing an inducible PTPN12-shRNA were quantified in the presence and absence of PTPN12 for tyrosine-phosphorylated peptides using a quantitative proteomic approach (described in Experimental Procedures). Interactions between the 69 PTPN12-regulated phosphoproteins were analyzed via (A) Ingenuity and (B) the HPRD.
(C) HER2 and EGFR RTKs interact with PTPN12 in HMECs. The left panel shows the experimental design of the BiFC system. PTPN12 was fused with the N terminus of YFP, and RTKs were fused with the C terminus of YFP. HMECs were transduced with retroviruses expressing PTPN12-N-YFP and individual RTK-C-YFP cDNAs. In the right panel the interaction between PTPN12 and HER family RTKs was assessed by cellular fluorescence. Asterisk indicates $p < 0.01$.
(D) Substrate-trapping PTPN12 mutant displays increased interaction with HER2. Breast cancer cells expressing PTPN12-WT-N-YFP or mutant PTPN12-C231S-N-YFP in combination with HER2-C-YFP were analyzed for cellular fluorescence.
(E) PTPN12 loss of function elicits hyperactivation of HER2, EGFR, and a MAPK-signaling cascade. HMECs engineered with an inducible PTPN12-shRNA were cultured \pm dox for 3 days, starved of growth factors, and analyzed for levels of the indicated total and phosphorylated proteins by western.
(F) PTPN12 suppresses HER2, EGFR, and MAPK signaling. HMECs engineered with an inducible PTPN12-cDNA were cultured and analyzed as in (E).
Error bars represent standard error.

We next evaluated the effects of PTPN12 suppression on known EGFR/HER2 effector pathways (RAS/MAPK and PI3K/AKT). PTPN12 depletion led to hyperactivation of ERK/RSK/S6 signaling but had no effect on phosphorylation of PI3K-effectors AKT and S6K1 (Figure 2E). Likewise, ectopic expression of PTPN12 decreased the phosphorylation of ERK/RSK/S6 but not PI3K signaling (Figure 2F). This is consistent with previous observations that pY1148 of EGFR serves as a binding site for the adaptor protein SHC and mediates activation of RAS-MAPK signaling (Batzer et al., 1995; Songyang et al., 1995). Furthermore, SHC is phosphorylated upon EGFR recruitment, and we found SHC1 phosphorylation on Y317 to be regulated by PTPN12 (Table S1). Taken together, these results indicate that loss of PTPN12 function leads to hyperphosphorylation of HER2/EGFR and activation of downstream RAS/MAPK signaling in HMECs.

To determine whether HER2/EGFR is required for transformation, TLM-HMECs expressing a dox-inducible PTPN12-shRNA were depleted of EGFR or HER2 (Figure 3A). Transformation by the PTPN12 shRNA was significantly impaired upon depletion of EGFR or HER2 (Figure 3B). Depletion of the adaptor protein SHC also reduced cellular transformation in response to a PTPN12 shRNA (Figures 3C and 3D), consistent with the hypothesis that PTPN12 suppresses transformation by inhibiting a HER2/EGFR/SHC/MAPK signaling axis. Furthermore, pharmacologic inhibition of HER2 and EGFR or MEK strongly suppressed transformation in cells depleted of PTPN12 (Figures 3E and 3F, respectively). Collectively, these data demonstrate that PTPN12 suppresses cellular transformation in HMECs by antagonizing HER2/EGFR phosphorylation and downstream MAPK signaling.

PTPN12 Is Inactivated by Mutation in Human TNBC

The role of PTPN12 in transformation and control of proto-oncogenic pathways led us to ask whether PTPN12 is inactivated in breast cancer. Initially, we examined whether the PTPN12 locus is deleted frequently in breast cancer by analyzing a publicly available data set of 243 human primary breast tumors and tumor-derived cell lines for which genomic copy number has been assessed (Beroukhi et al., 2010). Indeed, 22.6% of breast cancers exhibit evidence of deletion (one homozygous deletion of 15.0 Mb) at the PTPN12 locus, though the deletions exhibit a median size of 22.9 Mb, suggesting that multiple driver mutations may exist in this region. PTPN12 deletion in lung cancer was also frequent (13.8%) and typically encompassed large chromosomal regions (median deletion size of 22.2 Mb; two homozygous deletions of 1.3 and 0.7 Mb). An analysis of focal deletions (<2.0 Mb) encompassing PTPN12 in these tumors revealed a minimum common region (MCR) of only 0.61 Mb that spans five genes (Figure S3). These data suggest that PTPN12 is inactivated, in part, via deletion in a wide range of cancers and support the hypothesis that PTPN12 is a frequently inactivated tumor suppressor.

Because PTPN12 depletion leads to hyperactivation of HER2/EGFR, PTPN12 inactivation may occur more frequently in non-HER2-amplified human breast cancers. Therefore, to search for potential tumorigenic sequence variants, we sequenced the

coding exons of PTPN12 in 83 TNBCs and cell lines (75 primary tumors and eight cell lines). Primary sequence analysis revealed nonsynonymous sequence alterations in PTPN12 in 4.8% of TNBCs (three primary tumors; one tumor-derived cell line) (Figure 4A). Three variants were heterozygous, one was homozygous, and none was present in reference genomes or single-nucleotide polymorphism (SNP) databases. These amino acid changes (shown in Figure 4B) occurred in the highly conserved catalytic cleft of PTPN12 (H230Y) and within close proximity to a known protein-interaction domain (E690G and W699G) (Pao et al., 2007). In contrast we found no evidence of sequence alterations in 202 primary breast cancers from the other predominant breast cancer subtypes (ER+ and HER2-amplified), suggesting that PTPN12 may be inactivated more frequently in the TNBC subtype ($p < 0.001$, Fisher's exact test).

To determine whether these sequence variants affected PTPN12 function, wild-type (WT) or mutant PTPN12 cDNAs lacking the 3'UTR were introduced into TLM-HMECs expressing PTPN12 shRNA targeting the PTPN12 3'UTR. All cDNAs restored PTPN12 protein to endogenous levels (Figures 4C and 4D, top panels). Similar to WT PTPN12, the R30Q mutant suppressed PTPN12-shRNA induced transformation. In contrast, the three remaining tumor-derived mutants (H230Y, E690G, and W699G) did not suppress transformation. In fact, TLM-HMECs expressing these mutants formed 25%–60% more colonies than cells with PTPN12 shRNA alone (Figures 4C and 4D, bottom panels), suggesting that these loss-of-function PTPN12 mutations are potentially dominant negative.

We further examined whether the defective H230Y variant perturbed PTPN12 function in an independent system (MCF10A acinar formation). WT and H230Y mutant PTPN12 cDNAs were transduced into MCF10A cells expressing control- or PTPN12-shRNAs and were expressed at comparable levels (Figure S4). In contrast to WT PTPN12, the H230Y mutant did not suppress aberrant acini formation in the presence of PTPN12-shRNA (Figures 4F and 4G). In addition the H230Y mutant elicited aberrant acini in the presence of endogenous PTPN12, again suggesting dominant-negative activity. Although we were unable to determine if these defective variants were somatic tumor mutations due to the lack of patient-matched nontumor DNA, our functional data indicate that these defective PTPN12 variants are likely causal in TNBCs.

During sequencing of the PTPN12 locus, we observed a SNP occurring more frequently in tumors (7.3%, $n = 274$) than in non-disease control patients (2.5%, $n = 1142$) ($p = 0.004$) (Easton et al., 2007). Notably, this SNP results in a threonine to alanine change in PTPN12 (T573A). We have previously shown that this threonine is phosphorylated in cells (Dephoure et al., 2008), suggesting that this residue may have a regulatory function for PTPN12. Based on these observations, we tested the hypothesis that the PTPN12-T573A allele may have reduced ability to suppress transformation. Indeed, a PTPN12-T573A cDNA did not completely suppress transformation in PTPN12-depleted TLM-HMECs (Figure 4E) and conferred aberrant acinar morphogenesis in 3D culture (Figure 4H). These results suggest that the PTPN12 T573A SNP is a partial loss-of-function allele with dominant-negative properties. Intriguingly, our analysis of primary data from a genome-wide association study (GWAS) of

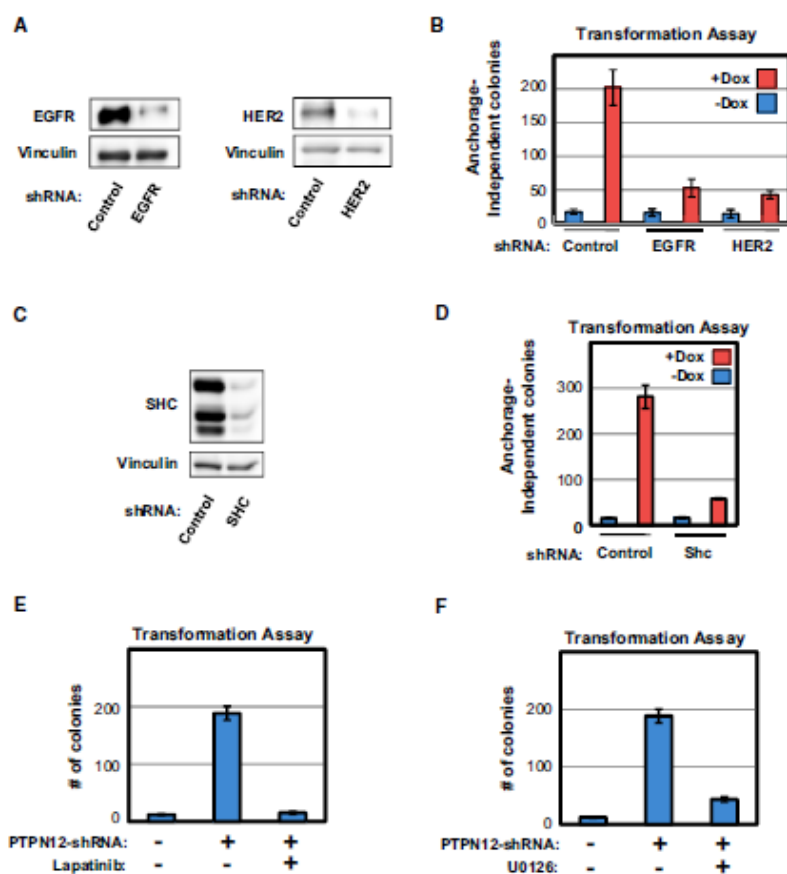


Figure 3. PTPN12 Suppresses Transformation by Inhibiting HER2/EGFR Signaling

(A) EGFR and HER2 depletion in TLM-HMECs. TLM-HMECs expressing control, EGFR, or HER2-targeting shRNAs were analyzed by western blotting for EGFR, HER2, and vinculin (loading control) as indicated.

(B) EGFR and HER2 RTKs are required for cellular transformation upon PTPN12 depletion. TLM-HMECs encoding an inducible PTPN12-shRNA were transduced with the indicated shRNAs and assessed for anchorage-independent proliferation \pm dox.

(C) SHC depletion in HMECs. TLM-HMECs expressing control or SHC-targeting shRNAs were analyzed by western for SHC and vinculin as indicated.

(D) SHC is required for cellular transformation upon PTPN12 depletion. TLM-HMECs encoding an inducible PTPN12-shRNA were transduced with the indicated shRNAs and assessed for anchorage-independent proliferation \pm dox.

(E) HER2/EGFR inhibitors block PTPN12 depletion-induced transformation. TLM-HMECs expressing the indicated shRNAs were assessed for anchorage-independent growth \pm a HER2/EGFR inhibitor (lapatinib).

(F) Transformation by PTPN12 inactivation requires MAPK signaling. TLM-HMECs expressing the indicated shRNAs were assessed for anchorage-independent proliferation \pm a MEK inhibitor (U0126).

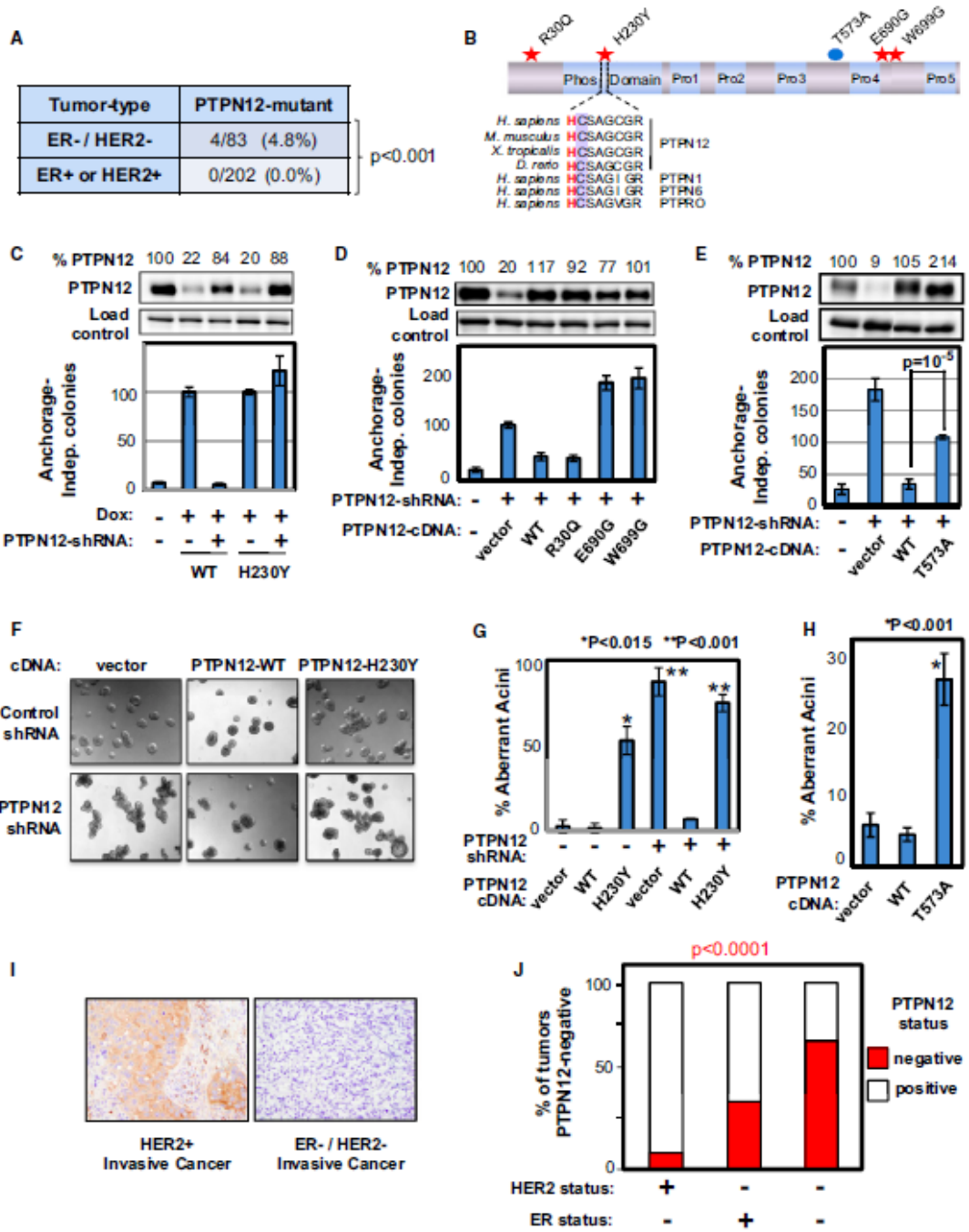
Error bars represent standard error.

SNPs contributing to breast cancer (Easton et al., 2007) revealed that the homozygous PTPN12-573A genotype occurred more frequently in the germline of patients with breast cancer. Although this observation did not reach statistical significance ($p = 0.2$), the trend (combined with our functional studies) is consistent with the allele conferring enhanced susceptibility to breast cancer. This raises the possibility that a relatively frequent allele of PTPN12 may confer a predisposition to breast cancer,

a hypothesis that will need to be rigorously tested in further experiments.

Loss of PTPN12 Expression Occurs More Frequently in TNBC

Our results suggest that PTPN12 functions as a suppressor of malignant transformation and may be inactivated in TNBC. Given the deletions and sequence alterations in PTPN12, we wished



to test whether PTPN12 function may also be frequently compromised by loss of expression. Unfortunately, PTPN12 mRNA expression is high in stromal compartments, thus precluding the use of RNA profiling to evaluate PTPN12 levels in public breast cancer data sets. To circumvent this problem we developed a specific immunohistochemical assay for PTPN12 protein (Figure S5A) and evaluated expression of PTPN12 in an independent cohort of 185 breast cancers. PTPN12 protein was consistently expressed in normal breast tissue (Figure S5B). In contrast, PTPN12 was undetectable in 37% of invasive breast cancers (example images shown in Figure 4I and Figure S5C). Strikingly, loss of PTPN12 expression occurred most frequently in TNBC (60.4% of TNBCs exhibit no detectable PTPN12 protein) (Figure 4J). In contrast, HER2-amplified tumors only rarely exhibited loss of PTPN12 expression (9.1% of HER2-amplified tumors). The near-mutual exclusivity of HER2 amplification and PTPN12 loss ($p < 0.0001$ by Fisher's exact test) suggests functional redundancy between these two events in tumorigenesis, and is consistent with the model that PTPN12 and HER2/EGFR RTKs operate in the same genetic pathway. Collectively, these results indicate that PTPN12 is frequently inactivated by deletion, sequence variation, or loss of protein expression, and PTPN12 loss of function may be a major determinant in aggressive TNBC.

PTPN12 Is Posttranscriptionally Regulated by a REST-miR-124 Network in Human Breast Cancer

Our observation that PTPN12 protein levels were frequently undetectable in primary human breast cancers led to us to examine the mechanism(s) by which PTPN12 expression is lost. By examining other suppressors of HMEC transformation, we observed that the tumor suppressor REST was also lost in primary breast cancers (example images in Figure 5A), and the expression of REST and PTPN12 was highly correlated ($p < 0.0001$; Figure 5B), suggesting that PTPN12 and REST may be

coordinately regulated. REST is a transcription factor that represses neuronal genes in non-neural tissues, and plays a prominent tumor suppressor role in epithelial tissues (Westbrook et al., 2005), though the mechanism by which REST suppresses tumorigenesis is poorly understood.

Based on the coordinate expression of REST and PTPN12 in human breast cancers and their similar phenotypes, we tested whether REST functions in a genetic pathway with PTPN12 by regulating its expression. Consistent with this hypothesis, transgenic REST expression led to a substantial increase in endogenous PTPN12 protein level in HCC70 (Figure 5C) and other TNBC cell lines (data not shown). Based on the established role of REST as a transcriptional repressor, we hypothesized that REST positively regulates PTPN12 expression via an indirect mechanism, perhaps by repressing an inhibitor of PTPN12 protein levels.

microRNAs are an emerging class of negative regulators, and we observed that the PTPN12 3'UTR has three evolutionarily conserved binding sites for miR-124 (Figure 5D), a microRNA suggested to play a role in neural development (Lim et al., 2005). Importantly, miR-124 is transcriptionally repressed by REST during organismal development, and REST inactivation leads to elevated miR-124 expression in cells and tissues (Conaco et al., 2006; Yoo et al., 2009). To determine whether miR-124 regulates PTPN12 protein levels, we ectopically expressed miR-124-3 in HMECs. Transgenic miR-124 expression led to a significant decrease in endogenous PTPN12 protein levels (Figure 5E), suggesting that miR-124 may in part mediate REST's ability to inhibit PTPN12 protein expression.

The ability of miR-124 to inhibit the PTPN12 tumor suppressor makes a strong prediction that miR-124 may function as an oncogene. Indeed, ectopic expression of miR-124 led to robust transformation of TLM-HMECs (Figure 5F), thus phenocopying PTPN12 loss of function. Consistent with the role of miR-124 as a putative human oncogene, we observed frequent and focal

Figure 4. PTPN12 Is Functionally Inactivated in Human TNBC via Multiple Mechanisms

(A) PTPN12 mutations occur more frequently in human TNBC. Frequency of mutations observed in TNBCs (75 primary tumors and eight cell lines) and 202 primary breast cancers positive for ER and/or HER2.
 (B) Schematic of PTPN12 mutations in TNBCs. Red stars indicate altered amino acids. The sequence surrounding the catalytic cysteine residue is expanded. The preceding histidine, H230, is conserved among all tyrosine phosphatases. The phosphatase domain (Phos Domain) and Proline rich regions (Pro1-5) are shown.
 (C) H230Y mutant PTPN12 fails to suppress transformation. TLM-HMECs expressing the PTPN12-shRNA were engineered with the indicated dox-inducible cDNAs. Cells were assessed for anchorage-independent growth.
 (D) E690 and W699 PTPN12 mutants fail to suppress transformation. TLM-HMECs expressing the PTPN12-shRNA were transfected with lentiviral PTPN12 cDNAs (as indicated) and assessed for anchorage-independent growth.
 (E) The PTPN12-T573A SNP is a partial loss-of-function allele for suppressing transformation. TLM-HMECs were transfected with PTPN12-shRNA in combination with lentiviral cDNAs encoding PTPN12-WT (threonine at residue 573), or PTPN12-T573A (alanine at residue 573). Cells were measured for anchorage-independent growth.
 (F) PTPN12-H230Y mutation disrupts proper acinar formation. MCF10A cells expressing control or PTPN12 shRNA in combination with wild-type or H230Y mutant PTPN12 were analyzed for 3D acinar formation (day 15 after seeding).
 (G) PTPN12-H230Y mutation disrupts proper acinar formation. Quantification of aberrant mammary acini from (F).
 (H) The PTPN12-T573A SNP allele disrupts acinar formation. MCF10A cells transfected with lentiviral cDNAs encoding control, PTPN12-WT (threonine at residue 573), or PTPN12-T573A (alanine at residue 573) as indicated were analyzed for 3D acinar morphogenesis in vitro (day 15 after seeding).
 (I) Loss of PTPN12 expression occurs more frequently in human TNBC. Primary human breast cancers ($n = 185$) were analyzed by immunohistochemistry for PTPN12 expression. Representative panels exhibiting positive PTPN12 expression in HER2-amplified breast cancer (left panel) and lack of expression in TNBC (right panel).
 (J) Loss of PTPN12 expression occurs predominantly in TNBC. Primary human breast cancers ($n = 185$) were analyzed by immunohistochemistry for PTPN12 expression. The number of samples showing no detectable PTPN12 expression (red area of bars) was quantified in HER2-positive, ER-positive, and triple-negative subtypes. Association between PTPN12 expression and breast cancer subtypes was tested by Fisher's exact test.
 Error bars represent standard error.

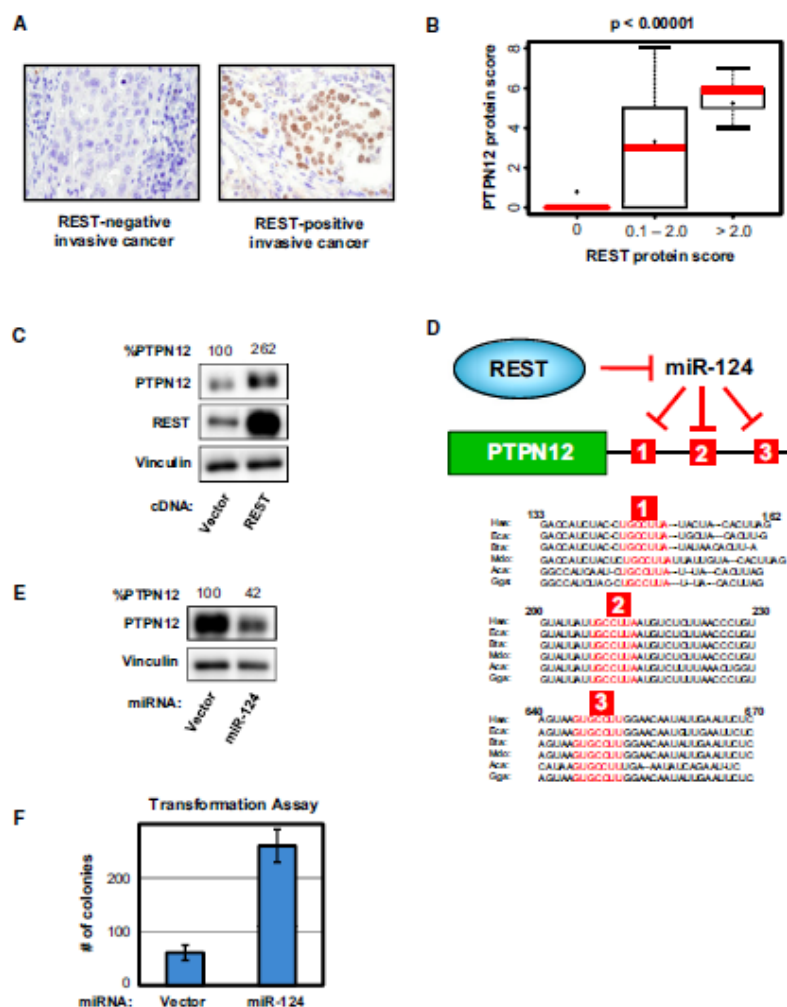


Figure 5. PTPN12 Is Regulated by the REST Tumor Suppressor via miR-124

(A) Loss of REST expression in human breast cancer. Primary human breast cancers (n = 185) were analyzed by immunohistochemistry for REST expression. Representative panels exhibiting negative and positive REST expression in invasive breast cancers.

(B) Loss of REST expression strongly correlates with loss of PTPN12 expression. Primary human breast cancers (n = 185) were analyzed by immunohistochemistry for REST and PTPN12 expression. The level of PTPN12 (y axis) is plotted for tumors with absent, intermediate, or high REST levels (x axis). The median and mean PTPN12 values for each group are represented by a solid red line and plus symbol, respectively. The boxes represent the 25th to 75th percentiles. Association between PTPN12 and REST expression was tested by Fisher's exact test. Error bars represent maximum and minimum observations within inner fences.

(C) Ectopic REST expression increases PTPN12 protein levels in REST-deficient TNBC cells. HCC70 TNBC cells were transfected with control or REST cDNA, cultured for 9 days, and analyzed for expression of REST and PTPN12 by western.

(D) Model for REST regulation of PTPN12 expression. REST regulates transcription of the neuronal microRNA miR-124. The PTPN12 3'UTR contains three conserved binding sites for miR-124. The sequences surrounding the three miR-124 binding sites are shown for human and five other vertebrate species.

(E) Ectopic miR-124 expression decreases PTPN12 protein levels in HMECs. HMECs were transfected with control or miR-124-containing plasmid, cultured for 7 days, and analyzed for PTPN12 expression by western.

(F) Ectopic miR-124 expression transforms TLM-HMECs. Cells from (E) were assessed for anchorage-independent proliferation. Error bars represent standard error.

amplifications of the miR-124-3 locus in human breast cancers (Figures S6A and S6C). In a cohort of 243 breast cancers (Beroukhi et al., 2010), 20.1% of tumors harbored amplifications in the miR-124-3 locus, defining a MCR of amplification of ~0.1 Mb and encompassing only two NCBI-annotated genes (including miR-124-3). miR-124-3 was similarly amplified (12.1%) in human lung cancers (Figures S6B and S6C), suggesting that miR-124-3 and possibly other oncogenes exist on these amplicons. Collectively, these data suggest that miR-124 may be a novel human oncogene in epithelial cancers that transforms cells, in part, by suppressing PTPN12 function.

PTPN12 Suppresses Growth and Metastasis of PTPN12-Deficient Breast Cancer Cells

The observations described above implicate PTPN12 as a tumor suppressor in TNBC. We next explored whether breast cancer cells are functionally dependent on PTPN12 inactivation. We first determined levels of PTPN12 in a panel of established breast cancer cell lines. PTPN12 levels were similar in normal HMECs and in HER2-amplified breast cancer cells (Figure 6A). In contrast, several TNBC cell lines exhibited low PTPN12 protein (Figure 6A), consistent with our observation that a significant fraction of TNBC tumors have low or undetectable PTPN12 protein (Figure 4J). To determine whether TNBC cells with low PTPN12 are sensitive to restoring PTPN12 levels, we transduced TNBC cells with control- or PTPN12-expressing retrovirus (Figure S7). As shown in Figures 6B and 6C, ectopic expression of PTPN12 decreased colony formation by TNBC cells, suggesting that these cells are sensitive to reconstituting PTPN12 function.

The ability of cancer cells to grow in microenvironments with altered or absent ECM is a hallmark of metastasis and is mimicked, in part, by *in vitro* culture in the absence of ECM support. Because our data indicate that PTPN12 is a potent suppressor of anchorage-independent proliferation (Figure 1), we tested the hypothesis that PTPN12 suppresses the metastatic propensity of TNBC cells. Notably, in our analysis of PTPN12 protein levels, we observed that the TNBC cell line MDA-MB231 exhibited high PTPN12, whereas a highly tumorigenic and metastatic subpopulation of MDA-MB231 ("MDA-MB231-LM2" cells; Minn et al. [2005]) exhibited 7-fold less PTPN12 (Figure 6D). We hypothesized that suppression of PTPN12 expression in this subpopulation of TNBC cells contributes to their aggressive tumorigenic and metastatic behavior. To test this hypothesis we engineered MDA-MB231-LM2 cells with a dox-inducible PTPN12 cDNA (Meerbrey et al., 2011) (termed "LM2-IP" cells) and tested whether PTPN12 restoration suppresses the tumorigenic and metastatic potential of LM2-IP cells. Addition of dox to LM2-IP cells resulted in PTPN12 protein levels comparable to parental MDA-MB231 cells (Figure 6D). To assay their tumorigenic potential, LM2-IP or parental MDA-MB231 cells were transplanted orthotopically into the mammary gland in the presence or absence of dox. As shown in Figure 6E, LM2-IP cells formed tumors rapidly. However, dox-induced PTPN12 expression significantly reduced the tumorigenicity of LM2-IP cells (Figure 6E; $p < 0.0001$) to the levels of parental MDA-MB231 cells. Lungs collected from these animals revealed significantly fewer metastases than dox-free animals (data not shown). However, interpretation of these results was partially

confounded by the significantly larger primary tumor burden of dox-free animals.

To circumvent the issue of tumor burden and directly assess the effects of PTPN12 on lung metastatic colonization and growth, we utilized an experimental model of metastasis (tail vein injection) that measures colonization and expansion in the lung. We injected LM2-IP cells into the tail vein, maintained animals in the presence or absence of dox, and monitored lung metastatic growth using luciferase luminescence-based imaging (examples shown in Figure 6F, top panels). LM2-IP cells injected into dox-free animals showed rapid expansion in the lung (Figure 6F, bottom panel), consistent with the previously reported behavior of MDA-MD231-LM2 cells (Minn et al., 2005). In contrast, LM2-IP cells exhibited a significantly reduced rate of expansion in dox-administered animals and showed no increase in lung metastatic growth after day 21. To confirm the luminescence-based readout, lungs were extracted from dox-positive and dox-negative animals at the experimental endpoint (day 35) and assessed for lung metastases. As shown in Figure 6G, dox-free animals showed significantly higher lung metastatic burden relative to dox-administered animals. Taken together, these data indicate that restoring PTPN12 function constrains the tumorigenic and metastatic behavior of aggressive TNBC cells.

PTPN12 Suppresses Proliferation and Tumorigenicity of TNBCs by Inhibiting Multiple RTKs

Together, our observations strongly suggest that restoring PTPN12 function impairs the tumorigenesis and proliferation of PTPN12-deficient TNBCs, suggesting that these cancers are dependent on the TK signaling constrained by PTPN12. Consequently, we sought to identify TKs regulated by PTPN12 in TNBC cells. Based on our observations that PTPN12 physically associates with and inhibits EGFR and HER2 RTKs in HMECs, we tested whether PTPN12 interacts with and regulates HER2 in PTPN12-deficient TNBC cells. BiFC analysis revealed a strong interaction between PTPN12 and HER2 in TNBC cells (Figure 7A, left panel). In addition, restoring PTPN12 expression in these cells decreased HER2 activity, as measured by HER2 tyrosine phosphorylation (Figure 7B). However, inhibition of HER family RTKs (HER2 and EGFR) with a pharmacologic inhibitor did not significantly affect the proliferation of these TNBC cells (Figure 7C), indicating that inhibition of HER2 and EGFR activity does not phenocopy PTPN12 restoration. Consequently, we hypothesized that PTPN12 regulates other TKs that, alone or in combination with HER2, are required for proliferation of TNBC cells.

To identify which additional TKs are regulated by PTPN12 in TNBC cells, we tested several candidate TKs from our proteomic analysis and previous reports (Cong et al., 2000; Markova et al., 2003) for interaction with PTPN12 in TNBC cells via BiFC. Notably, we observed a strong interaction between PTPN12 and PDGFR- β (Figure 7A, right panel), and ectopic PTPN12 expression reduced tyrosine phosphorylation of endogenous PDGFR- β (Figure 7B), suggesting that PTPN12 regulates this RTK in TNBCs. Notably, whereas inhibition of PDGFR- β alone had only a modest effect on TNBC proliferation, combined inhibition of HER2 family and PDGFR- β RTKs significantly impaired TNBC proliferation (Figure 7C).

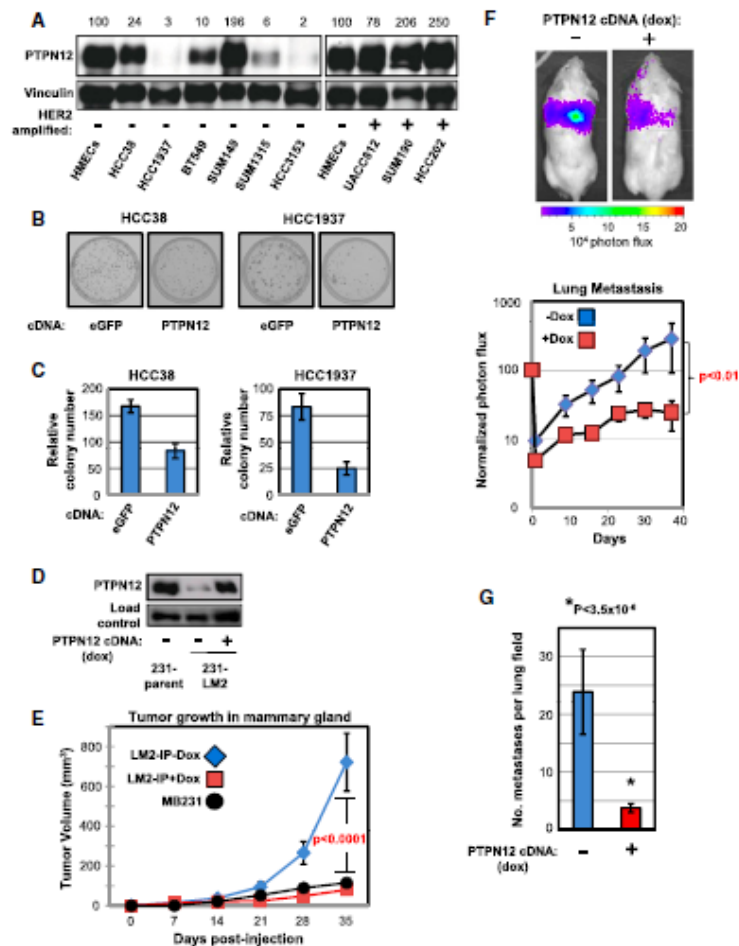


Figure 6. PTPN12 Suppresses Growth and Metastasis of TNBC Cells

(A) PTPN12 expression is reduced in TNBC cell lines. PTPN12 protein levels were quantified by western in HMECs, TNBC cells, and HER2-amplified breast cancer cells as indicated.

(B) Reconstituting PTPN12 expression suppresses proliferation in PTPN12-deficient breast cancer cells. TNBC cells expressing low endogenous PTPN12 were transduced with equivalent multiplicity of infection (moi) of retrovirus encoding eGFP (control) or PTPN12 cDNAs and analyzed for macroscopic colony formation in vitro.

(C) Reconstituting PTPN12 expression suppresses proliferation in PTPN12-deficient breast cancer cells. Quantification of colony number from cells in (B).

(D) PTPN12 expression is reduced in aggressive lung metastatic subpopulation of TNBC MDA-MB231 cells. PTPN12 protein expression was assessed in MDA-MB231 breast cancer cells (231-parent) and in MDA-MB231-LM2 subpopulation that exhibits enhanced primary and lung metastatic tumor growth. MDA-MB231-LM2 cells were engineered with an inducible PTPN12-cDNA (LM2-IP cells) that expresses similar PTPN12 levels as parental MDA-MB231 cells upon addition of dox.

(E) Restoring PTPN12 expression suppresses primary tumor growth in aggressive TNBC cells. Cells from (D) were transplanted in the mouse mammary gland and monitored for primary tumor growth in the presence or absence of dox (n = 12 for each group).

(F) Restoring PTPN12 expression suppresses lung metastatic growth in aggressive TNBC cells. Cells from (D) were tail vein injected and monitored for lung metastatic growth (via luminescence detection) in the presence or absence of dox (n = 6 for each group). Representative +dox and -dox images and quantification are shown in upper and lower panels, respectively.

(G) Restoring PTPN12 expression suppresses lung metastatic growth in aggressive TNBC cells. Cells from (D) were tail vein injected (as in F) in the presence or absence of dox (n = 7) and analyzed for lung metastatic lesions via standard H&E.

Error bars represent standard error.

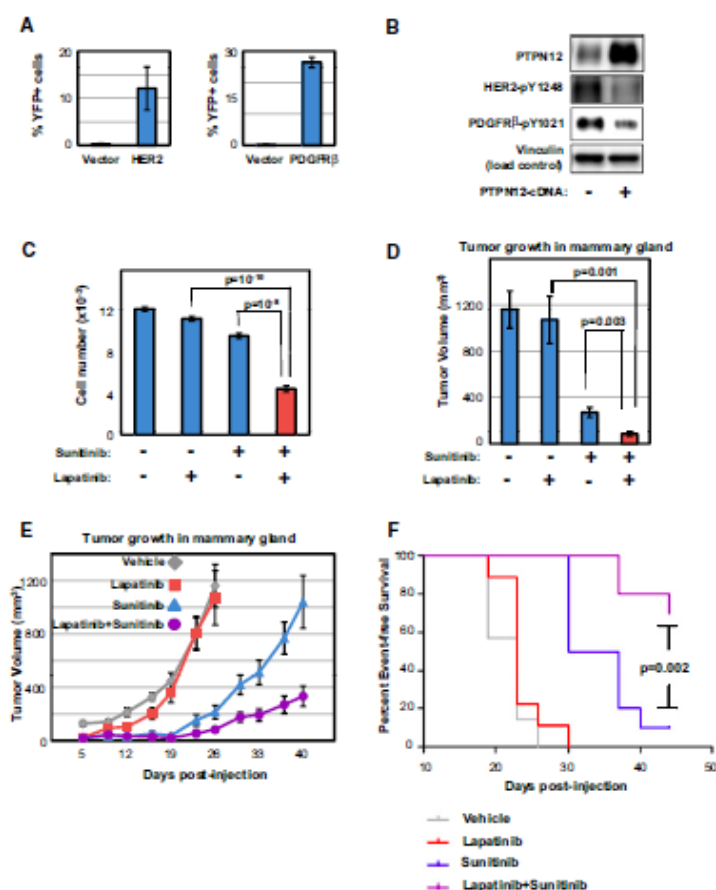


Figure 7. PTPN12 Inhibits Proliferation and Survival of TNBCs by Inhibiting Multiple RTKs

(A) HER2 and PDGFR- β RTKs interact with PTPN12 in TNBC cells. HCC1937 cells expressing PTPN12-N-YFP and individual RTK-C-YFP cDNAs (as indicated) were analyzed for cellular fluorescence using flow cytometry.

(B) Ectopic PTPN12 expression inhibits HER2 and PDGFR- β RTK signaling in TNBC cells. HCC1937 cells engineered with control or PTPN12-cDNA were assessed for PTPN12 expression and levels of phosphorylated HER2 and PDGFR- β by western.

(C) Combined HER family and PDGFR inhibitors suppress proliferation of PTPN12-deficient TNBC cells. HCC1937 cells were cultured \pm HER2/EGFR inhibitor lapatinib (1 μ M) \pm PDGFR inhibitor sunitinib (5 μ M) for 8 days. Cell numbers were determined by DAPI cell counting.

(D and E) Combined HER family and PDGFR inhibitors suppress tumorigenicity of PTPN12-deficient TNBC cells. MDA-MB231-LM2 cells were transplanted in the mouse mammary gland and monitored for primary tumor growth in the presence or absence of HER2/EGFR inhibitor (lapatinib) and PDGFR inhibitor (sunitinib) as indicated ($n = 10$ for each group). Tumor volumes on day 26 postinjection are shown in (D). Tumor growth curves are shown in (E).

(F) Combined HER family and PDGFR inhibitors extend event-free survival of animals harboring PTPN12-deficient TNBC tumors. Animals transplanted with MDA-MB231-LM2 cells (as above) were treated with the indicated inhibitor and monitored for tumor volume. Events are denoted as animals with tumors greater than 1000 mm³. Error bars represent standard error.

To determine whether PTPN12-deficient TNBCs are combinatorially dependent on the HER family and additional RTKs, such as PDGFR- β *in vivo*, we tested the effects of the pharmacologic inhibitors lapatinib and sunitinib alone or in combination on the tumorigenicity of aggressive PTPN12-deficient TNBCs. Lapatinib is a dual inhibitor of HER2 and EGFR, and sunitinib is an inhibitor of PDGFR- β and other TKs. MDA-MB231-LM2 cells were transplanted orthotopically, and mice were treated for 40 days with the indicated agents. Both agents were well tolerated by all animals at the administered doses (alone and in combination). Treatment with sunitinib alone resulted in a decrease in tumor growth rate (Figures 7D and 7E). Strikingly, whereas lapatinib alone did not affect tumor growth, lapatinib treatment significantly increased the efficacy of sunitinib in reducing tumor growth rate and burden ($p = 0.003$; Figures 7D and 7E). In addition, combination therapy resulted in a significant extension in event-free animal survival ($p = 0.002$; Figure 7F). These data suggest that PTPN12-deficient TNBC tumors may be combinatorially dependent on HER2 family and other RTKs.

Although our interaction and signaling studies suggest that PDGFR- β is one of these additional RTKs, and this is supported by the efficacy of sunitinib, given the broad specificity of sunitinib, it is possible that RTKs in addition to PDGFR- β may be involved. Thus, additional genetic and pharmacologic studies are necessary to determine the precise identities of the relevant RTKs driving tumorigenesis in tumors lacking PTPN12. Collectively, these studies identify PTPN12 as a significant tumor suppressor and illustrate a dependency on PTPN12-regulated TK signaling in TNBC, suggesting that these tumors may be successfully treated with the appropriate combination of TK inhibitors.

DISCUSSION

The Tyrosine Phosphatase PTPN12 Is a Tumor Suppressor in Human Breast Cancer

In this study, we demonstrate that the tyrosine phosphatase PTPN12 is a potent tumor suppressor in human breast cancer. Loss of PTPN12 phosphatase activity leads to aberrant acinar



morphogenesis and cellular transformation in mammary epithelial cells. PTPN12 is frequently compromised in breast cancer by deletion, inactivating sequence variants, or loss of expression. Importantly, in breast cancer cells exhibiting PTPN12 deficiency, restoring PTPN12 expression to levels observed in normal mammary epithelial cells suppresses proliferation, tumorigenesis, and metastasis. Together, these observations strongly support the conclusion that PTPN12 is a suppressor of human breast cancer.

A Network Governing Cellular Transformation and Tumor Suppression

Our study shows that PTPN12 functions in concert with a collection of other oncogenes and tumor suppressors in a serial inhibitory network culminating in the regulation of proto-oncogenic RTKs. We previously discovered that the oncogenic F box protein β -TRCP acts to negatively regulate the REST tumor suppressor (Westbrook et al., 2008). Here, we find that REST positively regulates PTPN12 levels, in part, by negatively regulating miR-124 that represses PTPN12 protein levels. Ectopic miR-124 expression can also transform HMECs, and miR-124 is focally and frequently amplified in epithelial cancers of the breast and lung, and is likely to act as an oncogene in these contexts. Thus, we have discovered an extensive network of serial negative regulation with alternating oncogenes and tumor suppressors consisting of β -TRCP, REST, miR-124, and PTPN12, which inhibits proto-oncogenic RTKs such as EGFR-HER2 to control cell proliferation, survival, and tumorigenesis.

The Role of PTPN12 and HER Family Receptors in "HER2-Negative" Breast Cancer

Approximately 20% of all breast cancers exhibit amplification and overexpression of HER2, and many of these malignancies are sensitive to HER2 inhibitors (Di Cosimo and Baselga, 2010). However, there is significant controversy as to whether HER2 and other HER family RTKs play a role in breast cancers that do not exhibit amplification/overexpression of the HER2 locus (termed "HER2-negative"). Our data support a model in which PTPN12 inactivation leads to HER2/EGFR hyperactivity and cellular transformation in HER2-negative breast cancers. This is supported by several observations. First, PTPN12 interacts with the HER2 and EGFR receptors in HMECs, and loss of PTPN12 function leads to hyperactivation of HER-receptor signaling in these cells. Conversely, transgenic expression of PTPN12 suppresses HER2 signaling in HMECs and PTPN12-deficient breast cancer cells. Second, PTPN12 inactivation leads to mammary epithelial cell transformation that is at least partially dependent on HER2 and EGFR. Third, HER2 activity is diminished in PTPN12-deficient breast cancers when PTPN12 expression is restored. Fourth, inhibitors of HER2 and EGFR, when combined with other TK inhibitors, reduce proliferation and tumorigenicity of HER2-negative breast cancers lacking PTPN12. Finally, we observe frequent inactivation of PTPN12 specifically in HER2-negative breast cancers (96% of PTPN12-deficient breast cancers were HER2 negative). This mutually exclusive relationship is consistent with PTPN12 and HER2 functioning in a common genetic pathway. Moreover, the frequent inactivation of PTPN12 in HER2-negative cancers suggests that

a significant subset of HER2-negative tumors may harbor aberrant HER2/EGFR signaling. Notably, whereas inhibitors targeting HER2 or EGFR individually have not been effective in HER2-negative breast cancers, dual EGFR/HER2 inhibitors have not been rigorously tested in HER2-negative cancers such as TNBC. Further studies will be necessary to determine whether dual EGFR/HER2 inhibitors in combination with other TK inhibitors are effective in HER2-negative cancers and whether PTPN12 represents a biomarker for sensitivity to such agents.

A New Rationale for Combinatorially Targeting TK Signaling in TNBC and Other Cancers

TKs have been shown to be critical pathogenetic drivers in some cancers, and the identification of oncogenic mutations and amplifications in TKs have provided important biomarkers for selecting cancers that are dependent on TK signaling and amenable to targeted therapies (Druker, 2004; Slamon et al., 1989). In contrast, TNBC is a particularly aggressive subtype of breast cancer for which no single, dominantly acting TK has been shown to drive the disease. Our discovery that PTPN12 is a tumor suppressor frequently inactivated in TNBC that acts as a negative regulator of HER2/EGFR and other TKs, such as PDGFR- β and ABL (Markova et al., 2003), raises the possibility that inhibitors of these proto-oncogenic TKs may be therapeutic in TNBC when used in the appropriate combination. In support of this prediction, our data indicate that lapatinib combined with another TK inhibitor (sunitinib) significantly reduces the proliferation and tumorigenicity of TNBCs. Given the prevalence of PTPN12 inactivation in TNBC and the addition of these cancers to PTPN12 dysfunction, it will be important to define the full spectrum of TKs that PTPN12 regulates in TNBC and other cancers in order to rationally combine agents targeting these kinases.

In summary, these studies establish an important role for tyrosine phosphatases in antagonizing tumorigenesis. Our observations raise the important prediction that many malignancies considered to be non-TK driven because of the absence of a dominant TK mutation may indeed be dependent on TK signaling. It is likely that in different cell types, different PTPs may play roles similar to PTPN12 in suppressing tumorigenesis, possibly by antagonizing different combinations of TKs. These studies provide a rationale for identifying and employing TK inhibitors to treat cancers not previously thought to be driven by TKs due to an absence of biomarkers for TK dependency. As noted above for TNBC, it is likely that these tumors would not be fully dependent on a single TK but, rather, a combination of TKs within the cell. Thus, a combinatorial inhibitor approach would be required to treat these cancers, most of which are likely to be untreatable today. Our studies warrant a closer examination of the status of tyrosine phosphorylation in what has been previously considered non-TK driven disease and the identification of TKs whose basal activity might combinatorially contribute to cancers harboring defects in PTPs.

EXPERIMENTAL PROCEDURES

Vectors

The shRNA library targeting human kinases and phosphatases (sh shRNAs/gene) was synthesized using published methods (Cleary et al., 2004) and

cloned into a MSCV-based retroviral vector. Individual GIPZ lentiviral shRNAs were from the Hannon-Bledge shRNA collection (Open Biosystems). shRNAs targeting the 3'UTR region of PTPN12 were designed using the BiopredSI and RNAi Codex algorithms. For inducible RNAi or overexpression experiments, shRNAs or cDNAs were subcloned into a dox-inducible lentiviral expression system (Meerbey et al., 2011).

Cell Culture

HMECs expressing hTERT and SV40 LT (TLM-HMECs) (Westbrook et al., 2005) were cultured in mammary epithelial growth medium (MEGM, Lonza). Lung metastatic MDA-MB231-LM2 cells (Minn et al., 2005) were cultured in DMEM (GIBCO) supplemented with 10% fetal bovine serum, 100 U/ml penicillin, and 100 µg/ml streptomycin. HCC1954, HCC38, and HCC1937 cells were cultured in RPMI-1640 (ATCC) supplemented with 10% fetal bovine serum, 100 U/ml penicillin, and 100 µg/ml streptomycin. MCF10A cells (from J. Brugge, Harvard Medical School) were grown as previously described (Petersen et al., 1992). All cell lines were incubated at 37°C and 5% CO₂. Stable cell lines expressing indicated shRNAs or cDNAs were generated by retroviral/lentiviral infection in the presence of 8 µg/ml polybrene, followed by selection with appropriate antibiotic-resistance markers.

Tumorigenicity and Experimental Metastasis Assays

Orthotopic tumorigenicity assays were performed as previously described (Minn et al., 2005). In drug treatment experiments, animals were gavaged with lapatinib (100 mg/kg) and/or sunitinib (40 mg/kg) once daily and monitored for tumor growth. For event-free survival analysis, events were denoted as animals with tumors greater than 1000 mm³. Comparison between groups was performed using Wilcoxon analysis. For experimental metastasis assays, NOD/SCID female mice (NCI) aged-matched between 5 and 7 weeks were treated with PBS or dox at 2 mg/kg by intraperitoneal (IP) injection. The 2 × 10⁵ cells were resuspended in 0.1 ml PBS and injected into the lateral tail vein. Lung metastatic progression was monitored and quantified using noninvasive bioluminescence as previously described (Minn et al., 2005). Linear model analyses (F test) were performed to test the effect of PTPN12 induction on tumorigenicity (tumor growth) or metastatic expansion (luminescence) in both assays.

SUPPLEMENTAL INFORMATION

Supplemental Information includes Extended Experimental Procedures, seven figures, and one table and can be found with this article online at doi:10.1016/j.cell.2011.02.003.

ACKNOWLEDGMENTS

We thank J. Luo, J. Rosen, and A. Lee for suggestions and critical reading of the manuscript. We are grateful to A. Lee, J. LaBaer, O. Lee, Z. Songyang, and J. Qin for providing reagents, and A. Ella for help with phosphopeptide analysis. This work was supported by a Susan G. Komen for the Cure Career Catalyst Award (KG090355) to T.F.W., S.P.O.R.E. developmental grant (P50 CA058183) to T.F.W., S.P.O.R.E. grant (P50 CA058183) to R.S. and C.K.O., grant HG3456 to S.P.G., and a U.S. Army Innovator Award (W81XWH0410197) to S.J.E. Research in the laboratory of M.B.-A. is supported by the Novartis Research Foundation, the European Research Council (ERC starting grant), the Swiss Cancer League, and the Krebsliga Belder Basel. S.J.E. is an investigator with the Howard Hughes Medical Institute. T.F.W. is a scholar of The V Foundation and Mary Kay Ash Foundation for Cancer Research.

Received: April 15, 2010
Revised: December 22, 2010
Accepted: February 1, 2011
Published: March 3, 2011

REFERENCES

- Angers-Loustau, A., Cote, J.F., Charest, A., Dowbenko, D., Spencer, S., Lasky, L.A., and Tremblay, M.L. (1999). Protein tyrosine phosphatase-PEST regulates focal adhesion disassembly, migration, and cytokinesis in fibroblasts. *J. Cell Biol.* 144, 1019–1031.
- Bakalanski, C.E., Elias, J.E., Villen, J., Haas, W., Gerber, S.A., Everley, P.A., and Gygi, S.P. (2008). The impact of peptide abundance and dynamic range on stable-isotope-based quantitative proteomic analyses. *J. Proteome Res.* 7, 4756–4765.
- Batzer, A.G., Blakie, P., Nelson, K., Schlessinger, J., and Margolis, B. (1995). The phosphotyrosine interaction domain of Shc binds an LKXNPXY motif on the epidermal growth factor receptor. *Mol. Cell Biol.* 15, 4403–4409.
- Beroukhi, R., Mermel, C.H., Porter, D., Wei, G., Raychaudhuri, S., Donovan, J., Barretina, J., Boehm, J.S., Dobson, J., Ueshima, M., et al. (2010). The landscape of somatic copy-number alteration across human cancers. *Nature* 463, 899–905.
- Bissell, M.J., Radisky, D.C., Rizki, A., Weaver, V.M., and Petersen, O.W. (2002). The organizing principle: microenvironmental influences in the normal and malignant breast. *Differentiation* 70, 537–548.
- Brandt, R., Eisenbrandt, R., Leenders, F., Zschiesche, W., Binas, B., Juergensen, C., and Theuring, F. (2000). Mammary gland specific hEGF receptor transgene expression induces neoplasia and inhibits differentiation. *Oncogene* 19, 2129–2137.
- Cleary, M.A., Kilian, K., Wang, Y., Bradshaw, J., Cavet, G., Ge, W., Kulkarni, A., Paddison, P.J., Chang, K., Sheth, N., et al. (2004). Production of complex nucleic acid libraries using highly parallel in situ oligonucleotide synthesis. *Nat. Methods* 1, 241–248.
- Conaco, C., Otto, S., Han, J.J., and Mandel, G. (2006). Reciprocal actions of REST and a microRNA promote neuronal identity. *Proc. Natl. Acad. Sci. USA* 103, 2422–2427.
- Cong, F., Spencer, S., Cote, J.F., Wu, Y., Tremblay, M.L., Lasky, L.A., and Goff, S.P. (2000). Cytoskeletal protein PSTPIP1 directs the PEST-type protein tyrosine phosphatase to the c-Abl kinase to mediate Abl dephosphorylation. *Mol. Cell* 6, 1413–1423.
- Debnath, J., Muthuswamy, S.K., and Brugge, J.S. (2003). Morphogenesis and oncogenesis of MCF-10A mammary epithelial cells grown in three-dimensional basement membrane cultures. *Methods* 30, 256–268.
- Debnath, J., Mills, K.R., Collins, N.L., Reginato, M.J., Muthuswamy, S.K., and Brugge, J.S. (2002). The role of apoptosis in creating and maintaining luminal space within normal and oncogene-expressing mammary acini. *Cell* 111, 29–40.
- Dephoure, N., Zhou, C., Villen, J., Beausoleil, S.A., Bakalanski, C.E., Eledge, S.J., and Gygi, S.P. (2008). A quantitative atlas of mitotic phosphorylation. *Proc. Natl. Acad. Sci. USA* 105, 10762–10767.
- Di Cosimo, S., and Baselga, J. (2010). Management of breast cancer with targeted agents: importance of heterogeneity. *Nat. Rev. Clin. Oncol.* 7, 139–147.
- Druker, B.J. (2004). Imatinib as a paradigm of targeted therapies. *Adv. Cancer Res.* 91, 1–30.
- Easton, D.F., Pooley, K.A., Dunning, A.M., Pharoah, P.D., Thompson, D., Ballinger, D.G., Struwing, J.P., Morrison, J., Field, H., Luben, R., et al. (2007). Genome-wide association study identifies novel breast cancer susceptibility loci. *Nature* 447, 1087–1093.
- Garton, A.J., Flint, A.J., and Tonks, N.K. (1996). Identification of p130(cas) as a substrate for the cytosolic protein tyrosine phosphatase PTP-PEST. *Mol. Cell Biol.* 16, 6408–6418.
- Garton, A.J., Bunham, M.R., Bouton, A.H., and Tonks, N.K. (1997). Association of PTP-PEST with the SH3 domain of p130cas: a novel mechanism of protein tyrosine phosphatase substrate recognition. *Oncogene* 15, 877–885.
- Glepmans, B.N., Adams, S.R., Ellsman, M.H., and Tsien, R.Y. (2008). The fluorescent toolbox for assessing protein location and function. *Science* 312, 217–224.



- Hemminki, A., Markie, D., Tomlinson, I., Avizienyte, E., Roth, S., Loukola, A., Bignell, G., Warren, W., Aminoff, M., Hoglund, P., et al. (1998). A serine/threonine kinase gene defective in Peutz-Jeghers syndrome. *Nature* 391, 184–187.
- Hsu, J.L., Huang, S.Y., Chow, N.H., and Chen, S.H. (2003). Stable-isotope dimethyl labeling for quantitative proteomics. *Anal. Chem.* 75, 6843–6852.
- Hunter, T. (2009). Tyrosine phosphorylation: thirty years and counting. *Curr. Opin. Cell Biol.* 21, 140–148.
- Hurvitz, S.A., and Finn, R.S. (2009). What's positive about 'triple-negative' breast cancer? *Future Oncol.* 5, 1015–1025.
- Jemal, A., Siegel, R., Ward, E., Hao, Y., Xu, J., Murray, T., and Thun, M.J. (2008). Cancer statistics, 2008. *CA Cancer J. Clin.* 58, 71–96.
- Keppola, T.K. (2006). Visualization of molecular interactions by fluorescence complementation. *Nat. Rev. Mol. Cell Biol.* 7, 449–458.
- Li, J., Yen, C., Liaw, D., Podsypanina, K., Bose, S., Wang, S.I., Puc, J., Milliaris, C., Rodgers, L., McCombie, R., et al. (1997). PTEN, a putative protein tyrosine phosphatase gene mutated in human brain, breast, and prostate cancer. *Science* 275, 1943–1947.
- Lim, L.P., Lau, N.C., Garrett-Engle, P., Grimson, A., Scheller, J.M., Castle, J., Bartel, D.P., Linsley, P.S., and Johnson, J.M. (2005). Microarray analysis shows that some microRNAs downregulate large numbers of target mRNAs. *Nature* 433, 769–773.
- Markova, B., Herrlich, P., Romstrand, L., and Bohmer, F.D. (2003). Identification of protein tyrosine phosphatases associating with the PDGF receptor. *Biochemistry* 42, 2691–2699.
- Matsuoka, S., Ballif, B.A., Smogorzewska, A., McDonald, E.R., 3rd, Hurov, K.E., Luo, J., Bakalarski, C.E., Zhao, Z., Solimini, N., Lerenthal, Y., et al. (2007). ATM and ATR substrate analysis reveals extensive protein networks responsive to DNA damage. *Science* 316, 1160–1168.
- Meerbrey, K.L., Hu, G., Kessler, J.D., Roarty, K., Li, M.Z., Fang, J.E., Herschkowitz, J.I., Burrows, A.E., Ciccia, A., Sun, T., et al. (2011). The pINDUCER lentiviral toolkit for inducible RNA interference in vitro and in vivo. *Proc. Natl. Acad. Sci. USA*. Published online February 9, 2011. 10.1073/pnas.1019736108.
- Mirn, A.J., Gupta, G.P., Siegel, P.M., Bos, P.D., Shu, W., Gif, D.D., Viale, A., Oshen, A.B., Gerald, W.L., and Massague, J. (2005). Genes that mediate breast cancer metastasis to lung. *Nature* 436, 518–524.
- Muller, W.J., Sinn, E., Pattengale, P.K., Wallace, R., and Lader, P. (1988). Single-step induction of mammary adenocarcinoma in transgenic mice bearing the activated *c-neu* oncogene. *Cell* 54, 105–115.
- Osborne, C.K. (1998). Tamoxifen in the treatment of breast cancer. *N. Engl. J. Med.* 339, 1609–1618.
- Pao, L.I., Badour, K., Siminovich, K.A., and Neel, B.G. (2007). Nonreceptor protein-tyrosine phosphatases in immune cell signaling. *Annu. Rev. Immunol.* 25, 473–523.
- Petersen, O.W., Ronnov-Jessen, L., Howlett, A.R., and Bissell, M.J. (1992). Interaction with basement membrane serves to rapidly distinguish growth and differentiation pattern of normal and malignant human breast epithelial cells. *Proc. Natl. Acad. Sci. USA* 89, 9064–9068.
- Slamon, D.J., Godolphin, W., Jones, L.A., Holt, J.A., Wong, S.G., Keith, D.E., Levin, W.J., Staut, S.G., Udove, J., Ullrich, A., et al. (1989). Studies of the *HER-2/neu* proto-oncogene in human breast and ovarian cancer. *Science* 244, 707–712.
- Songyang, Z., Margolis, B., Chaudhuri, M., Shoelson, S.E., and Cantley, L.C. (1995). The phosphotyrosine interaction domain of SHC recognizes tyrosine-phosphorylated NPXY motif. *J. Biol. Chem.* 270, 14863–14866.
- Tonks, N.K. (2006). Protein tyrosine phosphatases: from genes, to function, to disease. *Nat. Rev. Mol. Cell Biol.* 7, 833–846.
- Westbrook, T.F., Martin, E.S., Schlabach, M.R., Leng, Y., Liang, A.C., Feng, B., Zhao, J.J., Roberts, T.M., Mandel, G., Hamon, G.J., et al. (2005). A genetic screen for candidate tumor suppressors identifies REST. *Cell* 121, 837–848.
- Westbrook, T.F., Hu, G., Ang, X.L., Mulligan, P., Pavlova, N.N., Liang, A., Leng, Y., Mashir, R., Shi, Y., Harper, J.W., and Elledge, S.J. (2008). SCFbeta-TRCP controls oncogenic transformation and neural differentiation through REST degradation. *Nature* 452, 370–374.
- Yang, Q., Co, D., Sommercorn, J., and Tonks, N.K. (1993). Cloning and expression of PTP-PEST. A novel, human, nontransmembrane protein tyrosine phosphatase. *J. Biol. Chem.* 268, 6622–6628.
- Yarden, Y., and Skolnik, M.X. (2001). Untangling the ErbB signalling network. *Nat. Rev. Mol. Cell Biol.* 2, 127–137.
- Yoo, A.S., Stash, B.T., Chen, L., and Crabtree, G.R. (2009). MicroRNA-mediated switching of chromatin-remodelling complexes in neural development. *Nature* 460, 642–646.

Supplemental Information

EXTENDED EXPERIMENTAL PROCEDURES

Vectors and Virus Production

Individual GIPZ lentiviral shRNAs targeting PTPN12 (V2LHS_170948, V2LHS_170950, V2LHS_170952), EGFR (V2LHS_200678), HER2 (V2LHS_17671), SHC (V2LHS_152915) were from the Hannon-Elledge shRNA collection (Open Biosystems). The PTPN12 cDNA was recombined into a retroviral pQCXIN expression vector or a pQCXIN-N-YFP fusion vector (amino acid residues 1-155 of YFP) for ectopic expression and BiFC experiments, respectively. Sequence-verified human RTK cDNAs were obtained from the Harvard Institute of Proteomics collection and individually recombined into retroviral vectors with C-terminal-YFP (amino acid residues 156-239 of YFP) tag. PTPN12 mutants were generated by site-directed mutagenesis using QuickChange (Stratagene). Lentiviral or retroviral supernatants were generated by transient transfection of 293T cells following Mirus Bio's TransIT® transfection protocols and harvested 48 hr after transfection.

Immunoblotting

Cells were lysed in 1X SDS sample buffer (62.5mM Tris-HCl, pH6.8, 10% glycerol, 2% SDS, 2.5% β -mercaptoethanol) and heated at 95°C for 10min. The following antibodies were used for Western blotting: PTPN12 (Sigma HPA0070970); PTPN12 (Sigma P9109, MCF10A Western blotting only); vinculin (Sigma V9131); HER2 (Millipore 06-562); SHC (BD Transduction Laboratories 610878); phosphotyrosine (4G10, Upstate 05-1050X); phospho-HER2 (Y1248, Upstate 06-229); EGFR (Cell signaling 2232); phospho-EGFR (Y1148, Cell signaling 4404); phospho-EGFR (Y992, Cell signaling 2235); phospho-EGFR (Y845, Invitrogen 44-784G); phospho-EGFR (Y1045, Cell signaling 2237); Akt (Cell Signaling 2938); phospho-Akt (S473, Cell signaling 9271); MAPK (Cell signaling 9102); phospho-MAPK (T202/Y204, Cell signaling 4377); P90RSK (Cell signaling 9355); phospho-P90RSK (S380, Cell signaling 9335); S6 (Cell signaling 2217), phospho-S6 (S235/S236, Cell signaling 2211); phospho-P70 S6 Kinase (T421/S424) (Cell signaling 9204); phospho-PDGFR β (Y1021, Cell signaling 2227); p130cas (BD Transduction Laboratories 610271); REST (Upstate).

shRNA Screen

A genetic screen for suppressors of HMEC transformation was performed as described (Westbrook et al., 2005) with the following modifications. Briefly, TLM-HMECs were transduced in 2 independent replicates with a pooled collection of shRNAs targeting all kinases and phosphatases (6 shRNAs per gene) and were subject to anchorage-independent proliferation assays as described above. Proviral shRNAs were identified from 530 anchorage-independent colonies by PCR-recovery and sequencing. shRNAs identified in both replicate screens were considered to be targeting candidate suppressors of transformation.

Three-Dimensional Culture and Transformation Assays and Proliferation Assays

MCF10A cells expressing a constitutive control (CTRL) or PTPN12 shRNA, or inducible CTRL or PTPN12 shRNA were grown in Growth Factor Reduced BD Matrigel Matrix (BD Biosciences) and stained with TO-PRO3 (Invitrogen) and anti-Ki67 antibody (Zymed) as previously described (Debnath et al., 2003). 500 ng/ml of doxycycline was added to the medium at the indicated day and refreshed every 2 days to induce and maintain the expression of the shRNA. For analysis of aberrant acini, at least 4 replicates were performed (150 acini counted per replicate). For proliferation analysis in 3D, Ki67-positive cells were counted in at least 50 acini per replicate (3 replicates per experiment) using image software. Two-tailed t tests were used to test differences between groups. Anchorage-independent proliferation assays were performed as described (Westbrook et al., 2005).

For colony formation assays, breast cancer cells were transduced with equivalent multiplicity of infection (moi) of retroviruses encoding eGFP (control) or PTPN12 cDNAs, seeded at a density of 6,000 cells per 6cm plate 2 days after infection, selected with 800 μ g/ml neomycin and cultured until macroscopic colonies formed. All assays were performed in triplicate or quadruplicate and were repeated at least twice. Two-tailed t tests were used to test differences between groups.

For in vitro 2D proliferation experiments, cells were seeded in 96-well plates, cultured +/- 1 μ M lapatinib, +/- 5 μ M sunitinib (8 replicates each) for 8 days, and incubated with 10 μ g/ml Hoechst 33342 (Invitrogen, H3570) for 15 min. Fluorescent microscopy was performed with an ImageXpress Micro microscope (Molecular devices). Cell numbers were determined by nuclei counts using the MetaXpress software. All assays were performed n = 12 for each treatment. Two-tailed t tests were used to test differences between groups.

Phosphotyrosine Peptides Quantitative Profiling

Tryptic phosphopeptide preparation and purification was performed as described (Matsuoka et al., 2007). In vitro dimethyl labeling of peptides was performed based on a previous method with modifications (Hsu et al., 2003). Briefly, 20 mg of peptides were dissolved in 7 ml of 1M HEPES (pH 7.5), 0.56 ml of 0.6M NaCNBH3 and 0.56 ml of 4% formaldehyde were added to PTP shRNA treated peptides for light labeling, and 0.56 ml of 0.6M NaCNBD3 and 0.56 ml of 4% formaldehyde-D2 (Sigma) were added to untreated control peptides for heavy labeling, vortexed and incubated at 25°C for 20 min. 1.68 ml of 100% AcOH was added to quench each reaction. Dimethylated peptides were desalted by using a Sep-Pak C18 cartridge (Waters) respectively, and the light and the heavy labeled eluates were combined together and lyophilized.

For pY phosphoantibody mediated immunoprecipitation, 40 mg peptides were dissolved in 1 ml of IP buffer (100mM MOPS, pH 7.2, 10 mM sodium phosphate, 50 mM NaCl), then mixed with 100 μ l of anti-phospho Tyrosine P-Tyr-100 antibody beads (Cell



Signaling) and incubated overnight at 4°C. After washing with IP buffer three times and ddH₂O twice, the bound phosphopeptides were eluted with 0.015% TFA and dried by speed vacuum. All eluted phosphopeptide samples were further cleaned up by stage tip chromatography. Each sample was analyzed by LC-MS/MS in a hybrid Orbitrap mass spectrometer (Thermo Eletron, CA). MS/MS spectra were searched via the SEQUEST algorithm against a composite data-base containing the human IP1 protein database and its reversed complement. Search parameters allowed for dynamic modifications of 80 Da (phosphorylation) on tyrosine, 26 Da for light labeled or 30 Da for heavy labeled on an N-terminal residue and any mis-cleaved Lysine residues. Matches were filtered with common parameters (mass deviation, XCorr, dCr), using decoy matches < 0.1% matches to reverse sequences as a guide. Automated peptide quantification was performed by using the Vista program (Bakalanski et al., 2008).

Network connections within the PTPN12-regulated protein set were analyzed via 2 resources: Ingenuity Pathway Analysis and the Human Protein Reference Database (HPRD). Data analysis with the Ingenuity Pathways Analysis package was performed as described (Ingenuity Systems, <http://www.ingenuity.com>). To determine protein-protein interaction networks within PTPN12-regulated proteins, the HPRD database of human protein interactions was obtained (<http://www.hprd.org/>), and all interactions between pairs of these proteins were identified. To examine the significance of the observed connectivity in the PTPN12-regulated network, a Monte Carlo procedure was utilized in which 69 random proteins (in the HPRD database) were analyzed for protein-protein interaction network. Two outcome statistics were calculated for each simulation: the size of the largest connected component of the network and the number of connections of the most connected node. We performed 10,000 such simulations to determine the distribution of the standard error measures for a network determined by random proteins.

Bimolecular Fluorescence Complementation (BiFC)

N-terminal domain (residues 1–155) of Venus YFP was fused N-terminal to PTPN12 (bait). C-terminal domain (residues 156–239) of Venus YFP was fused C-terminal to 35 human RTKs (prey). TLM-HMECs were transduced with retroviruses encoding bait and individual preys. Cell fluorescence was analyzed by flow cytometry in triplicate.

Copy Number Analysis

The Tumorscape segmented copy number data from 243 human breast cancers and 734 human lung cancers was downloaded from the Tumorscape website (Beroukhi et al., 2010) and loaded into a MySQL database where analysis could be performed. Focal events were defined to be no greater than 2.0 Mb in length and (log₂ratio > 0.15 (amplification) or < -0.15 (deletion)). The resulting dataset was queried for focal events that overlapped the target gene in the desired cancer type from the tumorscape segmental events database.

Tumor Sequencing

Genomic DNA was extracted from a cohort of 277 primary breast cancers (The Lester and Sue Smith Breast Center at BCM) and 8 breast cancer cell lines (ATCC). All coding exons of PTPN12 were amplified and sequenced using standard Sanger methods (primer sequences and sequencing data available upon request).

Immunohistochemistry of Primary Breast Cancers

A PTPN12 immunohistochemical assay (antibody: Sigma HPA007097) was optimized and validated on paraffin-embedded cell pellets from human mammary epithelial cells (HMECs with or without PTPN12-shRNA expression (to confirm depletion of immuno-reactive signal). The specificity of the antibody was also confirmed as a single immuno-reactive species by western analysis on HMECs with a control- or PTPN12-shRNA. PTPN12 protein expression was analyzed in a cohort of 185 human invasive breast cancers (purchased from Asterand, plc). ER, PR, and HER2 status were provided by Asterand, plc. and confirmed by independent IHC (J.H. and I.M., unpublished data). Four μm sections of primary tumors were immunostained using standard protocols. Briefly, antigen retrieval was performed by heating in 0.1 M Tris-HCl buffer (pH 9.0). Sections were incubated with PTPN12 primary antibody at a dilution of 1:100. Slides were incubated with secondary biotinylated antibody and subsequently with streptavidin-peroxidase. The enzyme was visualized after a 15 min incubation with diaminobenzidine (DAB). Slides were counterstained with hematoxylin. Positive and negative controls were included in each staining.

Cytoplasmic PTPN12 was evaluated according to the percentage of positively stained cells and staining intensity based on a score that ranges from 0 to 4: 0 = negative; 1 = < 50% of cells positive with low intensity; 2 = > 50% of cells positive with low intensity or < 50% with intermediate intensity; 3 = > 50% of cells positive with intermediate intensity or < 50% with high intensity; 4 = > 50% of cells positive with high intensity). PTPN12 expression was evaluated by a pathologist (IM) who was blinded to tumor characteristics. The association between PTPN12 expression and subtype or HER2-status was tested by Fisher's Exact test.

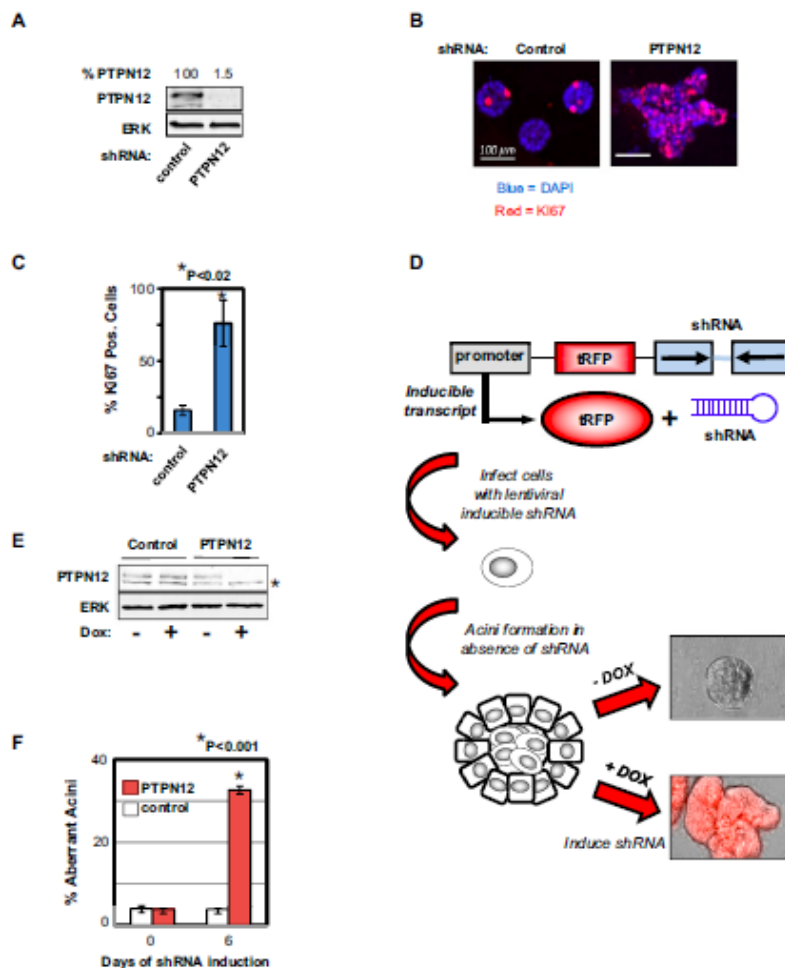


Figure S1. PTPN12 Is Required for Establishment and Maintenance of Proliferative Arrest during Mammary Acinar Morphogenesis, Related to Figure 1

(A) PTPN12 depletion in MCF10A cells expressing control or PTPN12-targeting shRNAs (from Figure 1E) were analyzed by western for PTPN12 and ERK2 (loading control) in top and bottom panels, respectively.

(B) PTPN12 regulates proliferation during acinar morphogenesis. MCF10A cells (from Figure 1F) expressing control or PTPN12 shRNA were cultured in 3D for 15 days and analyzed for Ki67 as a marker of proliferation.

(C) Quantification of Ki67-positive cells in mammary acini from (B).

(D) Schematic of experimental design for testing PTPN12 function in established mammary acini using an inducible (doxycycline-dependent) shRNA system. Inducible shRNA lentiviral vector (top panel) expresses a cassette encoding Turbo-RFP (tRFP) and the shRNA of interest. MCF10A cells transduced with an inducible shRNA vector targeting PTPN12 (or control) were seeded into 3D culture in the absence of doxycycline. After formation of acini (day 9), cells were cultured ± doxycycline for 6 days and analyzed for aberrant acini.

(E) PTPN12 depletion in MCF10A cells expressing inducible PTPN12 shRNA. MCF10A cells were infected with lentivirus expressing doxycycline-inducible control or PTPN12 shRNA and tRFP cDNA. Cells were cultured ± doxycycline for 3 days and analyzed by western for the indicated proteins. Asterisk (*) indicates non-specific band.

(F) PTPN12 is required to maintain proliferative arrest in established mammary acini. MCF10A cells expressing dox-inducible control- or PTPN12-targeting shRNAs and tRFP cDNA (from E) were quantified for aberrant acini formation. In the presence of dox, only acini exhibiting red fluorescence were analyzed for normal and aberrant acini.

Error bars represent standard error.

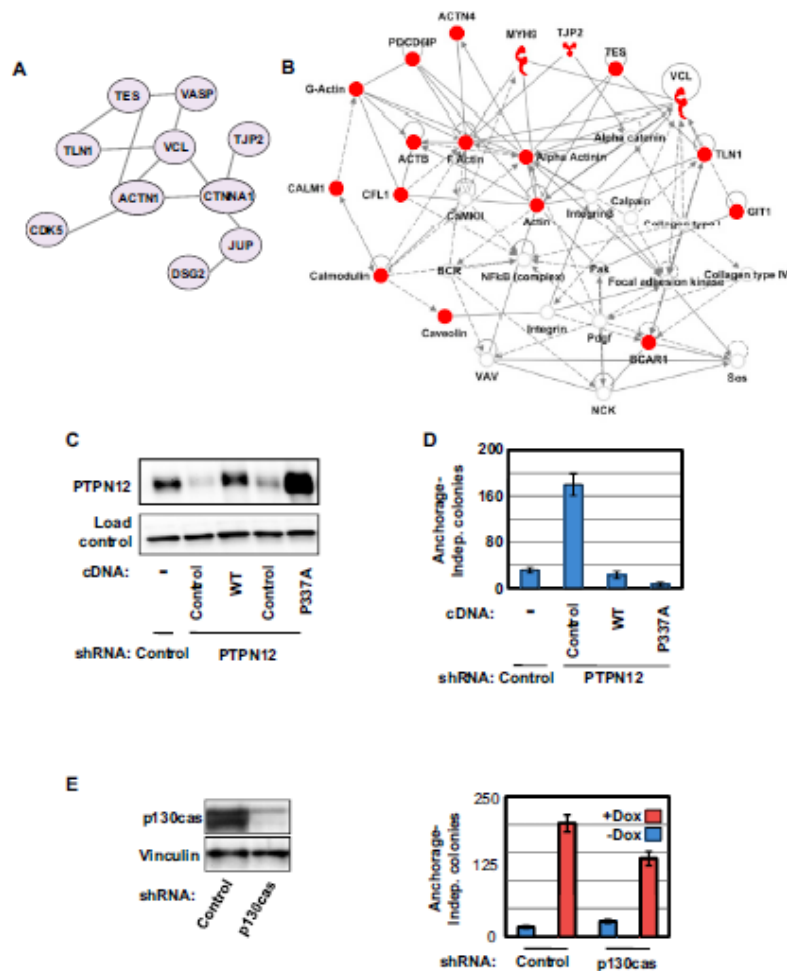


Figure S2. Cytoskeletal Networks of PTPN12-Regulated Phosphoproteins and Determination that p130CAS Is Not a Primary Mediator of PTPN12's Suppression of HMEC Transformation, Related to Figure 2

(A and B) HMECs expressing an inducible PTPN12-shRNA were profiled in the presence and absence of PTPN12 for tyrosine-phosphorylated peptides using a quantitative proteomic approach (described in Experimental Procedures). Interactions between the 69 PTPN12-regulated phosphoproteins were analyzed via (A) the Human Protein Reference Database and (B) Ingenuity and visualized using a custom software package. Shown are protein networks involved in regulating the actin-cytoskeleton.

(C) TLM-HMECs expressing control or PTPN12-shRNA were transduced with lentiviral vectors expressing cDNAs encoding PTPN12-WT or a mutant PTPN12-P337A defective in binding p130CAS (Garton et al., 1997) as indicated. Cellular lysates were analyzed for PTPN12 expression.

(D) PTPN12-P337 mutant suppresses transformation. TLM-HMECs engineered with the indicated shRNAs and cDNAs (cells from (C)) were measured for anchorage-independent proliferation.

(E) Depletion of p130CAS has a modest effect on transformation upon PTPN12-depletion. TLM-HMECs encoding an inducible PTPN12-shRNA were transduced with control or p130CAS-targeting shRNAs and assessed for p130CAS expression by western (left panel) and anchorage-independent proliferation \pm doxycycline (right panel).

Error bars represent standard error.

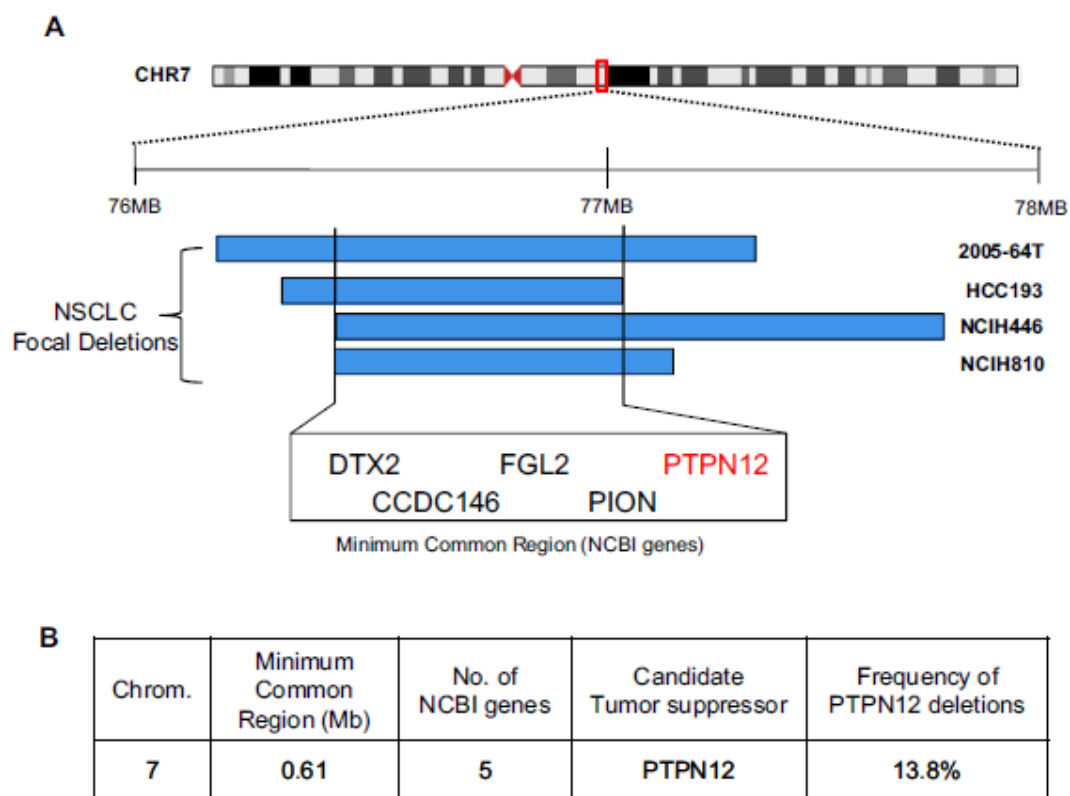


Figure S3. PTPN12 Is Focally and Frequently Deleted in Human Lung Cancer, Related to Figure 4

(A) Focal deletions target the PTPN12 locus in human non-small cell lung cancers (NSCLCs). Segmental copy-number data for 734 NSCLC samples was retrieved from Tumorscape (Beroukhi et al., 2010) and analyzed for focal deletions less than 2 Mb. 4 focal deletions targeting the PTPN12 locus were identified, with a minimum common region (MCR) of 0.61 Mb encompassing 5 NCBI-annotated genes.

(B) The PTPN12 locus is targeted by focal and frequent deletions in NSCLC. Table listing the characteristics of an MCR targeting PTPN12. The far right column indicates the total percentage of NSCLC tumors with evidence of PTPN12 deletion.

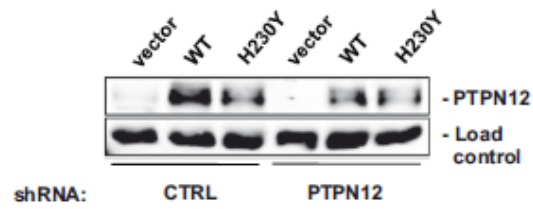


Figure S4. Restoring PTPN12 Expression in PTPN12-shRNA MCF10A Cells, Related to Figure 4
MCF10A cells were transduced with a lentiviral shRNA targeting endogenous PTPN12 in combination with lentiviruses encoding control, PTPN12-WT, or PTPN12-H230Y cDNAs as indicated. These cells were analyzed in Figure 4G.

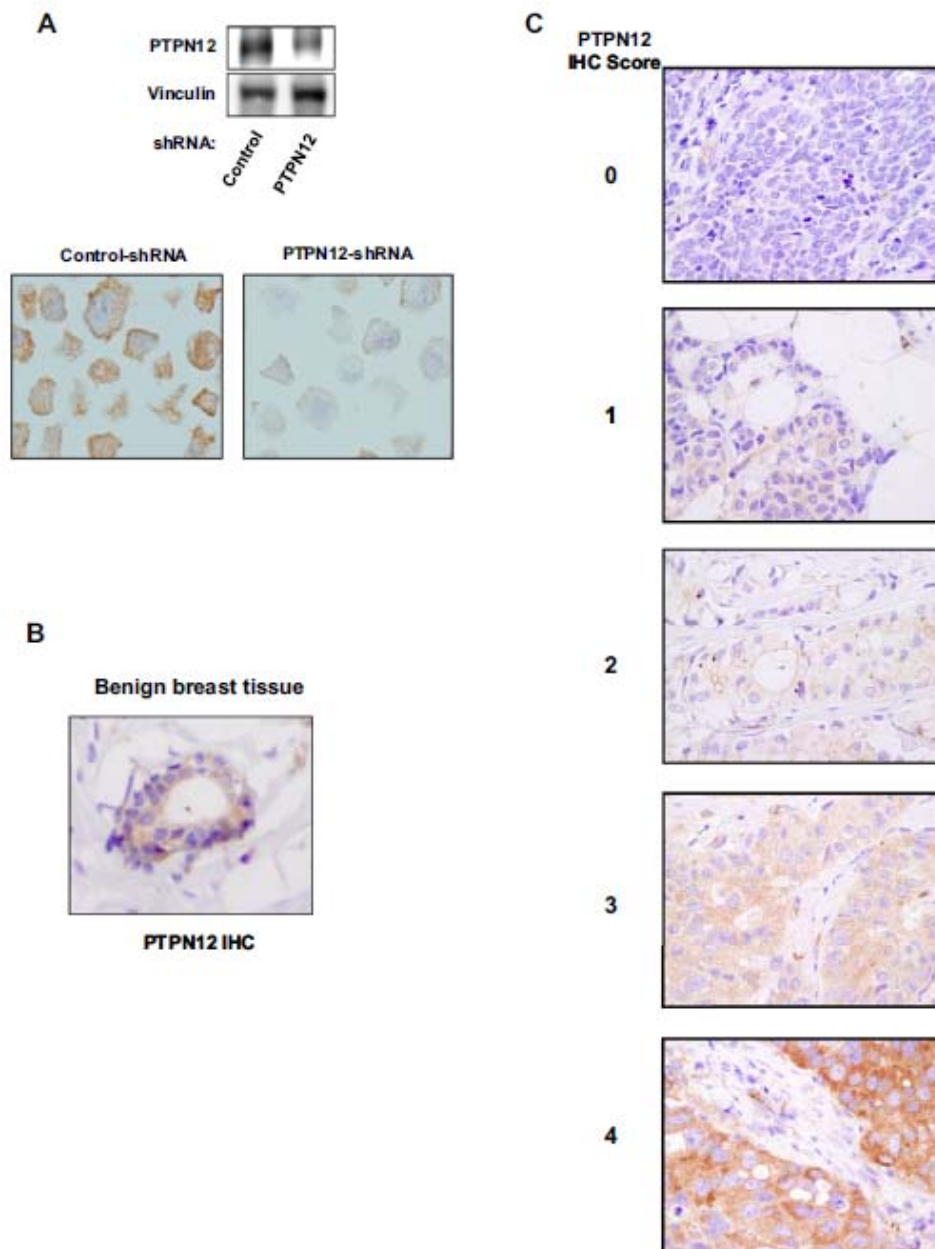


Figure S5. Immunohistochemical Analysis of PTPN12 Protein in Human Breast Cancer, Related to Figure 5

(A) HMECs expressing control or PTPN12-shRNA were analyzed for PTPN12 expression via western (top panels) or immunohistochemistry (bottom panels).

(B) PTPN12 is expressed in normal human mammary gland. Benign tissue from a biopsy was stained with anti-PTPN12.

(C) Analysis of PTPN12 levels in human breast cancers. PTPN12 proteins levels were evaluated in 185 primary human breast cancers via immunohistochemistry. Shown are representative images from each of the 5 classes of PTPN12 levels observed.

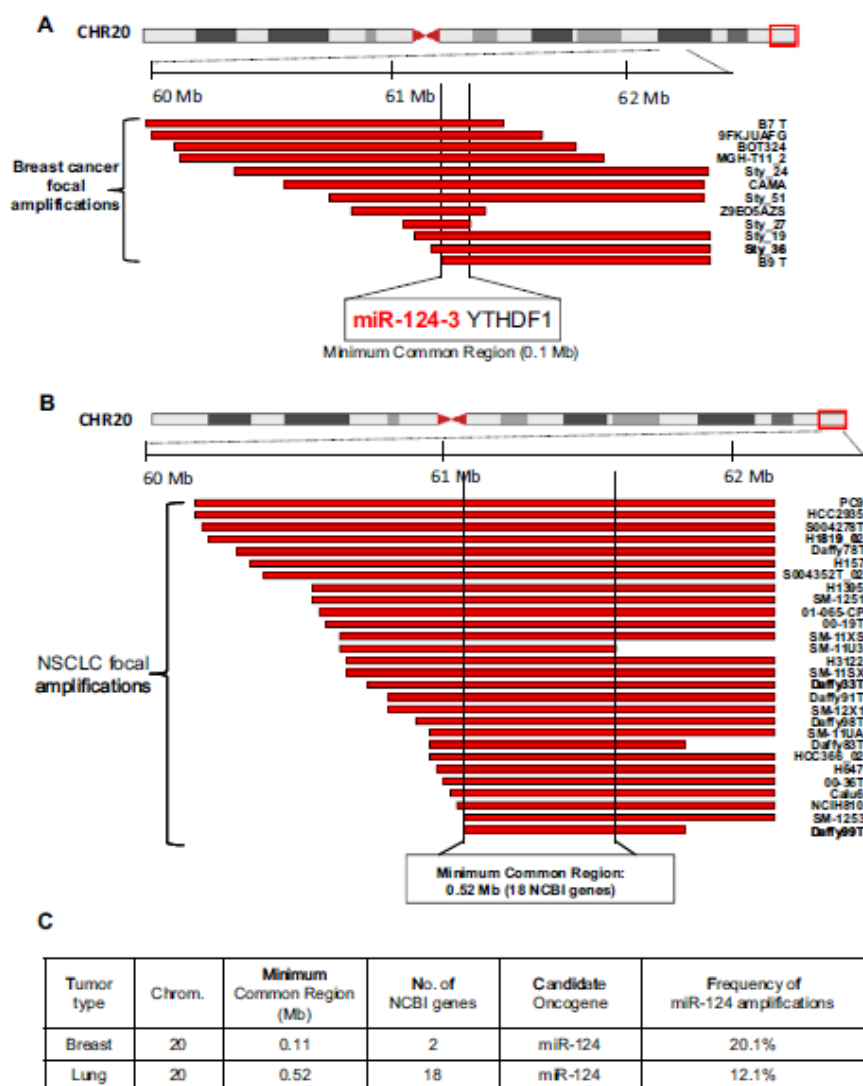


Figure S6. miR-124 Is Focally Amplified in Human Breast and Lung Cancer, Related to Figure 5

(A) Focal amplifications target the miR-124-3 locus in human breast cancer. Segmental copy-number data for 243 human breast cancer samples was retrieved from tumorscape (Beroukhi et al., 2010) and analyzed for focal amplifications less than 2 Mb. 13 focal amplifications targeting the miR124-3 locus were identified, with a minimum common region of 0.10 Mb encompassing 2 NCBI-annotated genes.

(B) Focal amplifications target the miR-124-3 locus in human non-small cell lung cancers (NSCLCs). Segmental copy-number data for 734 NSCLC samples was retrieved from tumorscape (Beroukhi et al., 2010) and analyzed for focal amplifications less than 2 Mb. 29 focal amplifications targeting the miR124-3 locus were identified, with a minimum common region of 0.61 Mb encompassing 18 NCBI-annotated genes.

(C) The miR-124-3 locus is targeted by focal and frequent amplifications in breast and lung cancer. Table listing the characteristics of a minimum common region (MCR) targeting miR-124-3 in breast and lung cancers (NSCLC). The far right column indicates the total percentage of breast and NSCLC tumors with evidence of miR-124 amplification.

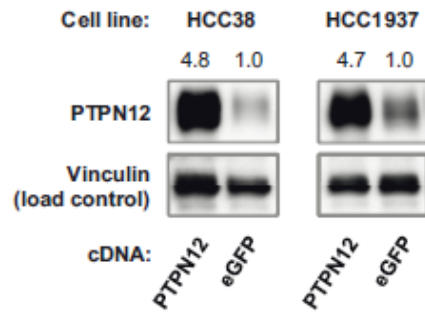


Figure S7. Ectopic Expression of PTPN12 in Human Breast Cancer Cell Lines, Related to Figure 6
 HCC38 and HCC1937 breast cancer cells were transduced with lentivirus encoding control or PTPN12 cDNA and assessed for PTPN12 expression by western. These cells were analyzed for colony formation in Figures 6B and 6C.

6. DISCUSSION AND OUTLOOK

We found opposing roles for SHP2 and PTPN12 in breast cancer: while SHP2 plays an oncogenic role and controls key networks of CSCs, PTPN12 acts as a tumor suppressor and constrains the activity of proto-oncogenic RTKs in TNBCs.

6.1 The role of SHP2 in CSCs

Recent studies have demonstrated the importance of CSCs in breast cancer. The signaling networks that govern CSCs remain ill-defined, and their delineation should pave the way for development of targeted, potentially curative cancer therapies when combined with other strategies. We provide new insights into the multiple roles of SHP2 in cancer. We found that SHP2 increases self-renewal of breast CSCs and is required for breast tumor maintenance and progression, demonstrating that SHP2 is a high quality target in human breast cancer.

Evidence that SHP2 increases self-renewal of breast CSCs is shown by several *in vitro* and *in vivo* models. Knockdown of SHP2 *in vitro* reduced the proportion of the CD44^{high}/CD24^{low} population and decreased tumorsphere-forming efficiency. In several *in vivo* models, SHP2 knockdown inhibited tumor maintenance and growth, reduced tumorsphere-forming efficiency of the cancer cells and dramatically decreased their capacity to seed new tumors when transplanted back at limiting dilutions in mice. These effects were accompanied by a blockage of invasion *in vivo* and in 3D cultures, and decreased metastatic ability *in vivo*.

6.2 SHP2 as a molecular hub linking stemness and EMT

It was reported recently that induction of an invasive phenotype in normal or neoplastic mammary epithelial cell populations increases the number of cells with CSC-like properties, suggesting a functional overlap between the invasion phenotype and the state of stemness (Mani, Guo et al. 2008). In line with this concept, CSCs are thought to be responsible for metastases. Our observations that SHP2 regulates CSCs and EMT, mediates the progression from DCIS to IDC and promotes metastatic spread suggest that SHP2 acts as a molecular hub for these fundamental phenomena.

6.3 Mechanism of action of SHP2 in CSCs

Previously, SHP2 was shown to activate both the ERK and AKT pathways by increasing the half-life of the activated form of RAS in breast cancer cells (Zhou and Agazie 2009). This was accomplished by dephosphorylating an autophosphorylation site on HER2 that serves as a docking platform for the SH2 domains of the RAS GTPase-activating protein (RASGAP). The net effect was an increase in the intensity and duration of GTP-RAS levels with the overall enhancement of ERK and AKT phosphorylation and cell transformation (Zhou and Agazie 2009). In addition, SHP2 has been shown to directly activate the SRC family member Fyn, downstream of integrin $\alpha 6\beta 4$, to induce invasiveness of breast cancer cells (Yang, Dutta et al. 2010), and to promote anchorage-independent growth *via* SRC/ERK activation downstream of MET/integrin $\beta 4$ (Bertotti, Comoglio et al. 2006).

We found that the effects of SHP2 on self-renewal of CSC and invasion of breast cancer cells require ERK pathway activation. Further, we show that SHP2 activation of ERK1/2 induces expression of the transcription factors ZEB1 and c-Myc, with c-Myc

mediating an increase in the expression of the RNA-binding protein LIN28B. Notably, the EMT-activator ZEB1 has been previously suggested to induce stemness in pancreatic and colorectal cancers (Wellner, Schubert et al. 2009). Moreover, LIN28B, a marker of undifferentiated human embryonic stem cells (Richards, Tan et al. 2004), promoted c-Myc-mediated proliferation and invasion in several cancer models (Chang, Zeitels et al. 2009; Wang, Chen et al. 2011). In our studies, c-Myc-induced LIN28B expression repressed let-7 miRNA leading to overexpression of let-7 targets, including RAS and other regulators of stemness. These findings uncover a novel mechanism of ERK regulation by SHP2 and identify an SHP2-dependent positive feedback loop required for the maintenance of CSC and for the invasiveness of breast cancer cells.

6.4 The “SHP2 signature” in human breast cancer

Our work has led to the discovery of an “SHP2 signature”, a set of genes that we found to be co-overexpressed in ~55% of human primary breast tumors. This signature reflects the existence of an SHP2-driven gene network, controlled by key transcription factors (e.g., c-Myc and ZEB1), and capable of maintaining stemness and invasiveness of breast tumors. Notably, the SHP2 signature genes are co-overexpressed in ~55% of all breast tumors and more frequently in TNBCs. These results suggest that inhibiting SHP2 might be particularly effective in human TNBCs, especially the ones we recently found to be dependent on active RTKs (Sun, Aceto et al. 2011).

6.5 SHP2 as a targets in breast cancer and in other malignancies

As SHP2 has been shown to activate the ERK pathway downstream of most growth factor and cytokine receptors, targeting SHP2 might be therapeutic in other cancers in which SHP2 is hyperactivated, e.g., downstream of the cytotoxin-associated antigen A (CagA) encoded by virulent *H. pylori* strains in gastric carcinoma, of the fusion protein NPM-ALK in anaplastic large cell lymphoma, and of EGFRvIII in glioma. Our findings warrant experiments to address whether SHP2 also regulates CSCs, tumor maintenance and progression in these malignancies.

Taken together, these findings reveal a fundamental SHP2-dependent positive feedback loop regulating CSCs. The facts that 1) SHP2 is a critical node required for signaling downstream of virtually all RTKs with transforming potential and 2) promotes self-renewal of CSCs, breast cancer maintenance, invasion and progression to metastasis, make this PTP a critical therapeutic target for breast cancer and provide a rationale for the development of selective inhibitors of this phosphatase.

6.6 The role of PTPN12 in TNBCs

In collaboration with the Elledge and Westbrook groups, we demonstrate that PTPN12 is a potent tumor suppressor in human breast cancer. We find that PTPN12 loss-of-function leads to aberrant acinar morphogenesis and cellular transformation in human mammary epithelial cells. Importantly, the tyrosine phosphatase activity of PTPN12 is required for suppression of cellular transformation. PTPN12 suppresses transformation by interacting with and inhibiting

multiple oncogenic tyrosine kinases including HER2, EGFR and PDGFR β . Moreover, PTPN12 function is frequently compromised in primary human TNBCs by inactivating mutations or loss of gene expression. Notably, in breast cancer cells exhibiting PTPN12 deficiency, restoring PTPN12 expression to levels observed in normal mammary epithelial cells suppresses proliferation, tumorigenesis and metastasis, suggesting that the malignant behaviour of these cancer cells is dependent on PTPN12 dysfunction. Together, these observations strongly support the conclusion that PTPN12 is a suppressor of human breast cancer of the TNBC subtype. We propose a model in which PTPN12 inactivation leads to HER2/EGFR/PDGFR β hyper-activity and cellular transformation in HER2-negative breast cancers. Importantly, loss of PTPN12 renders TNBCs sensitive to RTK inhibitors. Indeed treatment of cancer cells lacking PTPN12 with the EGFR/HER2 inhibitor lapatinib and the PDGFR β inhibitor sunitinib reduced tumor growth and increased overall survival. Therefore, our studies warrant a closer examination of the status of tyrosine phosphorylation in what has been previously considered non-RTK driven diseases.

6.7 Concluding remarks and future directions

Recently, we have witnessed important discoveries on the function of some members of the PTP family. Although PTPs were initially thought to exert tumor-suppressive activity because of their antagonistic effects on oncogenic PTKs signaling, the emerging notion that some PTPs can act as oncogenes has led to their consideration as drug targets. The development of potent and selective inhibitors for these enzymes is therefore of great clinical importance.

6.7.1 SHP2 as a drug target in breast cancer:

The better characterized example of an oncogenic PTP is the non-transmembrane phosphatase SHP2. The activity of SHP2 is required for self-renewal of breast CSCs and for promotion of breast cancer maintenance and progression to metastases. These effects are mediated *via* SHP2 activation of the ERK/MAPK pathway and the transcription factors ZEB1 and c-Myc. These findings should encourage academic institutes and pharmaceutical companies to develop selective inhibitors of SHP2.

These discoveries lead us to explore new directions:

1) the fact that SHP2 regulates the expression of mature let-7 miRNA (via c-Myc and LIN28B), raises the question of whether this phosphatase also regulates the biogenesis or activity of other miRNAs. PTPs play very essential roles in eukaryotic systems, and the involvement of members of this family in the control of fundamental regulatory elements like miRNAs would not be unexpected.

2) we have preliminary evidences of a nuclear localization of SHP2 in breast cancer cell lines. The role of SHP2 in the nucleus is unknown, as well as if its phosphatase activity is at all required in this cellular compartment. Our laboratory is currently addressing these interesting questions.

3) the direct substrate(s) of SHP2 in breast cancer is unclear. We performed preliminary SHP2-immunoprecipitation experiments followed by mass-spectrometry to identify SHP2 binding partners and substrates. Efforts in this direction should provide a direct molecular explanation of the observed downstream signaling cascade, eventually provide

novel mechanisms of action of this PTP, and potentially identify additional targets for the treatment of breast cancer.

6.7.2 PTPN12 as a tumor suppressor in TNBC:

PTPN12 is a tumor-suppressor phosphatase which constrains EGFR, HER2 and PDGFR β in breast cells. In the absence of activating mutations or overexpression of oncogenic enzymes like EGFR, HER2 or PDGFR β , loss of PTPN12 leads to hyperactivation of these RTKs. This might also be true for other RTKs regulated by other tumor suppressor PTPs. Therefore, this concept provides a rationale for targeting tyrosine kinases in TNBC and other cancers based on their profile of tyrosine phosphatase activity.

Finally, the pathophysiological role of the majority of PTPs in breast cancer is poorly characterized. Further studies using physiologically relevant models are required to reveal the functions of the “PTP-ome” in breast cancer. Given that the design of drugs targeting PTPs presents significant technical challenges, including the high polarity that the compounds must have to interact with the PTP domain and the consequent poor cell permeability and bioavailability, several efforts are currently made to solve these issues. In particular, transmembrane PTPs seem to be suitable targets for development of chemical inhibitors or antibodies targeting their extracellular domain, while non-transmembrane PTPs require specific and cell-permeable chemical inhibitors or antisense-based therapeutics. As further progress will be made in understanding the role of PTPs in breast cancer and in defining their substrates, new insights into the molecular mechanisms driving tumorigenesis should be revealed. This should ultimately lead to the development of new targeted therapies for the treatment of cancer.

7. REFERENCES

- Agazie, Y. M., N. Movilla, et al. (2003). "The phosphotyrosine phosphatase SHP2 is a critical mediator of transformation induced by the oncogenic fibroblast growth factor receptor 3." *Oncogene* **22**(44): 6909-6918.
- Agus, D. B., R. W. Akita, et al. (2002). "Targeting ligand-activated ErbB2 signaling inhibits breast and prostate tumor growth." *Cancer Cell* **2**(2): 127-137.
- Al-Hajj, M., M. S. Wicha, et al. (2003). "Prospective identification of tumorigenic breast cancer cells." *Proc Natl Acad Sci U S A* **100**(7): 3983-3988.
- Al-Hajj, M., M. S. Wicha, et al. (2003). "Prospective identification of tumorigenic breast cancer cells." *Proceedings of the National Academy of Sciences of the United States of America* **100**(7): 3983-3988.
- Allred, D. C., Y. Wu, et al. (2008). "Ductal carcinoma in situ and the emergence of diversity during breast cancer evolution." *Clin Cancer Res* **14**(2): 370-378.
- Alonso, A., J. Sasin, et al. (2004). "Protein tyrosine phosphatases in the human genome." *Cell* **117**(6): 699-711.
- Anders, C. and L. A. Carey (2008). "Understanding and treating triple-negative breast cancer." *Oncology (Williston Park)* **22**(11): 1233-1239; discussion 1239-1240, 1243.
- Anders, L., P. Mertins, et al. (2006). "Furin-, ADAM 10-, and gamma-secretase-mediated cleavage of a receptor tyrosine phosphatase and regulation of beta-catenin's transcriptional activity." *Mol Cell Biol* **26**(10): 3917-3934.
- Andersen, J. N., O. H. Mortensen, et al. (2001). "Structural and evolutionary relationships among protein tyrosine phosphatase domains." *Mol Cell Biol* **21**(21): 7117-7136.
- Angers-Loustau, A., J. F. Cote, et al. (1999). "Protein tyrosine phosphatase-PEST regulates focal adhesion disassembly, migration, and cytokinesis in fibroblasts." *The Journal of cell biology* **144**(5): 1019-1031.
- Ardini, E., R. Agresti, et al. (2000). "Expression of protein tyrosine phosphatase alpha (RPTPalpha) in human breast cancer correlates with low tumor grade, and inhibits tumor cell growth in vitro and in vivo." *Oncogene* **19**(43): 4979-4987.
- Arias-Romero, L. E., S. Saha, et al. (2009). "Activation of Src by protein tyrosine phosphatase 1B is required for ErbB2 transformation of human breast epithelial cells." *Cancer Res* **69**(11): 4582-4588.
- Baselga, J., K. A. Gelmon, et al. (2010). "Phase II trial of pertuzumab and trastuzumab in patients with human epidermal growth factor receptor 2-positive metastatic breast cancer that progressed during prior trastuzumab therapy." *J Clin Oncol* **28**(7): 1138-1144.
- Baselga, J. and S. M. Swain (2009). "Novel anticancer targets: revisiting ERBB2 and discovering ERBB3." *Nat Rev Cancer* **9**(7): 463-475.
- Behbod, F., F. S. Kittrell, et al. (2009). "An intraductal human-in-mouse transplantation model mimics the subtypes of ductal carcinoma in situ." *Breast Cancer Res* **11**(5): R66.
- Bennett, A. M., T. L. Tang, et al. (1994). "Protein-tyrosine-phosphatase SHPTP2 couples platelet-derived growth factor receptor beta to Ras." *Proc Natl Acad Sci U S A* **91**(15): 7335-7339.
- Bentires-Alj, M., S. G. Gil, et al. (2006). "A role for the scaffolding adapter GAB2 in breast cancer." *Nat Med* **12**(1): 114-121.
- Bentires-Alj, M. and B. G. Neel (2007). "Protein-tyrosine phosphatase 1B is required for HER2/Neu-induced breast cancer." *Cancer Res* **67**(6): 2420-2424.
- Bentires-Alj, M., J. G. Paez, et al. (2004). "Activating mutations of the noonan syndrome-associated SHP2/PTPN11 gene in human solid tumors and adult acute myelogenous leukemia." *Cancer Res* **64**(24): 8816-8820.

References

- Bertotti, A., P. M. Comoglio, et al. (2006). "Beta4 integrin activates a Shp2-Src signaling pathway that sustains HGF-induced anchorage-independent growth." *J Cell Biol* **175**(6): 993-1003.
- Bilwes, A. M., J. den Hertog, et al. (1996). "Structural basis for inhibition of receptor protein-tyrosine phosphatase-alpha by dimerization." *Nature* **382**(6591): 555-559.
- Bissell, M. J., D. C. Radisky, et al. (2002). "The organizing principle: microenvironmental influences in the normal and malignant breast." *Differentiation* **70**(9-10): 537-546.
- Bjorge, J. D., A. Pang, et al. (2000). "Identification of protein-tyrosine phosphatase 1B as the major tyrosine phosphatase activity capable of dephosphorylating and activating c-Src in several human breast cancer cell lines." *J Biol Chem* **275**(52): 41439-41446.
- Blanquart, C., S. E. Karouri, et al. (2009). "Implication of protein tyrosine phosphatase 1B in MCF-7 cell proliferation and resistance to 4-OH tamoxifen." *Biochem Biophys Res Commun* **387**(4): 748-753.
- Bocanegra, M., A. Bergamaschi, et al. "Focal amplification and oncogene dependency of GAB2 in breast cancer." *Oncogene* **29**(5): 774-779.
- Bocanegra, M., A. Bergamaschi, et al. (2010). "Focal amplification and oncogene dependency of GAB2 in breast cancer." *Oncogene* **29**(5): 774-779.
- Bompard, G., C. Puech, et al. (2002). "Protein-tyrosine phosphatase PTPL1/FAP-1 triggers apoptosis in human breast cancer cells." *J Biol Chem* **277**(49): 47861-47869.
- Bonnet, D. and J. E. Dick (1997). "Human acute myeloid leukemia is organized as a hierarchy that originates from a primitive hematopoietic cell." *Nature medicine* **3**(7): 730-737.
- Bos, P. D., X. H. Zhang, et al. (2009). "Genes that mediate breast cancer metastasis to the brain." *Nature* **459**(7249): 1005-1009.
- Burdon, T., C. Stracey, et al. (1999). "Suppression of SHP-2 and ERK signalling promotes self-renewal of mouse embryonic stem cells." *Dev Biol* **210**(1): 30-43.
- Carey, L. A., C. M. Perou, et al. (2006). "Race, breast cancer subtypes, and survival in the Carolina Breast Cancer Study." *JAMA : the journal of the American Medical Association* **295**(21): 2492-2502.
- Chan, G., D. Kalaitzidis, et al. (2008). "The tyrosine phosphatase Shp2 (PTPN11) in cancer." *Cancer Metastasis Rev* **27**(2): 179-192.
- Chan, R. J., Y. Li, et al. (2006). "Shp-2 heterozygous hematopoietic stem cells have deficient repopulating ability due to diminished self-renewal." *Exp Hematol* **34**(9): 1230-1239.
- Chang, T. C., L. R. Zeitels, et al. (2009). "Lin-28B transactivation is necessary for Myc-mediated let-7 repression and proliferation." *Proc Natl Acad Sci U S A* **106**(9): 3384-3389.
- Charest, A., J. Wagner, et al. (1997). "Coupling of the murine protein tyrosine phosphatase PEST to the epidermal growth factor (EGF) receptor through a Src homology 3 (SH3) domain-mediated association with Grb2." *Oncogene* **14**(14): 1643-1651.
- Chellaiah, M. A. and M. D. Schaller (2009). "Activation of Src kinase by protein-tyrosine phosphatase-PEST in osteoclasts: comparative analysis of the effects of bisphosphonate and protein-tyrosine phosphatase inhibitor on Src activation in vitro." *Journal of cellular physiology* **220**(2): 382-393.
- Clevers, H. (2011). "The cancer stem cell: premises, promises and challenges." *Nature medicine* **17**(3): 313-319.
- Cong, F., S. Spencer, et al. (2000). "Cytoskeletal protein PSTPIP1 directs the PEST-type protein tyrosine phosphatase to the c-Abl kinase to mediate Abl dephosphorylation." *Molecular cell* **6**(6): 1413-1423.
- Cortesio, C. L., K. T. Chan, et al. (2008). "Calpain 2 and PTP1B function in a novel pathway with Src to regulate invadopodia dynamics and breast cancer cell invasion." *J Cell Biol* **180**(5): 957-971.
- Cousin, H. and D. Alfandari (2004). "A PTP-PEST-like protein affects alpha5beta1-integrin-dependent matrix assembly, cell adhesion, and migration in *Xenopus* gastrula." *Developmental biology* **265**(2): 416-432.

References

- Creighton, C. J., X. Fu, et al. (2010). "Proteomic and transcriptomic profiling reveals a link between the PI3K pathway and lower estrogen-receptor (ER) levels and activity in ER+ breast cancer." Breast cancer research : BCR **12**(3): R40.
- Creighton, C. J., X. Li, et al. (2009). "Residual breast cancers after conventional therapy display mesenchymal as well as tumor-initiating features." Proceedings of the National Academy of Sciences of the United States of America **106**(33): 13820-13825.
- D'Alessio, A., D. Califano, et al. (2003). "The tyrosine phosphatase Shp-2 mediates intracellular signaling initiated by Ret mutants." Endocrinology **144**(10): 4298-4305.
- Dadke, S., S. Cotteret, et al. (2007). "Regulation of protein tyrosine phosphatase 1B by sumoylation." Nat Cell Biol **9**(1): 80-85.
- Dadke, S., A. Kusari, et al. (2001). "Phosphorylation and activation of protein tyrosine phosphatase (PTP) 1B by insulin receptor." Mol Cell Biochem **221**(1-2): 147-154.
- Dean, M., T. Fojo, et al. (2005). "Tumour stem cells and drug resistance." Nat Rev Cancer **5**(4): 275-284.
- Debnath, J., K. R. Mills, et al. (2002). "The role of apoptosis in creating and maintaining luminal space within normal and oncogene-expressing mammary acini." Cell **111**(1): 29-40.
- den Hertog, J., A. Groen, et al. (2005). "Redox regulation of protein-tyrosine phosphatases." Arch Biochem Biophys **434**(1): 11-15.
- den Hertog, J., S. Tracy, et al. (1994). "Phosphorylation of receptor protein-tyrosine phosphatase alpha on Tyr789, a binding site for the SH3-SH2-SH3 adaptor protein GRB-2 in vivo." EMBO J **13**(13): 3020-3032.
- Di Cosimo, S. and J. Baselga (2010). "Management of breast cancer with targeted agents: importance of heterogeneity. [corrected]." Nat Rev Clin Oncol **7**(3): 139-147.
- Diehn, M., R. W. Cho, et al. (2009). "Association of reactive oxygen species levels and radioresistance in cancer stem cells." Nature **458**(7239): 780-783.
- Dontu, G., W. M. Abdallah, et al. (2003). "In vitro propagation and transcriptional profiling of human mammary stem/progenitor cells." Genes Dev **17**(10): 1253-1270.
- Dontu, G., M. Al-Hajj, et al. (2003). "Stem cells in normal breast development and breast cancer." Cell Prolif **36 Suppl 1**: 59-72.
- Dromard, M., G. Bompard, et al. (2007). "The putative tumor suppressor gene PTPN13/PTPL1 induces apoptosis through insulin receptor substrate-1 dephosphorylation." Cancer Res **67**(14): 6806-6813.
- Duss, S., S. Andre, et al. (2007). "An oestrogen-dependent model of breast cancer created by transformation of normal human mammary epithelial cells." Breast Cancer Res **9**(3): R38.
- Elchebly, M., P. Payette, et al. (1999). "Increased insulin sensitivity and obesity resistance in mice lacking the protein tyrosine phosphatase-1B gene." Science **283**(5407): 1544-1548.
- Elson, A. (1999). "Protein tyrosine phosphatase epsilon increases the risk of mammary hyperplasia and mammary tumors in transgenic mice." Oncogene **18**(52): 7535-7542.
- Elson, A. and P. Leder (1995). "Protein-tyrosine phosphatase epsilon. An isoform specifically expressed in mouse mammary tumors initiated by v-Ha-ras OR neu." J Biol Chem **270**(44): 26116-26122.
- Falet, H., S. Pain, et al. (1998). "Tyrosine unphosphorylated platelet SHP-1 is a substrate for calpain." Biochem Biophys Res Commun **252**(1): 51-55.
- Felberg, J. and P. Johnson (1998). "Characterization of recombinant CD45 cytoplasmic domain proteins. Evidence for intramolecular and intermolecular interactions." J Biol Chem **273**(28): 17839-17845.
- Feng, G. S. (2007). "Shp2-mediated molecular signaling in control of embryonic stem cell self-renewal and differentiation." Cell Res **17**(1): 37-41.
- Ferlay, J., P. Autier, et al. (2007). "Estimates of the cancer incidence and mortality in Europe in 2006." Ann Oncol **18**(3): 581-592.
- Finkel, T. (2003). "Oxidant signals and oxidative stress." Curr Opin Cell Biol **15**(2): 247-254.

References

- Forbes, J. F., J. Cuzick, et al. (2008). "Effect of anastrozole and tamoxifen as adjuvant treatment for early-stage breast cancer: 100-month analysis of the ATAC trial." *Lancet Oncol* **9**(1): 45-53.
- Fox, A. N. and K. Zinn (2005). "The heparan sulfate proteoglycan syndecan is an in vivo ligand for the Drosophila LAR receptor tyrosine phosphatase." *Curr Biol* **15**(19): 1701-1711.
- Frangioni, J. V., A. Oda, et al. (1993). "Calpain-catalyzed cleavage and subcellular relocation of protein phosphotyrosine phosphatase 1B (PTP-1B) in human platelets." *EMBO J* **12**(12): 4843-4856.
- Freiss, G., G. Bompard, et al. (2004). "[PTPL1, a proapoptotic protein tyrosine phosphatase in breast cancers]." *Bull Cancer* **91**(4): 325-332.
- Garton, A. J., M. R. Burnham, et al. (1997). "Association of PTP-PEST with the SH3 domain of p130cas; a novel mechanism of protein tyrosine phosphatase substrate recognition." *Oncogene* **15**(8): 877-885.
- Garton, A. J. and N. K. Tonks (1994). "PTP-PEST: a protein tyrosine phosphatase regulated by serine phosphorylation." *EMBO J* **13**(16): 3763-3771.
- Garton, A. J. and N. K. Tonks (1999). "Regulation of fibroblast motility by the protein tyrosine phosphatase PTP-PEST." *The Journal of biological chemistry* **274**(6): 3811-3818.
- Gil-Henn, H. and A. Elson (2003). "Tyrosine phosphatase-epsilon activates Src and supports the transformed phenotype of Neu-induced mammary tumor cells." *J Biol Chem* **278**(18): 15579-15586.
- Glondou-Lassis, M., M. Dromard, et al. (2010). "PTPL1/PTPN13 regulates breast cancer cell aggressiveness through direct inactivation of Src kinase." *Cancer Res* **70**(12): 5116-5126.
- Grossmann, K. S., M. Rosario, et al. "The tyrosine phosphatase Shp2 in development and cancer." *Adv Cancer Res* **106**: 53-89.
- Grossmann, K. S., M. Rosario, et al. (2010). "The tyrosine phosphatase Shp2 in development and cancer." *Adv Cancer Res* **106**: 53-89.
- Gu, M. and P. W. Majerus (1996). "The properties of the protein tyrosine phosphatase PTPMEG." *J Biol Chem* **271**(44): 27751-27759.
- Halle, M., Y. C. Liu, et al. (2007). "Caspase-3 regulates catalytic activity and scaffolding functions of the protein tyrosine phosphatase PEST, a novel modulator of the apoptotic response." *Molecular and cellular biology* **27**(3): 1172-1190.
- Hatakeyama, M. (2004). "Oncogenic mechanisms of the Helicobacter pylori CagA protein." *Nat Rev Cancer* **4**(9): 688-694.
- Hennessy, B. T., A. M. Gonzalez-Angulo, et al. (2009). "Characterization of a naturally occurring breast cancer subset enriched in epithelial-to-mesenchymal transition and stem cell characteristics." *Cancer research* **69**(10): 4116-4124.
- Horsch, K., M. D. Schaller, et al. (2001). "The protein tyrosine phosphatase-PEST is implicated in the negative regulation of epidermal growth factor on PRL signaling in mammary epithelial cells." *Molecular endocrinology* **15**(12): 2182-2196.
- Huang, T. S., J. Y. Hsieh, et al. (2008). "Functional network reconstruction reveals somatic stemness genetic maps and dedifferentiation-like transcriptome reprogramming induced by GATA2." *Stem Cells* **26**(5): 1186-1201.
- Hunter, T. (1987). "A thousand and one protein kinases." *Cell* **50**(6): 823-829.
- Hunter, T. (2009). "Tyrosine phosphorylation: thirty years and counting." *Curr Opin Cell Biol* **21**(2): 140-146.
- Hynes, N. E. and H. A. Lane (2005). "ERBB receptors and cancer: the complexity of targeted inhibitors." *Nat Rev Cancer* **5**(5): 341-354.
- Iliopoulos, D., H. A. Hirsch, et al. (2009). "An epigenetic switch involving NF-kappaB, Lin28, Let-7 MicroRNA, and IL6 links inflammation to cell transformation." *Cell* **139**(4): 693-706.
- Jemal, A., R. Siegel, et al. (2010). "Cancer statistics, 2010." *CA Cancer J Clin* **60**(5): 277-300.
- Johnson, K. G., A. P. Tenney, et al. (2006). "The HSPGs Syndecan and Dallylike bind the receptor phosphatase LAR and exert distinct effects on synaptic development." *Neuron* **49**(4): 517-531.

References

- Johnson, K. J., A. R. Peck, et al. (2010). "PTP1B Suppresses Prolactin Activation of Stat5 in Breast Cancer Cells." *Am J Pathol* **177**(6): 2971-2983.
- Johnson, S. M., H. Grosshans, et al. (2005). "RAS is regulated by the let-7 microRNA family." *Cell* **120**(5): 635-647.
- Julien, S. G., N. Dube, et al. (2011). "Inside the human cancer tyrosine phosphatome." *Nature reviews. Cancer* **11**(1): 35-49.
- Julien, S. G., N. Dube, et al. (2007). "Protein tyrosine phosphatase 1B deficiency or inhibition delays ErbB2-induced mammary tumorigenesis and protects from lung metastasis." *Nat Genet* **39**(3): 338-346.
- Kamata, H., S. Honda, et al. (2005). "Reactive oxygen species promote TNFalpha-induced death and sustained JNK activation by inhibiting MAP kinase phosphatases." *Cell* **120**(5): 649-661.
- Ke, Y., E. E. Zhang, et al. (2007). "Deletion of Shp2 in the brain leads to defective proliferation and differentiation in neural stem cells and early postnatal lethality." *Mol Cell Biol* **27**(19): 6706-6717.
- Klaman, L. D., O. Boss, et al. (2000). "Increased energy expenditure, decreased adiposity, and tissue-specific insulin sensitivity in protein-tyrosine phosphatase 1B-deficient mice." *Molecular and cellular biology* **20**(15): 5479-5489.
- Klein, C. A. (2009). "Parallel progression of primary tumours and metastases." *Nature reviews. Cancer* **9**(4): 302-312.
- Kordon, E. C. and G. H. Smith (1998). "An entire functional mammary gland may comprise the progeny from a single cell." *Development* **125**(10): 1921-1930.
- Levea, C. M., C. T. McGary, et al. (2000). "PTP LAR expression compared to prognostic indices in metastatic and non-metastatic breast cancer." *Breast Cancer Res Treat* **64**(2): 221-228.
- Lewis Phillips, G. D., G. Li, et al. (2008). "Targeting HER2-positive breast cancer with trastuzumab-DM1, an antibody-cytotoxic drug conjugate." *Cancer Res* **68**(22): 9280-9290.
- Li, C., D. G. Heidt, et al. (2007). "Identification of pancreatic cancer stem cells." *Cancer research* **67**(3): 1030-1037.
- Li, F., B. Tiede, et al. (2007). "Beyond tumorigenesis: cancer stem cells in metastasis." *Cell Res* **17**(1): 3-14.
- Li, X., M. T. Lewis, et al. (2008). "Intrinsic resistance of tumorigenic breast cancer cells to chemotherapy." *J Natl Cancer Inst* **100**(9): 672-679.
- Liu, S., Y. Sugimoto, et al. (2002). "Estrogenic down-regulation of protein tyrosine phosphatase gamma (PTP gamma) in human breast is associated with estrogen receptor alpha." *Anticancer Res* **22**(6C): 3917-3923.
- Liu, S., Y. Sugimoto, et al. (2004). "Function analysis of estrogenically regulated protein tyrosine phosphatase gamma (PTPgamma) in human breast cancer cell line MCF-7." *Oncogene* **23**(6): 1256-1262.
- Loh, M. L., S. Vattikuti, et al. (2004). "Mutations in PTPN11 implicate the SHP-2 phosphatase in leukemogenesis." *Blood* **103**(6): 2325-2331.
- Lyons, P. D., J. M. Dunty, et al. (2001). "Inhibition of the catalytic activity of cell adhesion kinase beta by protein-tyrosine phosphatase-PEST-mediated dephosphorylation." *The Journal of biological chemistry* **276**(26): 24422-24431.
- Mani, S. A., W. Guo, et al. (2008). "The epithelial-mesenchymal transition generates cells with properties of stem cells." *Cell* **133**(4): 704-715.
- Mauri, D., N. Pavlidis, et al. (2006). "Survival with aromatase inhibitors and inactivators versus standard hormonal therapy in advanced breast cancer: meta-analysis." *J Natl Cancer Inst* **98**(18): 1285-1291.
- Mauro, L. J. and J. E. Dixon (1994). "'Zip codes' direct intracellular protein tyrosine phosphatases to the correct cellular 'address'." *Trends Biochem Sci* **19**(4): 151-155.
- Meerbrey, K. L., G. Hu, et al. (2011). "The pINDUCER lentiviral toolkit for inducible RNA interference in vitro and in vivo." *Proc Natl Acad Sci U S A*.

References

- Mendoza, N., G. L. Phillips, et al. (2002). "Inhibition of ligand-mediated HER2 activation in androgen-independent prostate cancer." *Cancer Res* **62**(19): 5485-5488.
- Meng, K., A. Rodriguez-Pena, et al. (2000). "Pleiotrophin signals increased tyrosine phosphorylation of beta beta-catenin through inactivation of the intrinsic catalytic activity of the receptor-type protein tyrosine phosphatase beta/zeta." *Proc Natl Acad Sci U S A* **97**(6): 2603-2608.
- Meng, T. C., D. A. Buckley, et al. (2004). "Regulation of insulin signaling through reversible oxidation of the protein-tyrosine phosphatases TC45 and PTP1B." *J Biol Chem* **279**(36): 37716-37725.
- Meng, T. C., T. Fukada, et al. (2002). "Reversible oxidation and inactivation of protein tyrosine phosphatases in vivo." *Mol Cell* **9**(2): 387-399.
- Meyer, D. S. and M. Bentires-Alj (2010). "Can phosphatidylinositol 3-kinase/mammalian target of rapamycin inhibition ERase them all?" *Breast Cancer Res* **12**(5): 315.
- Meyer, M. J., J. M. Fleming, et al. (2009). "Dynamic regulation of CD24 and the invasive, CD44posCD24neg phenotype in breast cancer cell lines." *Breast cancer research : BCR* **11**(6): R82.
- Miller, T. W., B. T. Hennesy, et al. (2010). "Hyperactivation of phosphatidylinositol-3 kinase promotes escape from hormone dependence in estrogen receptor-positive human breast cancer." *The Journal of clinical investigation* **120**(7): 2406-2413.
- Modi, S., A. T. Stopeck, et al. (2007). "Combination of trastuzumab and tanespimycin (17-AAG, KOS-953) is safe and active in trastuzumab-refractory HER-2 overexpressing breast cancer: a phase I dose-escalation study." *J Clin Oncol* **25**(34): 5410-5417.
- Mody, N., J. Leitch, et al. (2001). "Effects of MAP kinase cascade inhibitors on the MKK5/ERK5 pathway." *FEBS Lett* **502**(1-2): 21-24.
- Mustelin, T., T. Vang, et al. (2005). "Protein tyrosine phosphatases and the immune response." *Nature reviews. Immunology* **5**(1): 43-57.
- Nagata, Y., K. H. Lan, et al. (2004). "PTEN activation contributes to tumor inhibition by trastuzumab, and loss of PTEN predicts trastuzumab resistance in patients." *Cancer Cell* **6**(2): 117-127.
- Nakshatri, H., E. F. Srouf, et al. (2009). "Breast cancer stem cells and intrinsic subtypes: controversies rage on." *Curr Stem Cell Res Ther* **4**(1): 50-60.
- Nam, H. J., F. Poy, et al. (1999). "Crystal structure of the tandem phosphatase domains of RPTP LAR." *Cell* **97**(4): 449-457.
- Nam, H. J., F. Poy, et al. (2005). "Structural basis for the function and regulation of the receptor protein tyrosine phosphatase CD45." *J Exp Med* **201**(3): 441-452.
- Nguyen, D. X., P. D. Bos, et al. (2009). "Metastasis: from dissemination to organ-specific colonization." *Nature reviews. Cancer* **9**(4): 274-284.
- Nguyen, D. X., P. D. Bos, et al. (2009). "Metastasis: from dissemination to organ-specific colonization." *Nat Rev Cancer* **9**(4): 274-284.
- O'Brien, C. A., A. Pollett, et al. (2007). "A human colon cancer cell capable of initiating tumour growth in immunodeficient mice." *Nature* **445**(7123): 106-110.
- Ostman, A., C. Hellberg, et al. (2006). "Protein-tyrosine phosphatases and cancer." *Nat Rev Cancer* **6**(4): 307-320.
- Panagopoulos, I., N. Pandis, et al. (1996). "The FHIT and PTPRG genes are deleted in benign proliferative breast disease associated with familial breast cancer and cytogenetic rearrangements of chromosome band 3p14." *Cancer Res* **56**(21): 4871-4875.
- Pawitan, Y., J. Bjohle, et al. (2005). "Gene expression profiling spares early breast cancer patients from adjuvant therapy: derived and validated in two population-based cohorts." *Breast Cancer Res* **7**(6): R953-964.
- Pawson, T. and M. Kofler (2009). "Kinome signaling through regulated protein-protein interactions in normal and cancer cells." *Curr Opin Cell Biol* **21**(2): 147-153.
- Pece, S., D. Tosoni, et al. "Biological and molecular heterogeneity of breast cancers correlates with their cancer stem cell content." *Cell* **140**(1): 62-73.

References

- Pece, S., D. Tosoni, et al. (2010). "Biological and molecular heterogeneity of breast cancers correlates with their cancer stem cell content." *Cell* **140**(1): 62-73.
- Perez-Pinera, P., Y. Chang, et al. (2007). "Anaplastic lymphoma kinase is expressed in different subtypes of human breast cancer." *Biochem Biophys Res Commun* **358**(2): 399-403.
- Perez-Pinera, P., O. Garcia-Suarez, et al. (2007). "The receptor protein tyrosine phosphatase (RPTP)beta/zeta is expressed in different subtypes of human breast cancer." *Biochem Biophys Res Commun* **362**(1): 5-10.
- Perou, C. M., T. Sorlie, et al. (2000). "Molecular portraits of human breast tumours." *Nature* **406**(6797): 747-752.
- Persson, C., T. Sjoblom, et al. (2004). "Preferential oxidation of the second phosphatase domain of receptor-like PTP-alpha revealed by an antibody against oxidized protein tyrosine phosphatases." *Proc Natl Acad Sci U S A* **101**(7): 1886-1891.
- Pierce, G. B. and W. C. Speers (1988). "Tumors as caricatures of the process of tissue renewal: prospects for therapy by directing differentiation." *Cancer research* **48**(8): 1996-2004.
- Playford, M. P., P. D. Lyons, et al. (2006). "Identification of a filamin docking site on PTP-PEST." *The Journal of biological chemistry* **281**(45): 34104-34112.
- Playford, M. P., K. Vadali, et al. (2008). "Focal adhesion kinase regulates cell-cell contact formation in epithelial cells via modulation of Rho." *Experimental cell research* **314**(17): 3187-3197.
- Polyak, K. and R. A. Weinberg (2009). "Transitions between epithelial and mesenchymal states: acquisition of malignant and stem cell traits." *Nat Rev Cancer* **9**(4): 265-273.
- Ponti, D., A. Costa, et al. (2005). "Isolation and in vitro propagation of tumorigenic breast cancer cells with stem/progenitor cell properties." *Cancer Res* **65**(13): 5506-5511.
- Portera, C. C., J. M. Walshe, et al. (2008). "Cardiac toxicity and efficacy of trastuzumab combined with pertuzumab in patients with [corrected] human epidermal growth factor receptor 2-positive metastatic breast cancer." *Clin Cancer Res* **14**(9): 2710-2716.
- Prat, A. and J. Baselga (2008). "The role of hormonal therapy in the management of hormonal-receptor-positive breast cancer with co-expression of HER2." *Nat Clin Pract Oncol* **5**(9): 531-542.
- Prat, A., J. S. Parker, et al. (2010). "Phenotypic and molecular characterization of the claudin-low intrinsic subtype of breast cancer." *Breast cancer research : BCR* **12**(5): R68.
- Pulford, K., S. W. Morris, et al. (2004). "Anaplastic lymphoma kinase proteins in growth control and cancer." *J Cell Physiol* **199**(3): 330-358.
- Pulido, R., A. Zuniga, et al. (1998). "PTP-SL and STEP protein tyrosine phosphatases regulate the activation of the extracellular signal-regulated kinases ERK1 and ERK2 by association through a kinase interaction motif." *EMBO J* **17**(24): 7337-7350.
- Quintana, E., M. Shackleton, et al. (2008). "Efficient tumour formation by single human melanoma cells." *Nature* **456**(7222): 593-598.
- Ramaswamy, B., S. Majumder, et al. (2009). "Estrogen-mediated suppression of the gene encoding protein tyrosine phosphatase PTPRO in human breast cancer: mechanism and role in tamoxifen sensitivity." *Mol Endocrinol* **23**(2): 176-187.
- Raouf, A., Y. Zhao, et al. (2008). "Transcriptome analysis of the normal human mammary cell commitment and differentiation process." *Cell Stem Cell* **3**(1): 109-118.
- Ren, J. M., P. M. Li, et al. (1998). "Transgenic mice deficient in the LAR protein-tyrosine phosphatase exhibit profound defects in glucose homeostasis." *Diabetes* **47**(3): 493-497.
- Revillion, F., C. Puech, et al. (2009). "Expression of the putative tumor suppressor gene PTPN13/PTPL1 is an independent prognostic marker for overall survival in breast cancer." *Int J Cancer* **124**(3): 638-643.
- Ricci-Vitiani, L., D. G. Lombardi, et al. (2007). "Identification and expansion of human colon-cancer-initiating cells." *Nature* **445**(7123): 111-115.
- Richards, M., S. P. Tan, et al. (2004). "The transcriptome profile of human embryonic stem cells as defined by SAGE." *Stem Cells* **22**(1): 51-64.

References

- Robinson, D. R., Y. M. Wu, et al. (2000). "The protein tyrosine kinase family of the human genome." *Oncogene* **19**(49): 5548-5557.
- Rosen, J. M. and C. T. Jordan (2009). "The increasing complexity of the cancer stem cell paradigm." *Science* **324**(5935): 1670-1673.
- Ruhe, J. E., S. Streit, et al. (2006). "EGFR signaling leads to downregulation of PTP-LAR via TACE-mediated proteolytic processing." *Cell Signal* **18**(9): 1515-1527.
- Sahai, E. and C. J. Marshall (2002). "RHO-GTPases and cancer." *Nature reviews. Cancer* **2**(2): 133-142.
- Salmeen, A., J. N. Andersen, et al. (2003). "Redox regulation of protein tyrosine phosphatase 1B involves a sulphenyl-amide intermediate." *Nature* **423**(6941): 769-773.
- Salmeen, A. and D. Barford (2005). "Functions and mechanisms of redox regulation of cysteine-based phosphatases." *Antioxid Redox Signal* **7**(5-6): 560-577.
- Sastry, S. K., P. D. Lyons, et al. (2002). "PTP-PEST controls motility through regulation of Rac1." *Journal of cell science* **115**(Pt 22): 4305-4316.
- Sastry, S. K., Z. Rajfur, et al. (2006). "PTP-PEST couples membrane protrusion and tail retraction via VAV2 and p190RhoGAP." *The Journal of biological chemistry* **281**(17): 11627-11636.
- Sattler, M., M. G. Mohi, et al. (2002). "Critical role for Gab2 in transformation by BCR/ABL." *Cancer Cell* **1**(5): 479-492.
- Schatton, T., G. F. Murphy, et al. (2008). "Identification of cells initiating human melanomas." *Nature* **451**(7176): 345-349.
- Shackleton, M., E. Quintana, et al. (2009). "Heterogeneity in cancer: cancer stem cells versus clonal evolution." *Cell* **138**(5): 822-829.
- Shackleton, M., F. Vaillant, et al. (2006). "Generation of a functional mammary gland from a single stem cell." *Nature* **439**(7072): 84-88.
- Shi, Z. Q., D. H. Yu, et al. (2000). "Molecular mechanism for the Shp-2 tyrosine phosphatase function in promoting growth factor stimulation of Erk activity." *Mol Cell Biol* **20**(5): 1526-1536.
- Shu, S. T., Y. Sugimoto, et al. (2010). "Function and regulatory mechanisms of the candidate tumor suppressor receptor protein tyrosine phosphatase gamma (PTPRG) in breast cancer cells." *Anticancer Res* **30**(6): 1937-1946.
- Sims, A. H., A. Howell, et al. (2007). "Origins of breast cancer subtypes and therapeutic implications." *Nature clinical practice. Oncology* **4**(9): 516-525.
- Singh, S. K., C. Hawkins, et al. (2004). "Identification of human brain tumour initiating cells." *Nature* **432**(7015): 396-401.
- Sirois, J., J. F. Cote, et al. (2006). "Essential function of PTP-PEST during mouse embryonic vascularization, mesenchyme formation, neurogenesis and early liver development." *Mechanisms of development* **123**(12): 869-880.
- Skelton, M. R., S. Ponniah, et al. (2003). "Protein tyrosine phosphatase alpha (PTP alpha) knockout mice show deficits in Morris water maze learning, decreased locomotor activity, and decreases in anxiety." *Brain research* **984**(1-2): 1-10.
- Slamon, D. J., G. M. Clark, et al. (1987). "Human breast cancer: correlation of relapse and survival with amplification of the HER-2/neu oncogene." *Science* **235**(4785): 177-182.
- Sleeman, K. E., H. Kendrick, et al. (2007). "Dissociation of estrogen receptor expression and in vivo stem cell activity in the mammary gland." *J Cell Biol* **176**(1): 19-26.
- Sorlie, T., C. M. Perou, et al. (2001). "Gene expression patterns of breast carcinomas distinguish tumor subclasses with clinical implications." *Proceedings of the National Academy of Sciences of the United States of America* **98**(19): 10869-10874.
- Stingl, J. and C. Caldas (2007). "Molecular heterogeneity of breast carcinomas and the cancer stem cell hypothesis." *Nat Rev Cancer* **7**(10): 791-799.
- Stingl, J., P. Eirew, et al. (2006). "Purification and unique properties of mammary epithelial stem cells." *Nature* **439**(7079): 993-997.

References

- Streuli, M., N. X. Krueger, et al. (1992). "Expression of the receptor-linked protein tyrosine phosphatase LAR: proteolytic cleavage and shedding of the CAM-like extracellular region." *EMBO J* **11**(3): 897-907.
- Streuli, M., N. X. Krueger, et al. (1990). "Distinct functional roles of the two intracellular phosphatase like domains of the receptor-linked protein tyrosine phosphatases LCA and LAR." *EMBO J* **9**(8): 2399-2407.
- Sun, T., N. Aceto, et al. (2011). "Activation of Multiple Proto-oncogenic Tyrosine Kinases in Breast Cancer via Loss of the PTPN12 Phosphatase " *Cell* **144**(5): 703-718.
- Sun, T., N. Aceto, et al. (2011). "Activation of Multiple Proto-oncogenic Tyrosine Kinases in Breast Cancer via Loss of the PTPN12 Phosphatase." *Cell* **144**(5): 703-718.
- Suzuki, H., A. R. Forrest, et al. (2009). "The transcriptional network that controls growth arrest and differentiation in a human myeloid leukemia cell line." *Nat Genet* **41**(5): 553-562.
- Takekawa, M., F. Itoh, et al. (1994). "Chromosomal localization of the protein tyrosine phosphatase G1 gene and characterization of the aberrant transcripts in human colon cancer cells." *FEBS letters* **339**(3): 222-228.
- Tartaglia, M., E. L. Mehler, et al. (2001). "Mutations in PTPN11, encoding the protein tyrosine phosphatase SHP-2, cause Noonan syndrome." *Nat Genet* **29**(4): 465-468.
- Tartaglia, M., C. M. Niemeyer, et al. (2003). "Somatic mutations in PTPN11 in juvenile myelomonocytic leukemia, myelodysplastic syndromes and acute myeloid leukemia." *Nat Genet* **34**(2): 148-150.
- Thurlimann, B., A. Keshaviah, et al. (2005). "A comparison of letrozole and tamoxifen in postmenopausal women with early breast cancer." *N Engl J Med* **353**(26): 2747-2757.
- Tonks, N. K. (2003). "PTP1B: from the sidelines to the front lines!" *FEBS letters* **546**(1): 140-148.
- Tonks, N. K. (2005). "Redox redux: revisiting PTPs and the control of cell signaling." *Cell* **121**(5): 667-670.
- Tonks, N. K. (2006). "Protein tyrosine phosphatases: from genes, to function, to disease." *Nat Rev Mol Cell Biol* **7**(11): 833-846.
- Vargo-Gogola, T. and J. M. Rosen (2007). "Modelling breast cancer: one size does not fit all." *Nature reviews. Cancer* **7**(9): 659-672.
- Visvader, J. E. (2009). "Keeping abreast of the mammary epithelial hierarchy and breast tumorigenesis." *Genes Dev* **23**(22): 2563-2577.
- Viswanathan, S. R., G. Q. Daley, et al. (2008). "Selective blockade of microRNA processing by Lin28." *Science* **320**(5872): 97-100.
- Vogelstein, B. and K. W. Kinzler (2004). "Cancer genes and the pathways they control." *Nat Med* **10**(8): 789-799.
- von Minckwitz, G., A. du Bois, et al. (2009). "Trastuzumab beyond progression in human epidermal growth factor receptor 2-positive advanced breast cancer: a german breast group 26/breast international group 03-05 study." *J Clin Oncol* **27**(12): 1999-2006.
- Voshol, H., M. Ehrat, et al. (2009). "Antibody-based proteomics: analysis of signaling networks using reverse protein arrays." *FEBS J* **276**(23): 6871-6879.
- Wang, L. S., Y. W. Huang, et al. (2006). "Conjugated linoleic acid (CLA) up-regulates the estrogen-regulated cancer suppressor gene, protein tyrosine phosphatase gamma (PTPgama), in human breast cells." *Anticancer Res* **26**(1A): 27-34.
- Wang, S., W. M. Yu, et al. (2009). "Noonan syndrome/leukemia-associated gain-of-function mutations in SHP-2 phosphatase (PTPN11) enhance cell migration and angiogenesis." *The Journal of biological chemistry* **284**(2): 913-920.
- Wang, Y., J. G. Klijn, et al. (2005). "Gene-expression profiles to predict distant metastasis of lymph-node-negative primary breast cancer." *Lancet* **365**(9460): 671-679.
- Wang, Y. C., Y. L. Chen, et al. (2011). "Lin-28B expression promotes transformation and invasion in human hepatocellular carcinoma." *Carcinogenesis* **31**(9): 1516-1522.

References

- Wellner, U., J. Schubert, et al. (2009). "The EMT-activator ZEB1 promotes tumorigenicity by repressing stemness-inhibiting microRNAs." *Nat Cell Biol* **11**(12): 1487-1495.
- Wharram, B. L., M. Goyal, et al. (2000). "Altered podocyte structure in GLEPP1 (Ptpro)-deficient mice associated with hypertension and low glomerular filtration rate." *The Journal of clinical investigation* **106**(10): 1281-1290.
- Wiener, J. R., B. J. Kerns, et al. (1994). "Overexpression of the protein tyrosine phosphatase PTP1B in human breast cancer: association with p185c-erbB-2 protein expression." *J Natl Cancer Inst* **86**(5): 372-378.
- Wu, D., Y. Pang, et al. (2009). "A conserved mechanism for control of human and mouse embryonic stem cell pluripotency and differentiation by shp2 tyrosine phosphatase." *PLoS One* **4**(3): e4914.
- Yang, T., J. S. Zhang, et al. (1999). "Leukocyte common antigen-related tyrosine phosphatase receptor: increased expression and neuronal-type splicing in breast cancer cells and tissue." *Mol Carcinog* **25**(2): 139-149.
- Yang, W., L. D. Klamann, et al. (2006). "An Shp2/SFK/Ras/Erk signaling pathway controls trophoblast stem cell survival." *Dev Cell* **10**(3): 317-327.
- Yang, X., U. Dutta, et al. (2010). "SHP2 mediates the localized activation of Fyn downstream of the alpha6beta4 integrin to promote carcinoma invasion." *Mol Cell Biol* **30**(22): 5306-5317.
- Yang, Z. F., D. W. Ho, et al. (2008). "Significance of CD90+ cancer stem cells in human liver cancer." *Cancer cell* **13**(2): 153-166.
- Yuan, T., Y. Wang, et al. "Protein-tyrosine phosphatase PTPN9 negatively regulates ErbB2 and epidermal growth factor receptor signaling in breast cancer cells." *J Biol Chem* **285**(20): 14861-14870.
- Yuan, T., Y. Wang, et al. (2010). "Protein-tyrosine phosphatase PTPN9 negatively regulates ErbB2 and epidermal growth factor receptor signaling in breast cancer cells." *J Biol Chem* **285**(20): 14861-14870.
- Zhan, L., A. Rosenberg, et al. (2008). "Deregulation of scribble promotes mammary tumorigenesis and reveals a role for cell polarity in carcinoma." *Cell* **135**(5): 865-878.
- Zhan, Y., G. J. Counelis, et al. (2009). "The protein tyrosine phosphatase SHP-2 is required for EGFRvIII oncogenic transformation in human glioblastoma cells." *Exp Cell Res* **315**(14): 2343-2357.
- Zhan, Y. and D. M. O'Rourke (2004). "SHP-2-dependent mitogen-activated protein kinase activation regulates EGFRvIII but not wild-type epidermal growth factor receptor phosphorylation and glioblastoma cell survival." *Cancer Res* **64**(22): 8292-8298.
- Zheng, J., S. K. Kulp, et al. (2000). "17 beta-estradiol-regulated expression of protein tyrosine phosphatase gamma gene in cultured human normal breast and breast cancer cells." *Anticancer Res* **20**(1A): 11-19.
- Zheng, X., R. J. Resnick, et al. (2008). "Apoptosis of estrogen-receptor negative breast cancer and colon cancer cell lines by PTP alpha and src RNAi." *Int J Cancer* **122**(9): 1999-2007.
- Zheng, Y., Y. Xia, et al. (2009). "FAK phosphorylation by ERK primes ras-induced tyrosine dephosphorylation of FAK mediated by PIN1 and PTP-PEST." *Molecular cell* **35**(1): 11-25.
- Zhi, H. Y., S. W. Hou, et al. (2010). "PTPH1 cooperates with vitamin D receptor to stimulate breast cancer growth through their mutual stabilization." *Oncogene*.
- Zhou, B. B., H. Zhang, et al. (2009). "Tumour-initiating cells: challenges and opportunities for anticancer drug discovery." *Nature reviews. Drug discovery* **8**(10): 806-823.
- Zhou, X. and Y. M. Agazie (2009). "Molecular mechanism for SHP2 in promoting HER2-induced signaling and transformation." *J Biol Chem* **284**(18): 12226-12234.
- Zhou, X., J. Coad, et al. (2008). "SHP2 is up-regulated in breast cancer cells and in infiltrating ductal carcinoma of the breast, implying its involvement in breast oncogenesis." *Histopathology* **53**(4): 389-402.
- Zhou, X. D. and Y. M. Agazie (2008). "Inhibition of SHP2 leads to mesenchymal to epithelial transition in breast cancer cells." *Cell Death Differ* **15**(6): 988-996.

References

Zhu, H. H., K. Ji, et al. (2011). "Kit-Shp2-Kit signaling acts to maintain a functional hematopoietic stem and progenitor cell pool." Blood.

8. ABBREVIATIONS

Dox	doxycycline
EGF(R)	epidermal growth factor (receptor)
EMT	epithelial-to-mesenchymal-transition
ERK	extracellular signal-regulated kinase
ER	estrogen receptor
FBS	fetal bovine serum
GAPDH	glycerhaldehyde-3-phosphate dehydrogenase
Gab2	GRB2-associated binding protein 2
HER2	epidermal growth factor receptor 2
HER3	epidermal growth factor receptor 3
MARA	motif activity response analysis
miR	short hairpin RNA ^{miR}
SHP2	Src-homology 2 domain-containing phosphatase
PDGFR β	platelet-derived growth factor receptor beta
PTPN11	protein tyrosine phosphatase non-receptor type 11
PTPN12	protein tyrosine phosphatase non-receptor type 12
RPA	reverse-phase protein array
TNBC	triple-negative breast cancer
ZEB1	zinc finger E-box binding homeobox 1

9. ACKNOWLEDGEMENTS

First I would like to thank Momo for giving me the opportunity to work in his lab, to enjoy the science during these years and to learn something new day after day. It was really a great experience. I also want to thank Nancy, Gerhard and Frank for being an exceptional support during these years, not only during the committee meetings but throughout the whole PhD.

Special thanks goes to all the facilities of the FMI and all the internal and external collaborators from Novartis Basel and Cambridge, University of Basel, Harvard and Baylor. I always had the luck of interacting with very professional and passionate people, which I hope to still interact with in the future.

I also would like to thank all the former and present colleagues at the FMI, I have learned a lot from all of you, and I am sure that we have established real friendships which will last for long time.

10. CURRICULUM VITAE

PERSONAL INFORMATIONS

Name	Nicola
Surname	Aceto
Address	Friedrich Miescher Institute for Biomedical Research (FMI) Maulbeerstrasse 66 CH-4058 Basel –SWITZERLAND-
Phone (lab)	+41 61 6976692
Phone (office)	+41 61 6978519
Mobile	+41 76 52 13 688 / +39 339 311 04 74
Email	nicola.aceto@fmi.ch
Date of birth	October 8, 1982
Nationality	Italian
Marital status	Married

EDUCATION

PhD in Biochemistry (2006 – Present)

Friedrich Miescher Institute for Biomedical Research (FMI), Basel, Switzerland

International PhD Program

Title of PhD thesis: “Opposing roles for protein tyrosine phosphatases SHP2 and PTPN12 in breast cancer”. Supervisor: Dr. Mohamed Bentires-Alj

MSc in Medical and Pharmaceutical Biotechnology (2004 – 2006)

University of Piemonte Orientale “Amedeo Avogadro”, Novara, Italy

Final exam mark of 110/110 summa cum laude

Title of the final year dissertation: “Molecular mechanisms of apoptosis induced by Taurolidine in Malignant Mesothelioma cells”. Supervisor: Prof. Giovanni Gaudino

BSc in Biotechnology (2001 – 2004)

University of Piemonte Orientale “Amedeo Avogadro”, Novara, Italy

Final exam mark of 110/110 magna cum laude

Title of the final year dissertation: “Akt dominant negative vector preparation. Evaluation of Taurolidine activity on Malignant Mesothelioma”. Supervisor: Prof. Giovanni Gaudino

PUBLICATIONS

Papers

- **“The Tyrosine Phosphatase SHP2 Promotes Breast Cancer Progression and Maintains the Cancer Stem Cell Population via Activation of Key Transcription Factors and Repression of the let-7 miRNA”**
Aceto N, Sausgruber N, Brinkhaus H, Gaidatzis D, Martiny-Baron G, Mazzarol G, Confalonieri S, Hu G, Balwierz P, Pachkov M, Elledge SJ, van Nimwegen E, Stadler MB, and Bentires-Alj M.
Nature Medicine. Submitted, in revision
- **“Epithelial Protein-Tyrosine Phosphatase 1B (PTP1B) Contributes to the Induction of Mammary Tumors by HER2/Neu but is Dispensable for Tumor Maintenance”**
Balavenkatraman KK, Aceto N, Britschgi A, Mueller U, Bence KK, Neel BG and Bentires-Alj M.
Cancer Res. Submitted, in revision
- **“Activation of Multiple Proto-oncogenic Tyrosine Kinases in Breast Cancer via Loss of the PTPN12 Phosphatase”**
Sun T, Aceto N, Meerbrey KL, Kessler JD, Zhou C, Migliaccio I, Nguyen DX, Pavlova NN, Botero M, Huang J, Bernardi RJ, Schmitt E, Hu G, Li MZ, Dephoure N, Gygi SP, Rao M, Creighton CJ, Hilsenbeck SG, Shaw CA, Muzny D, Gibbs RA, Wheeler DA, Osborne CK, Schiff R, Bentires-Alj M, Elledge SJ, Westbrook TF.
Cell. 2011 Mar 4; 144, 703-718. PMID: 21376233
- **“Taurolidine and oxidative stress: a rationale for local treatment of mesothelioma”**
Aceto N, Bertino P, Barbone D, Tassi G, Manzo L, Porta C, Mutti L, Gaudino G.
Eur Respir J. 2009 Dec;34(6):1399-407. PMID: 19460788.
- **“Genome profiling of chronic myelomonocytic leukemia: frequent alterations of RAS and RUNX1 genes”**
Gelsi-Boyer V, Trouplin V, Adelaide J, Aceto N, Remy V, Pinson S, Houdayer C, Arnoulet C, Sainty D, Bentires-Alj M, Olschwang S, Vey N, Mozziconacci MJ, Birnbaum D and Chaffanet M.
BMC Cancer. 2008 Oct 16; 8(1):299. PMID: 18925961.

Patent

- **“Protein tyrosine phosphatase, non-receptor type 11 (PTPN11) and tumor initiating cells”**

Inventors: **N. Aceto** and M. Bentires-Alj

Filed on March 2010. Filing number: EP10158207.0

Posters

- **“A Cell Autonomous Role for Protein-Tyrosine Phosphatase 1B (PTP1B) in Her2/Neu-evoked Mammary Tumors”**

Kamal Kumar Balavenkatraman, **Nicola Aceto**, Adrian Britschgi, Emanuela Milani, Georg M Baron and Mohamed Bentires-Alj.

Gordon Research Conference on Mammary Gland Biology 2010. June 6-11th 2010, Il Ciocco Hotel and Resort, Lucca, Italy.

- **“The Role of Memo in Breast Cancer Development and Metastasis”**

Gwen MacDonald, **Nicola Aceto**, Mohamed Bentires-Alj, Susanne Lienhard, Arno Doelemeyer, Manuela Vecchi and Nancy Hynes.

Gordon Research Conference on Mammary Gland Biology 2010. June 6-11th 2010, Il Ciocco Hotel and Resort, Lucca, Italy.

- **“Dissecting the Role of the Protein Phosphatase 1B (PTP1B) in Breast Cancer”**

Kamal Kumar Balavenkatraman, **Nicola Aceto**, Emanuela Milani, Urs Mueller and Mohamed Bentires-Alj.

FMI Annual Meeting 2009. October 1-2nd 2009, Novartis Campus St. Johann, Basel, Switzerland.

- **“The Role of Delta-HER2 in Breast Cancer”**

Abdullah Alajati, **Nicola Aceto**, Dominique Meyer, Stephan Duss, Heinz Gut and Mohamed Bentires-Alj.

FMI Annual Meeting 2009. October 1-2nd 2009, Novartis Campus St. Johann, Basel, Switzerland.

- **“Role of PTPs in Breast Cancer Invasion and Metastases”**
Nicola Aceto, Dominique Meyer, Kamal Kumar Balavenkatraman, Urs Mueller and Mohamed Bentires-Alj.
FMI Annual Meeting 2008. September 19-22nd 2008, Grindelwald, Switzerland.
- **“The Role of Protein Tyrosine Phosphatases in Breast Cancer and Drug Resistance”**
Dominique Meyer, Nicola Aceto, Kamal Kumar Balavenkatraman, Urs Mueller, Mohamed Bentires-Alj.
FMI Annual Meeting 2008. September 19-22nd 2008, Grindelwald, Switzerland.
- **“RHAU is Essential for the Growth of RAS-Transformed MEF Cells”**
Janice Lai, Stephane Thiry, Nicola Aceto, Mohamed Bentires-Alj and Yoshikuni Nagamine.
FMI Annual Meeting 2008. September 19-22nd 2008, Grindelwald, Switzerland.
- **“Role of PTPs in Breast Cancer and Metastasis”**
Nicola Aceto, Kamal K. Balavenkatraman, Dominique Meyer, Emanuela Milani, Urs Mueller and Mohamed Bentires-Alj.
FMI Annual Meeting 2007. September 19-22nd 2007, Grindelwald, Switzerland.
- **“The Role of PTPs in Breast Cancer and Drug Resistance”**
Dominique Meyer, Nicola Aceto, Kamal Kumar Balavenkatraman, Emanuela Milani, Urs Mueller and Mohamed Bentires-Alj.
FMI Annual Meeting 2007. September 19-22nd 2007, Grindelwald, Switzerland.
- **“Role of the Protein Tyrosine Phosphatase 1B (PTP1B) in Breast Cancer”**
Kamal K. Balavenkatraman, Nicola Aceto, Urs Mueller and Mohamed Bentires-Alj.
FMI Annual Meeting 2007. September 19-22nd 2007, Grindelwald, Switzerland.
- **“Role of the Protein Tyrosine Phosphatase 1B (PTP1B) in Breast Cancer”**
Kamal K. Balavenkatraman, Nicola Aceto, Urs Mueller and Mohamed Bentires-Alj.

Novartis Postdoc retreat. September 9-12th 2007, Boston, MA, USA.

- **“Role of PTPs in breast carcinogenesis and metastasis”**
Mohamed Bentires-Alj’s lab: **Nicola Aceto**, Heike Brinkhaus, Emanuela Milani.
FMI Annual meeting 2006. September 21th-24th 2006, Murten, Switzerland.

FELLOWSHIPS AND PRIZES

- **STARTCUP TORINO PIEMONTE for BUSINESS IDEAS and BUSINESS PLAN Finalist (2006)**
Finalist with a team of 6 people for the best business idea and business plan.
STARTCUP and I3P, Torino, ITALY.

RELEVANT CONFERENCES ATTENDED AND TALKS GIVEN

- **FMI 40th Anniversary Symposium 2010.**
September 20-21st 2010, Congress Center, Basel, Switzerland.
- **FMI Annual Meeting 2009.**
October 1-2nd 2009, Novartis Campus St. Johann, Basel, Switzerland.
Talk title: Role of the Protein Tyrosine Phosphatase SHP2 in Breast Cancer
- **FMI Annual Meeting 2008.**
September 19-22nd 2008, Congress Center, Grindelwald, Switzerland.
- **Mechanisms and Models of Cancer, CSHL Meeting, New York.**
August 13-17th 2008, Cold Spring Harbor Laboratory, New York, USA.
- **FMI Annual Meeting 2007.**
September 19-22nd 2007, Congress Center, Grindelwald, Switzerland.
- **Targeting the Kinome meeting.**
December 4th - 6th 2006, Congress Center, Basel, Switzerland
- **FMI Annual Meeting 2006.**
September 21th-24th 2006, Centre Löwenberg, Murten, Switzerland.

MEMBERSHIP

- **European Association for Cancer Research (EACR)**
Member of EACR from July 2007

CERTIFICATES

- **Education for persons carrying out animal experiments**
Course in accordance with the Ordinance Governing Training and Ongoing Education of Specialists for Animal Experiments of 6 March 2007 (SR 455.171.2) Section 2 and 3 (Art. 4-11) in correspondence with the FELASA-Category B.
- **Biosafety**
Instruction course in Biosafety on January 10, 2007 at the Friedrich Miescher Institute, Basel, Switzerland.
- **Radiation protection**
2-days instruction course in radiation protection on November 28-29th, 2006 at the Friedrich Miescher Institute, Basel, Switzerland.

WORK EXPERIENCE

I have good experience with all basic molecular biology techniques and cell culture, three-dimensional cultures in matrigel, mammosphere and tumorsphere culture for the analysis of stem and progenitor cells and FACS analysis of cell lines or cells obtained from primary tissues. I am also very familiar with in vivo techniques in mouse models, such as orthotopic xenografts breast cancer models, lung metastases studies, serial dilution transplantations from primary mouse tumors and intraductal injection into the primary duct of the mouse mammary gland. At the biochemical level, I am experienced with western blotting, immunoprecipitation, reverse-phase protein array (RPA) and proteomics from both cell lines and primary tissues. At the genomic level, I have insights into microarray data generation and analysis and motif activity response analysis (MARA). At the informatic level, I am experienced in handling all Microsoft Office programs, Endnote, Adobe

Illustrator, Photoshop and Acrobat, VectorNTI and several imaging programs (e.g., ZEN, Imaris and ImageJ).

LANGUAGES

Excellent knowledge of both spoken and written English (TOEFL). English is my working language. I have a basic knowledge of French and German. My mother tongue is Italian.

LEADERSHIP SKILLS

Training of:

- **Christina Holzer, MSc Biochemistry student, University of Basel, Switzerland**
From 1/9/2008 to 31/8/2009
- **Thomas Feutren, MD student, University of Strasbourg, France**
From 1/7/2008 to 31/8/2008

